Magnetic nanoparticles: synthesis, properties and biomedical applications

Olivier Sandre

olivier.sandre@u-bordeaux.fr
@olive_free

MAGNETIC NANOPARTICLES: SYNTHESIS, PROPERTIES AND BIOMEDICAL APPLICATIONS

Olivier Sandre, senior CNRS researcher at Univ. Bordeaux, France

LCPO
Laboratoire de Chimie des Polymères Organiques

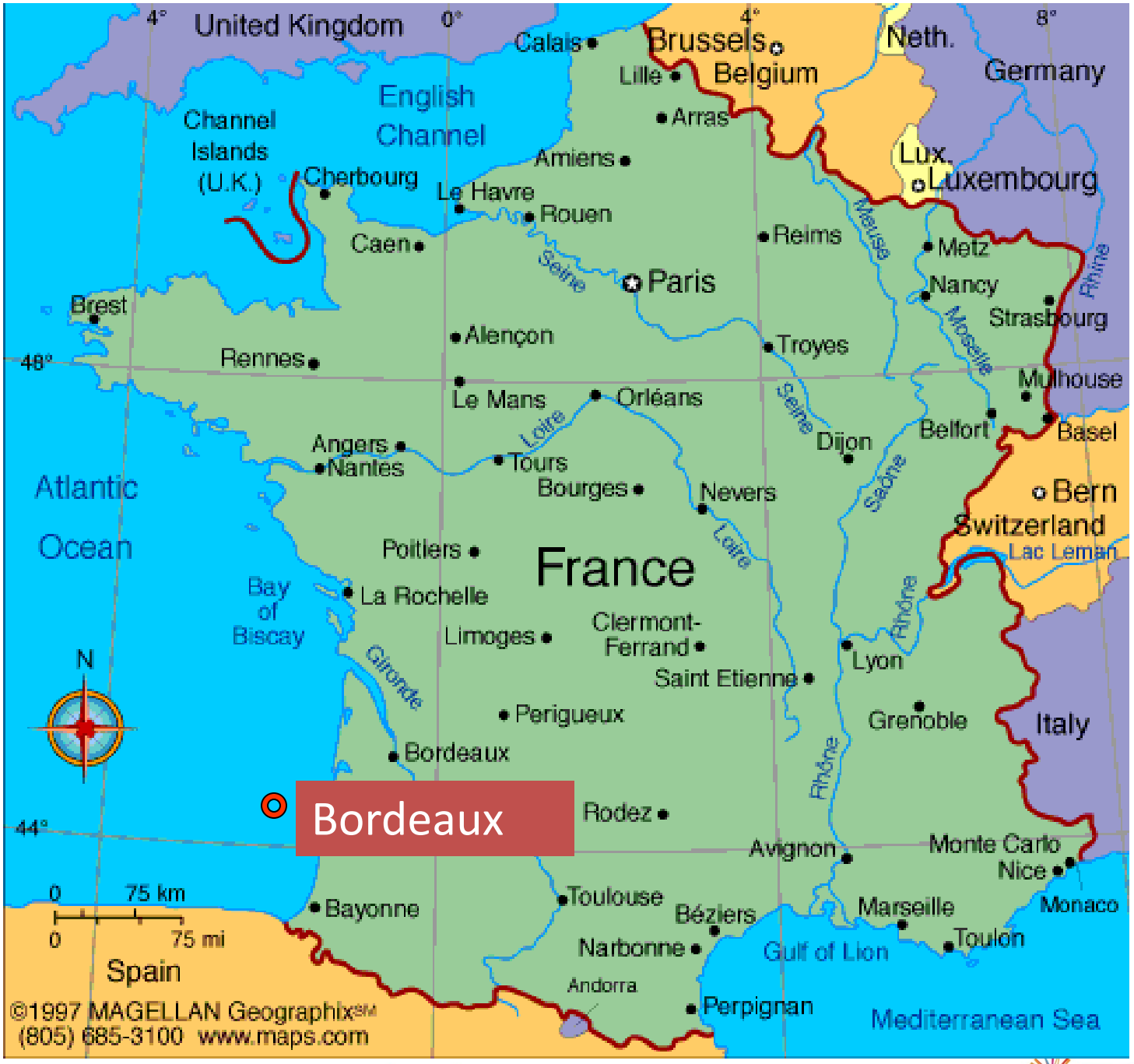

LCPO
Laboratoire de Chimie des Polymères Organiques

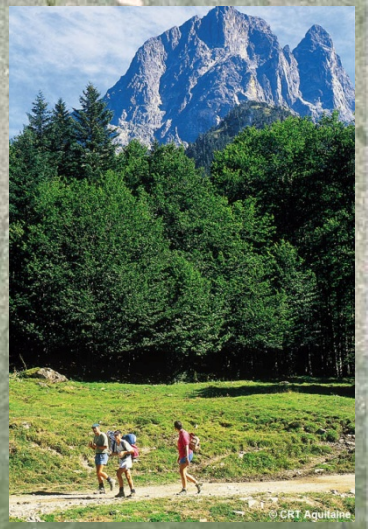

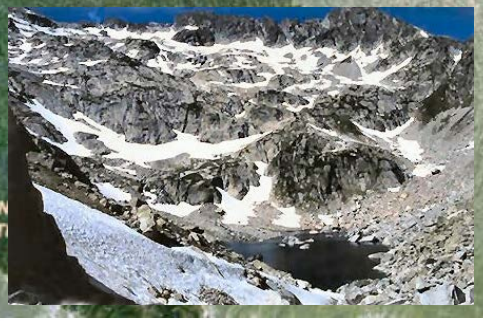

Magnetic nanoparticles (MNPs) Part 1: Synthesis and physical properties

• Part 1A: Chemistry of iron oxides and oxo-hydroxides:
Diversity of methods to prepare colloidal nanoparticles, either in non aqueous solvents: hydrothermal synthesis, polyol synthesis, thermal decomposition…
or in water: alkaline co-precipitation of iron salts (also in EG, DEG…)

• Part 1B: Magnetic behavior (ferro- /ferri- /antiferro- /superpara– magnetism…) and optical properties of MNPs (UV-vis absorption, magnetic birefringence)

• Part 1C: MNPs as contrast agents in Magnetic Resonance Imaging
Universal law for relaxometry (T_1/T_2 of water H spins near MNPs)

All properties are highly sensitive on MNP's size and shape (poly)dispersity!

• Part 2A Magnetic Hyperthermia ('Tumor catabolism')

• Part 2B Nanomedicines – Magnetic carrier – Magnetic Guiding ('Tumor homing')

• Part 2C Drug Delivery Systems (DDS) based on Magnetic Core@Polymer Shells, Magnetic Polymer Shells, Magnetic Micelles, or Vesicles ('Polymersomes')

Diversity of iron oxides and oxo-hydroxides

The Iron Oxides (Rochelle M. Cornell, Udo Schwertmann)

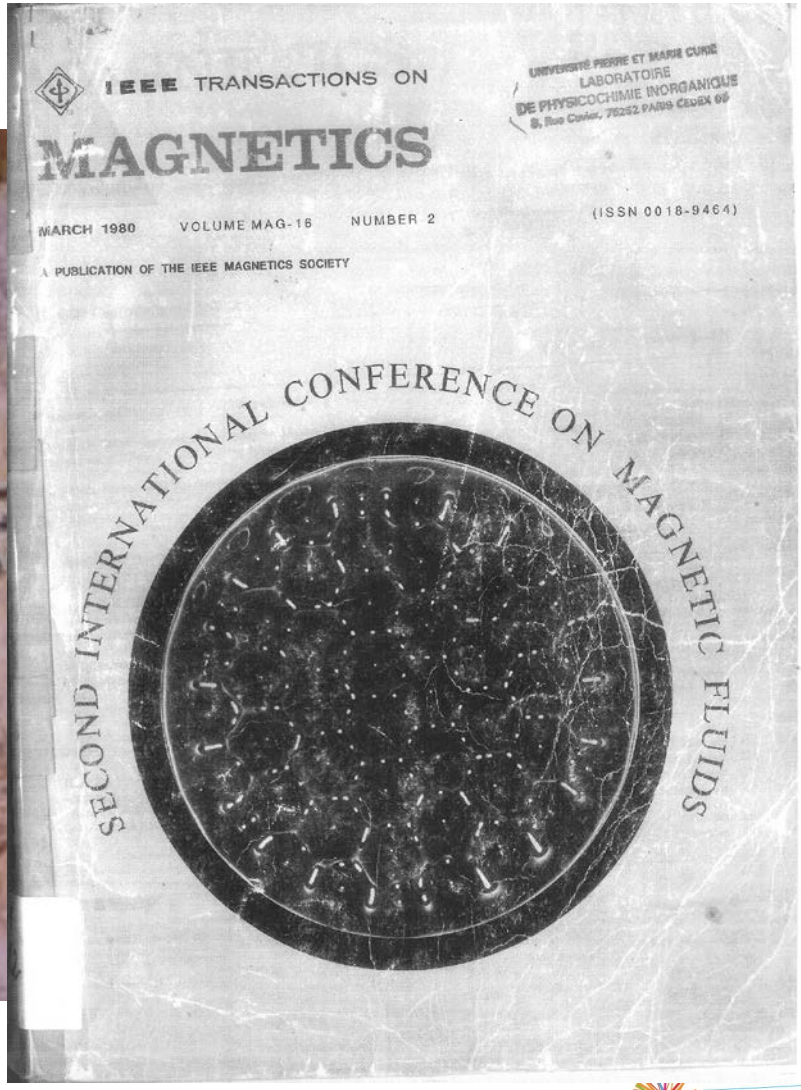

From solution of Fe^{2+} et Fe^{3+} salts towards solid phase

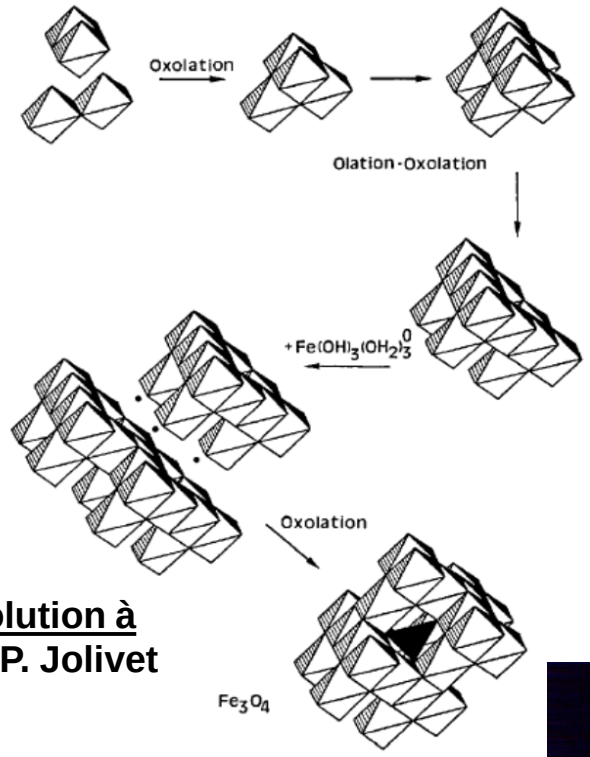

in De la solution à l'oxyde, J.-P. Jolivet

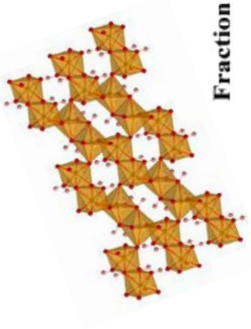

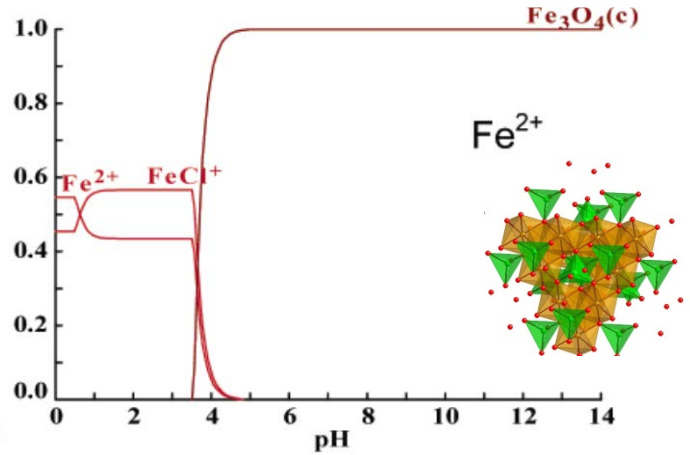

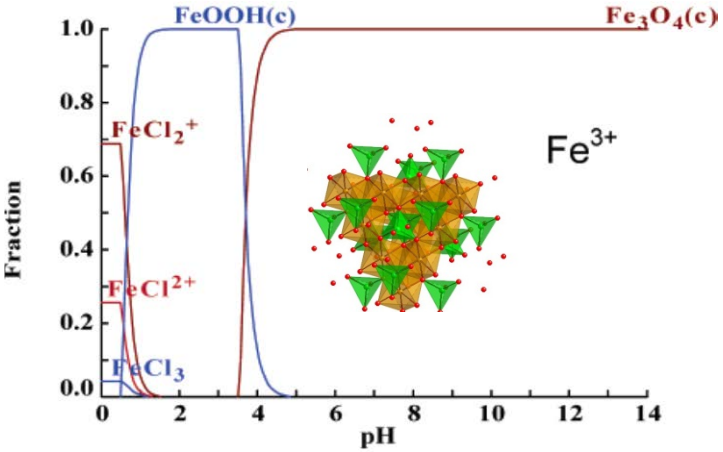

D.K. Kim et al.,
Chem. Mater. 2003, 15, 1617-1627

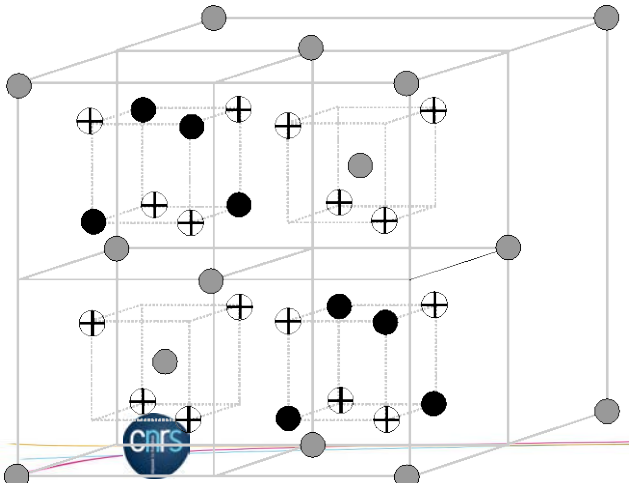

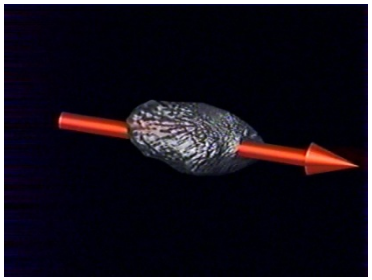

O^{2-}

Fe^{3+} tetrahedral site

Fe^{2+}/Fe^{3+} octahedral site

Spinelle structure

Very narrow pH stability of $Fe^{3+}(H_2O)_6$ soluble ion

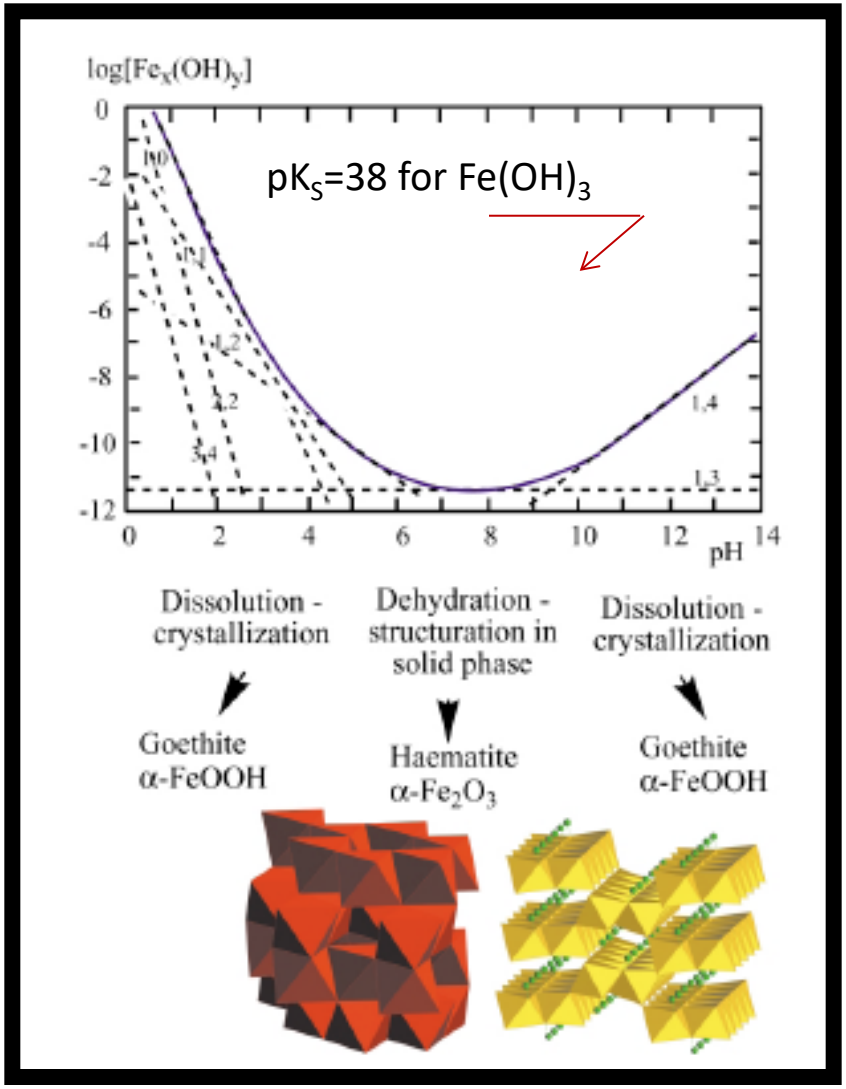

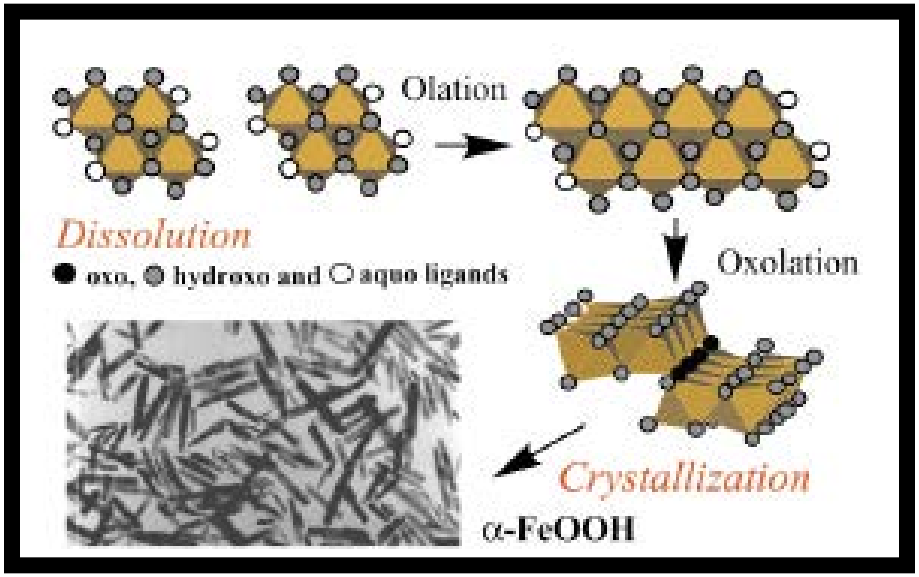

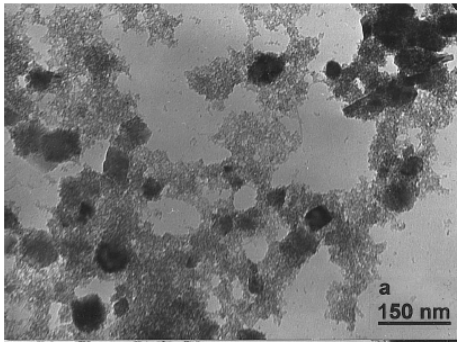

Jean-Pierre Jolivet, *Chem. Commun.*, 2004, 481-487

Antiferromagnetic clays made of iron^{+III} oxo-hydroxides

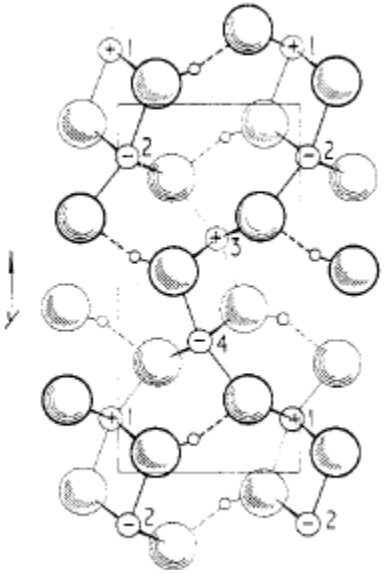

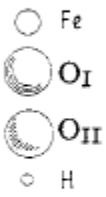

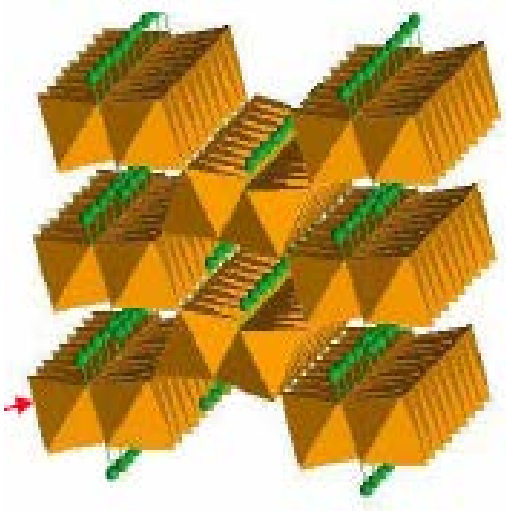

Orthorombic structure of γ–FeOOH
(Fe^{3+} in octahedral sites)

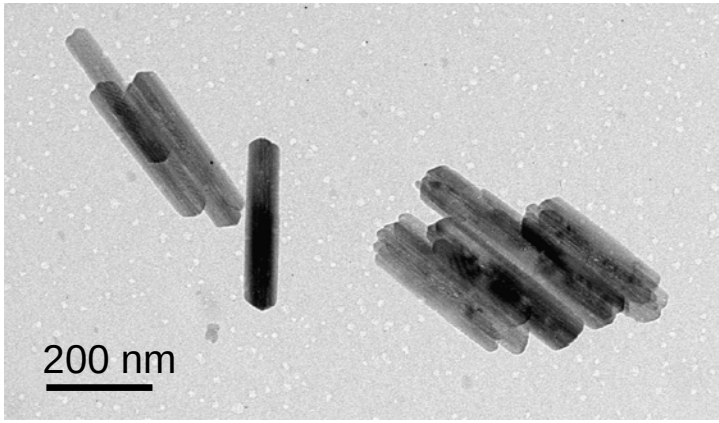

Goethite nanolaths γ–FeOOH
(rod-like)

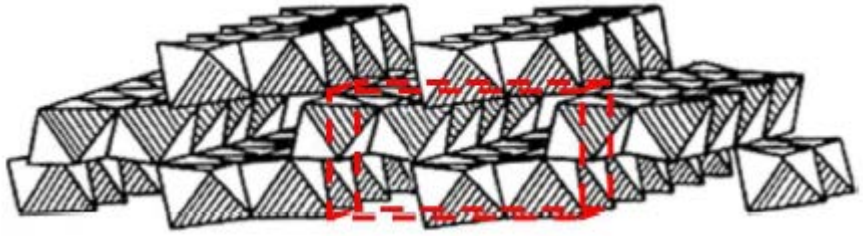

Goethite is antiferromagnetic

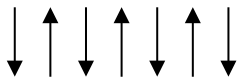

= 0 Resulting magnetization

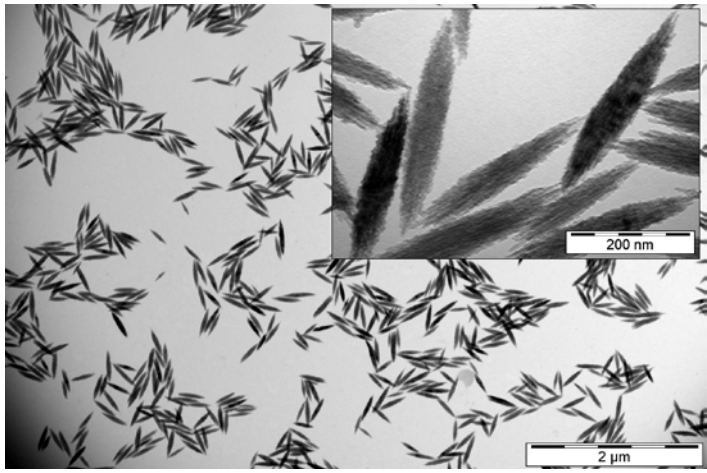

Accicular Haematite α–Fe_2O_3
(spindle-like)

Synthesis of antiferromagnetic goethite nanorods

1/ ferrihydrite alkaline precipitation

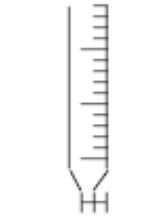

NaOH
1M

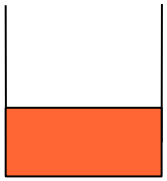

0.1M $Fe(NO_3)_3$

$Ni(NO_3)_2$ ou $Co(NO_3)_2$

2/ Slow dissolution X days at pH>11
→ goethite formation (ochre)

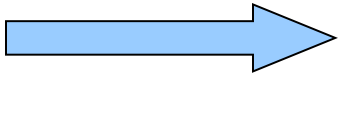

$\alpha - FeOOH$

3/ Washings H_2O
(5000 rpm)

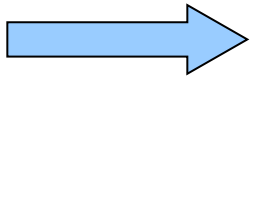

Dispersion in HNO_3 at pH=3

- PhD thesis J. Hernandez (UPMC 1998):
  10 days ageing at T=25C & pH13

- S. Krehula et al. (Mat. Lett. 2002): hydrophobic base (TMAOH)
  Ageing during 1 – 21 days + "forced hydrolysis" (T=60 – 160C)

- D. Thies-Weesie et al. (Chem. Mater. 2007)
  Size-sorting by centrifugation steps

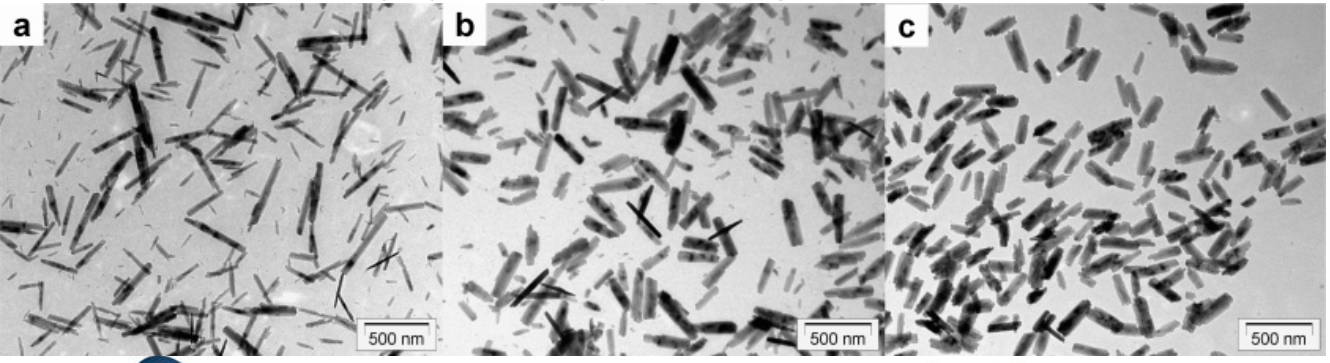

- Thermal decomposition Fe^{III}-oleate
  Taekyung Yu et al. (JACS 2007)

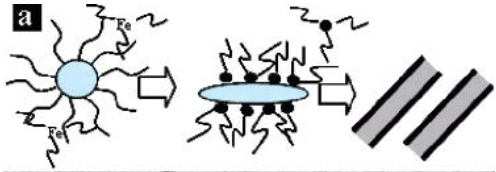

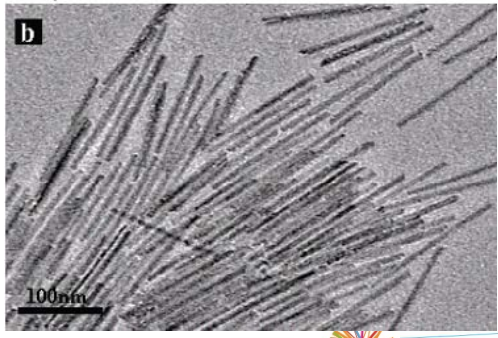

Doping of goethite nanorods with M^{n+} cations

- U. Schwertmann & R.M. Cornell, Iron Oxides in the Laboratory (1991)
- B. Sing et al., Clay Minerals 2002 → Cr^{3+}, Mn^{3+}, Ni^{2+}
- M. Mohapatra et al., Hydromelallurgy 2002 → Cu^{2+}, Ni^{2+}, Co^{2+}, Mat. Chem. Phys. 2005 → Ce^{4+}

Ageing conditions: 24h in oven at 70° C - pH=11-12

Sample	pH_{ageing}	Ni/Fe	Φ v/v	D_{hyd} nm
T	11.1	0	0.21%	205
1Ni	11	0.6%	0.19%	198
5Ni	11.9	2.4%	0.17%	142
10Ni	12	2.8%	0.10%	168

Sample	pH_{ageing}	Co/Fe	Φ v/v	D_{hyd} nm
T	11.1	0	0.21%	205
1Co	12	1.0%	0.25%	284
5Co	12.2	2.6%	0.15%	169
10Co	12.2	9.6%	0.02%	238

XRPD: no trace of $Ni(OH)_2$ → nickel on surface

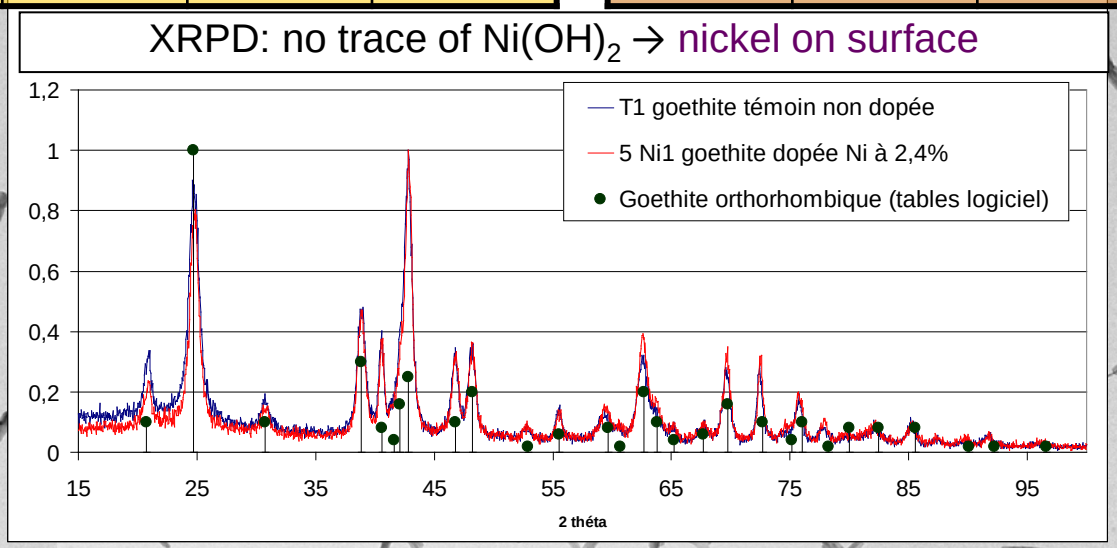

α–FeOOH: orthorombic mesh a=9.95Å b=3.01Å c=4.62Å

1 µm

1 µm

Goethite nanorods doped with Co^{2+}

Goethite doped at 1%Co

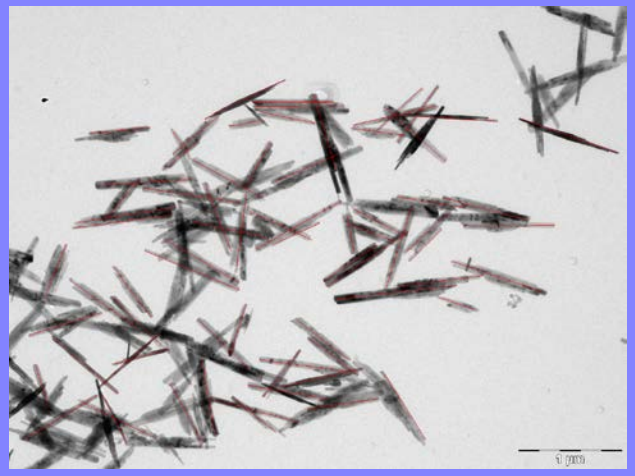

Hydrodynamic diameter = 284 nm
Mean length by TEM = 715 nm

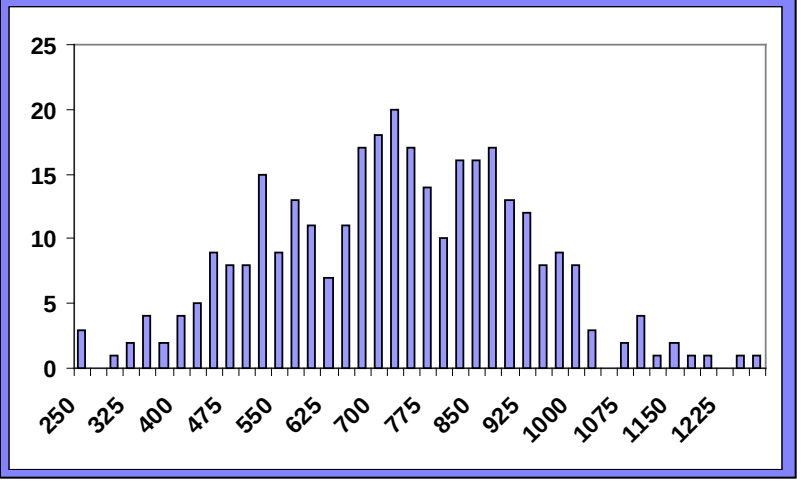

Goethite doped at 10%Co

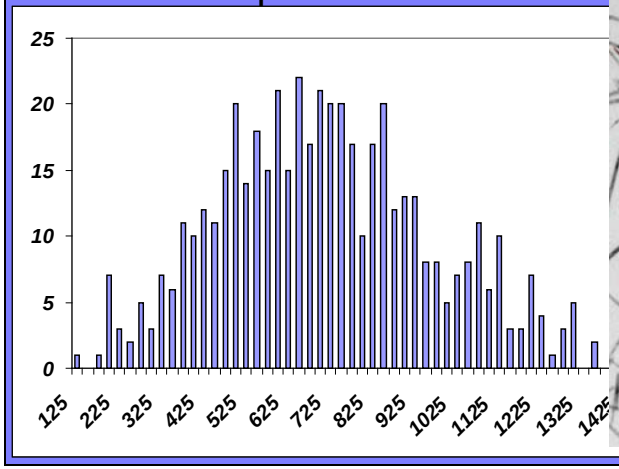

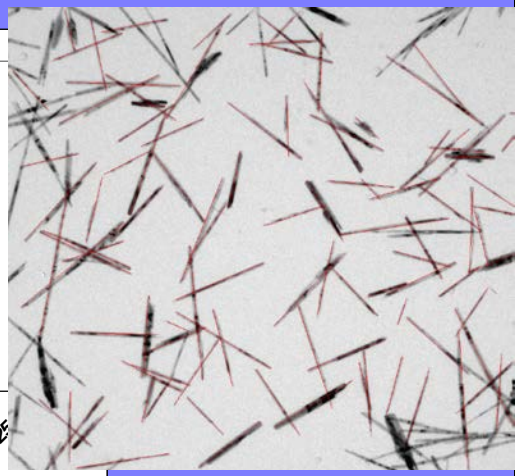

Large size associated with interesting magnetic properties (1Co1 sample)

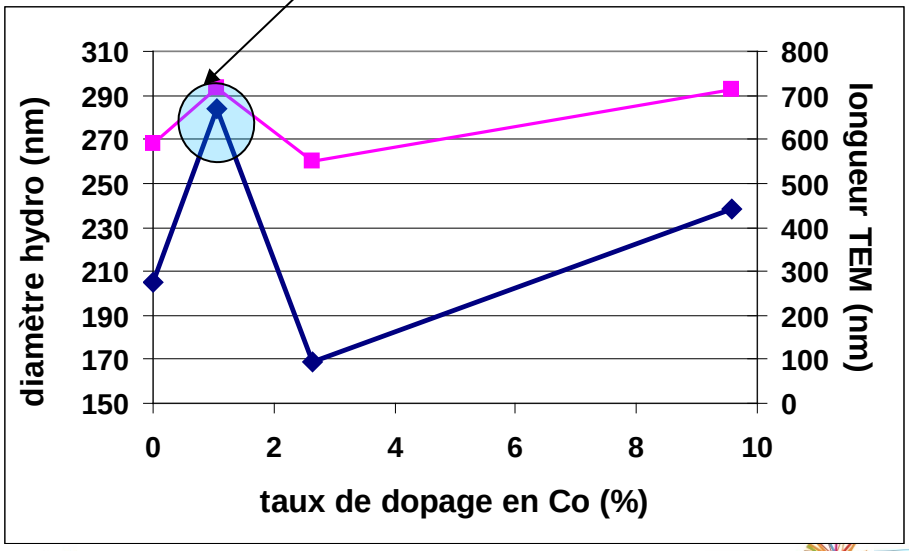

Non monotonous effect of Co doping on rods' size:

Antiferromagnetic nanorods of even smaller sizes

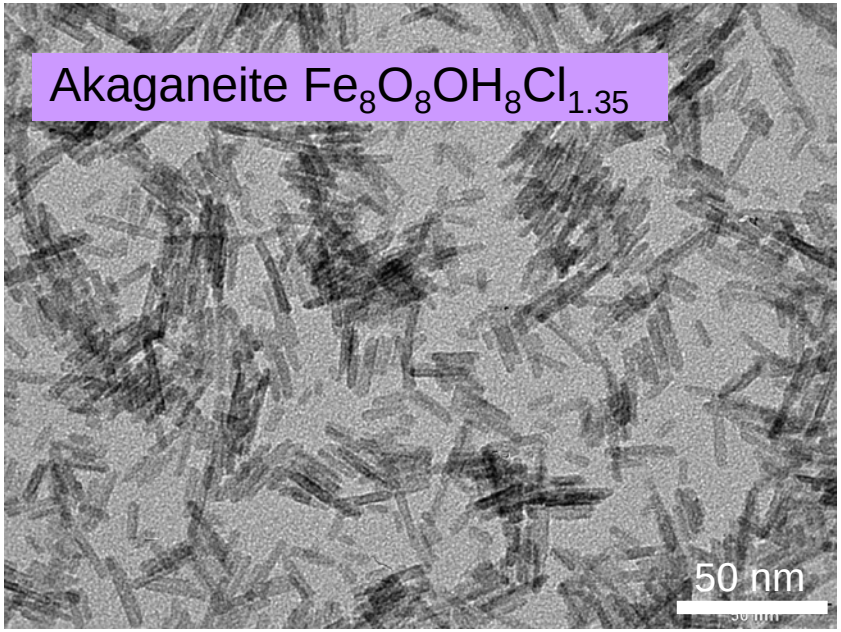

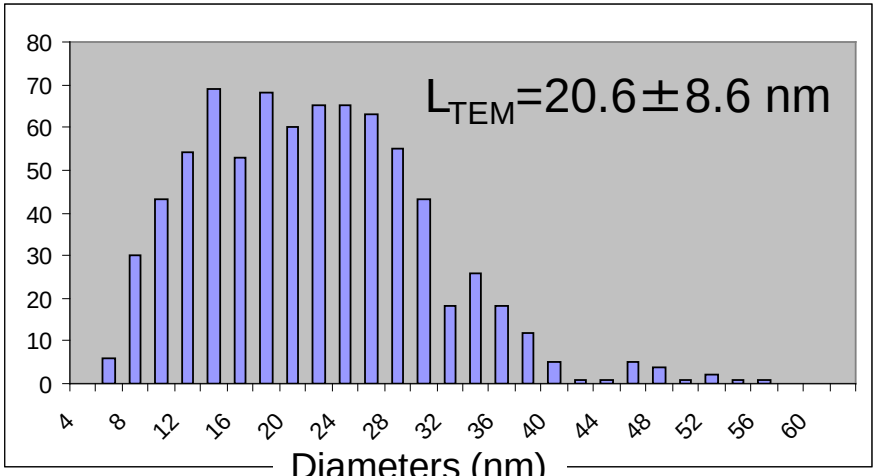

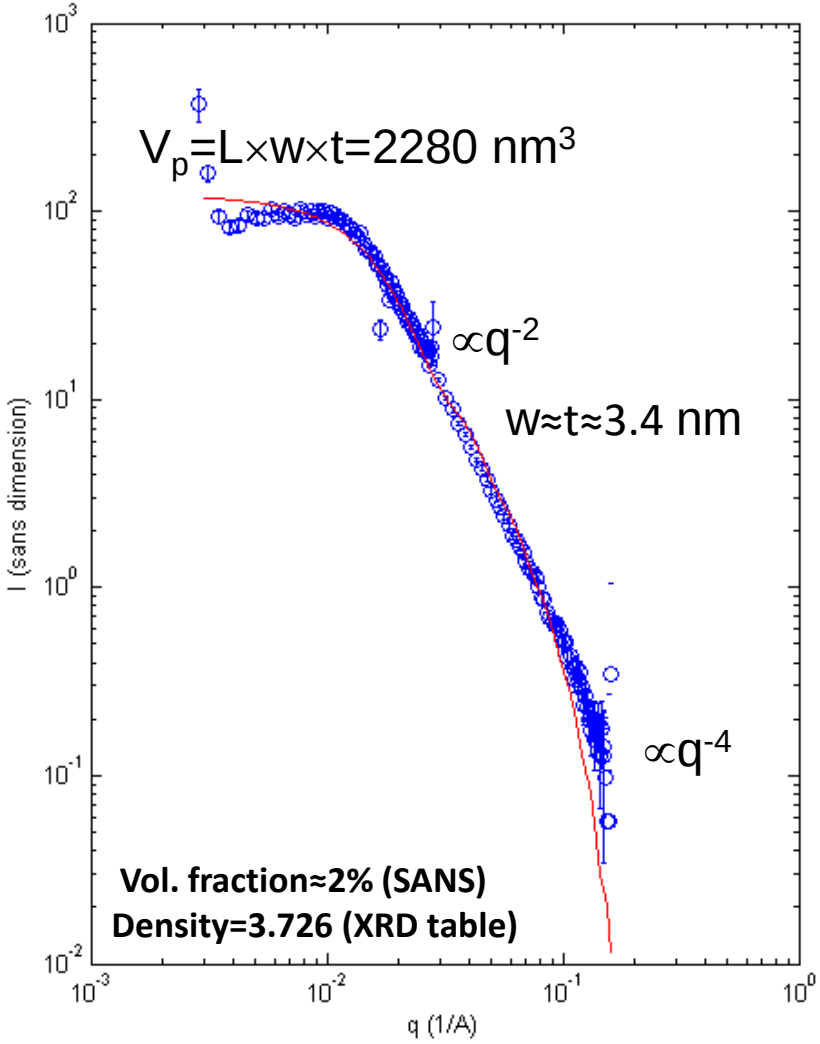

SANS on PAXY LLB-Saclay (oct. 2008)

Magneto-orientational behavior of a suspension of anti-ferromagnetic nanoparticles (NAF)

J. Phys.: Condens. Matter **20** (2008) 204120 Yu L Raikher, V. I. Stepanov (Perm, Russia) :

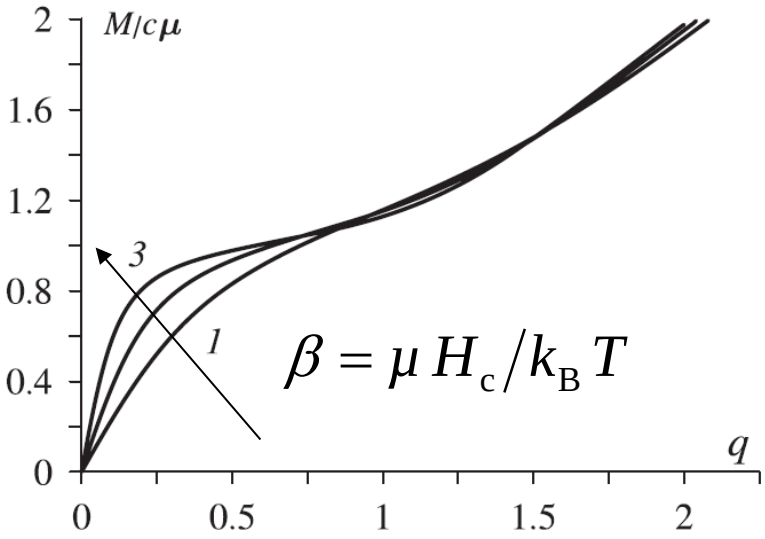

$$U = -\mu\,(\vec{e}.\vec{H}) + \tfrac{1}{2}\chi_A V(\vec{e}.\vec{H})^2$$

Figure 1. Reduced static magnetization of a NAF colloid

$$H_c = \mu / \chi_A V$$

$\chi_A = \chi_{||} - \chi_{\perp}$

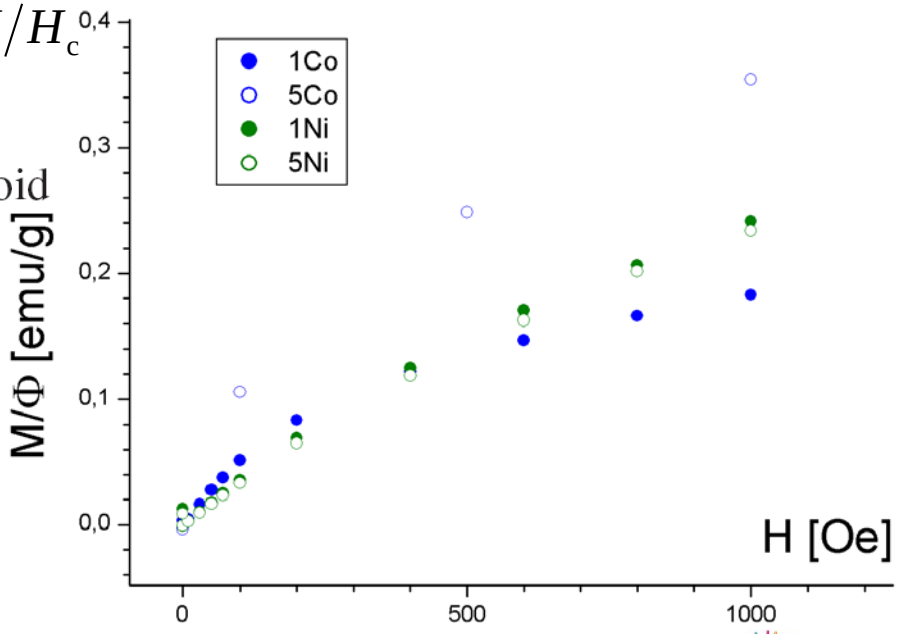

Magnetic behavior of antiferromagnetic nanorods

SQUID magnetometry at ambient temperature*

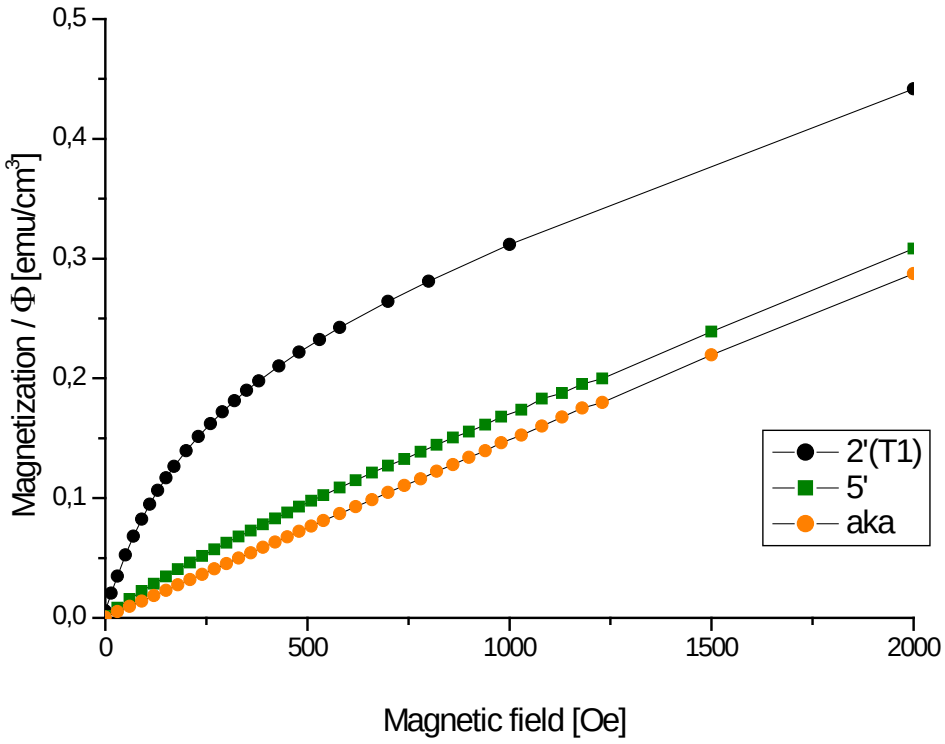

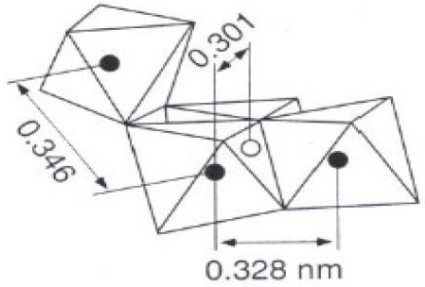

$\mu_{Fe+III}=5\ \mu_B$

$\mu \approx 10000\ \mu_B \approx (N_{Fe})_{surf}^{1/2}\ \mu_{Fe}$

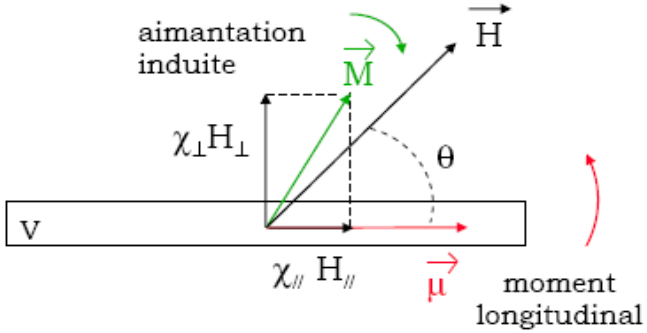

B. Lemaire, P. Davidson (LPS Orsay)

*measurement at INSP lab. (UPMC)

Magnetite: Crystalline Structure

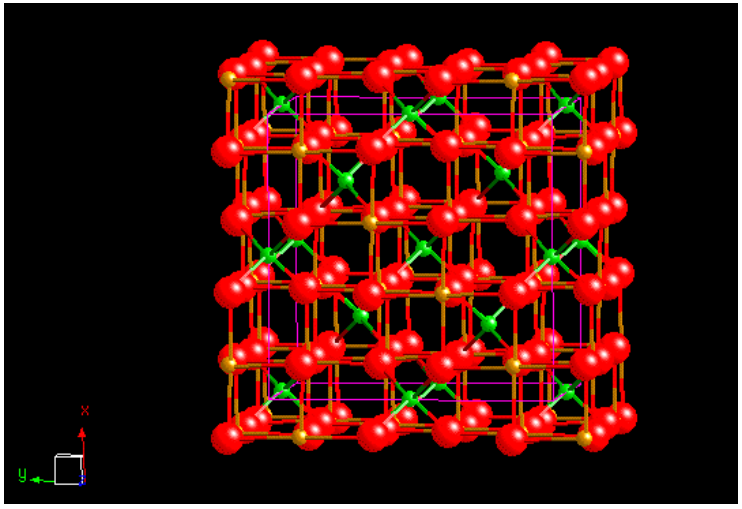

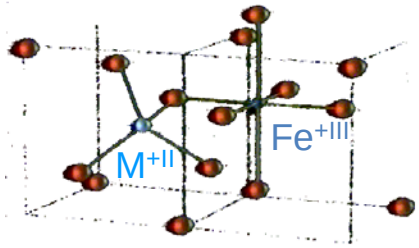

$MO.Fe_2O_3$

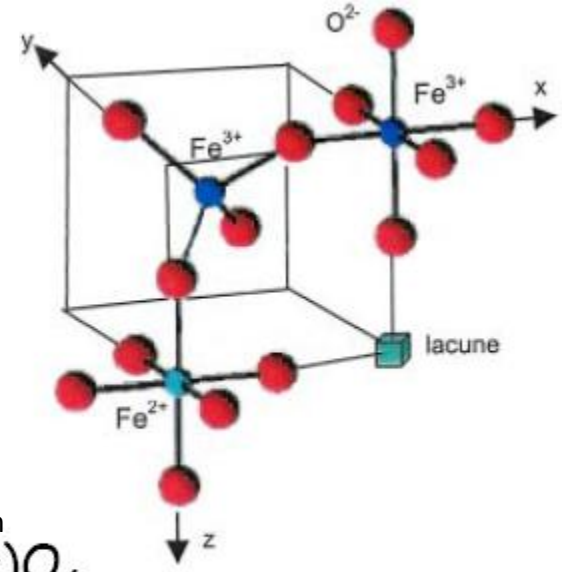

Spinelle structure:
direct or inverse

[4]=T_d [6]=O_h

$(Fe^{3+})(Fe^{3+}\ Fe^{2+})O_4$

Fe^{2+} (d^6)=4 μ_B

Fe^{3+} (d^5)=5 μ_B

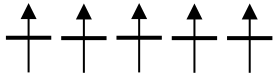

Magnetite is ferrimagnetic

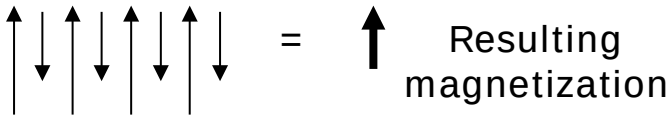

<u>Exercise:</u> 1/calculate specific volume ($cm^3 \cdot mol^{-1}$) and mesh size a

<u>Data:</u> one unit cell is cubic and contains 8 Fe_3O_4 molecules

Mass density $\rho = 5.18 \times 10^3$ $kg \cdot m^{-3}$, Molar mass M=231.535 $g \cdot mol^{-1}$

1 Bohr magneton $\mu_B = 9.274 \times 10^{-24}$ $A \cdot m^2$

2/calculate the specific magnetization M_S of bulk Fe_3O_4 in $A \cdot m^{-1}$

<u>Answers:</u>

v=45 $cm^3 \cdot mol^{-1}$

a=8.396 Å

$M_S = 5 \times 10^5$ $A \cdot m^{-1}$

Magnetic domains and Bloch boundaries (walls)

Macroscopic magnets (bulk materials) are multi-domains

Size of mono-domain: ~ 30-50 nm for iron oxides

Curie-Weiss domains

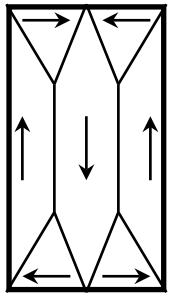

Bloch walls

Rosensweig 1965, Néel 1955, Kittel 1946, Elmore 1938

One ~10 nm nanoparticle is a magnetic single domain

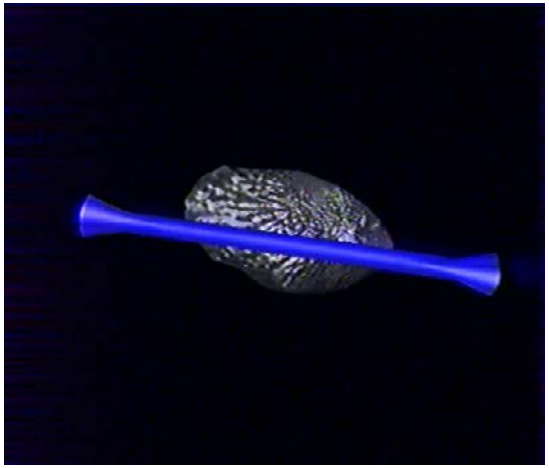

Exercise:

1:calculate magnetic moment (in nb of μ_B/MNP) for diameters: d=4 / 8 / 16 nm

2: calculate total nb of Fe ions per MNP for all d's

3: calculate nb of Fe ions on surface per MNP for all d's

Data:

1 Bohr magneton $\mu_B = 9.274 \times 10^{-24}$ A·m^2

For nano-crystalline Fe_3O_4, $M_S = 4 \times 10^5$ A·m^{-1}

Answer:

1: 1500 / 11000 / 90000 2: 1400 / 10700 / 87000

3: 290 (20%) / 1100 (10%) / 4500 (5%)

Shape anisotropy contribution to birefringence

"Rock-like" particles: S1C fraction, coated with PAA_{2k}

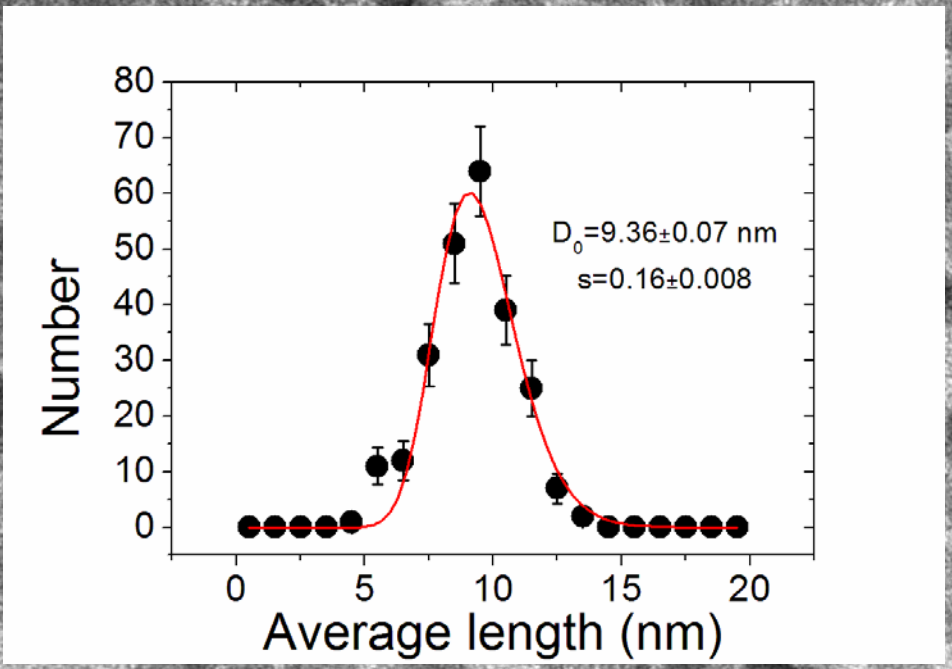

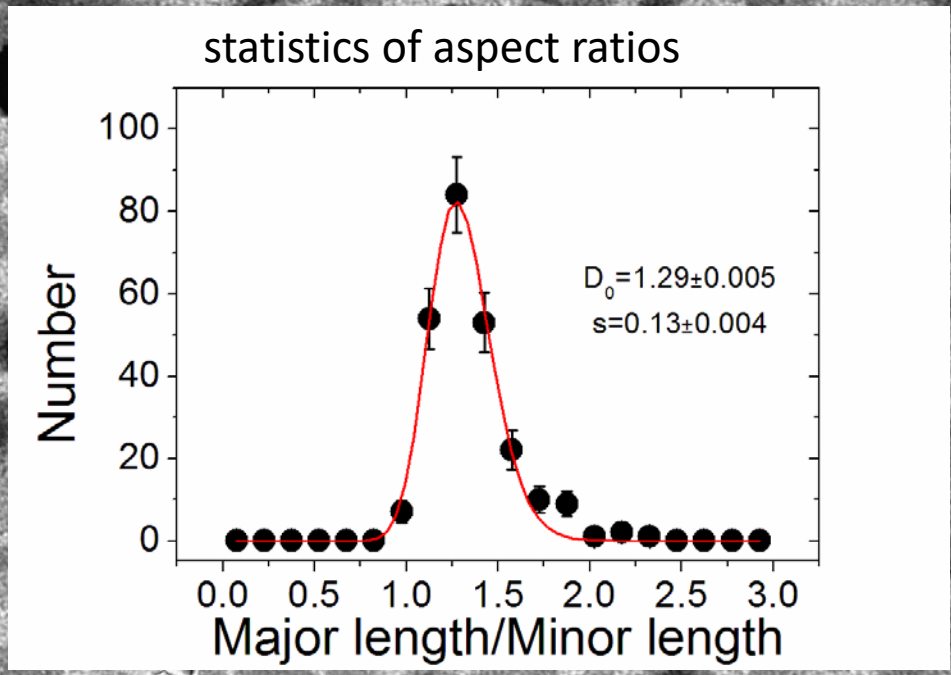

50 nm

Birefringence measurement under H field

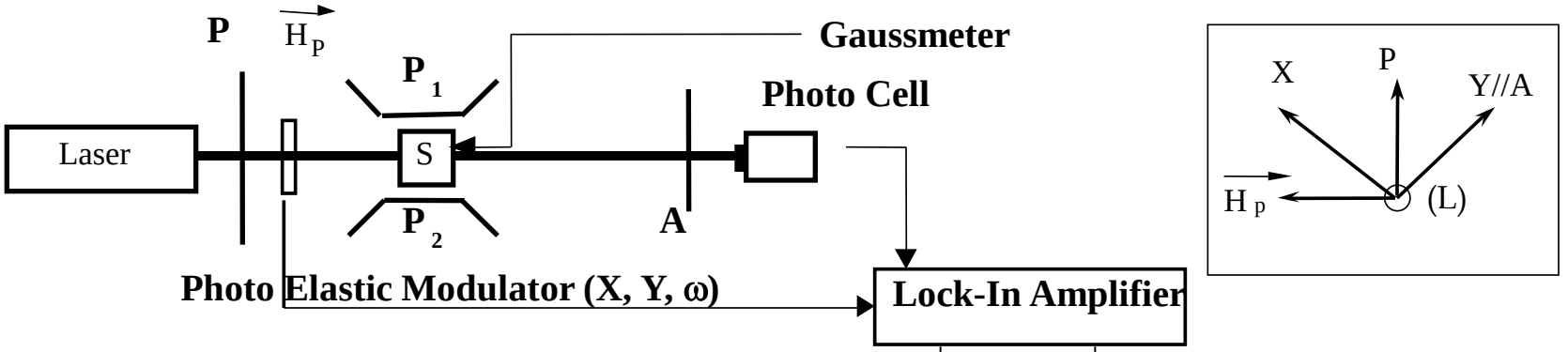

E. Hasmonay et al. EPJB 1998

$I_1(\omega) \propto |\sin(\varphi)|$ $I_2(2\omega) \propto (t_{\parallel} - t_{\perp})$ dichroism

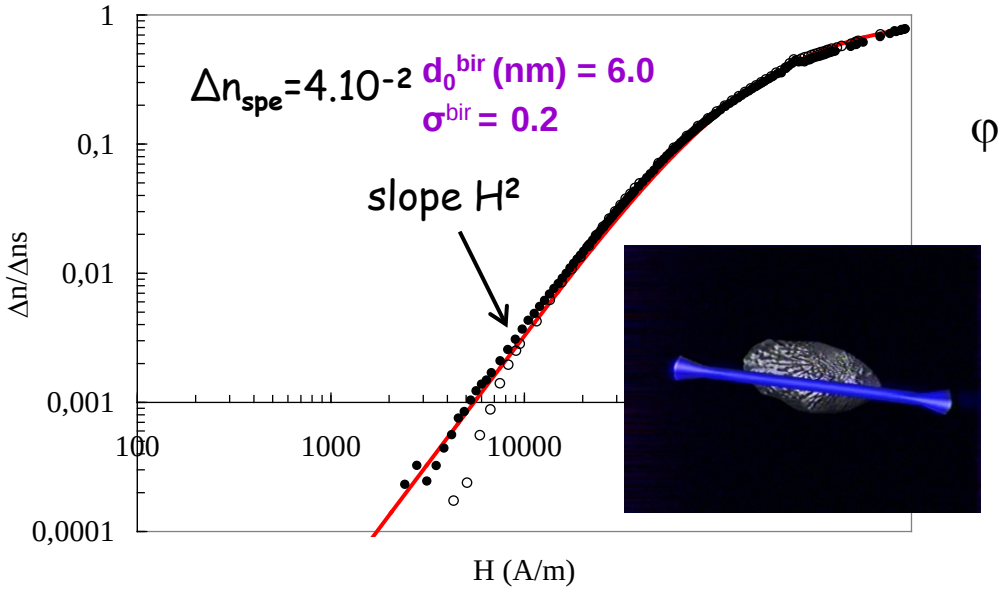

$\varphi = 2\pi \Delta n\, e / \lambda$ → $\Delta n = (n_{\parallel} - n_{\perp})$ birefringence

Plateau: $\Delta n_{sat} = \Delta n_{spe}\, \Phi$

Ferrofluid sample (maghemite γ-Fe_2O_3)

Starting materials : "True" ferrofluid

Ferrofluid = colloidal suspension of magnetic nanoparticles
which remains <u>stable whatever the intensity of applied magnetic field</u>

- no attraction of nanoparticles under B field gradient nor chaining by dipolar interaction

- but progressive orientation of dipoles according to Langevin's laws:

Magnetization

$m_s = 3{,}1.10^5$ A/m (SI) $m_s / 4\pi = 300$ G (CGS)

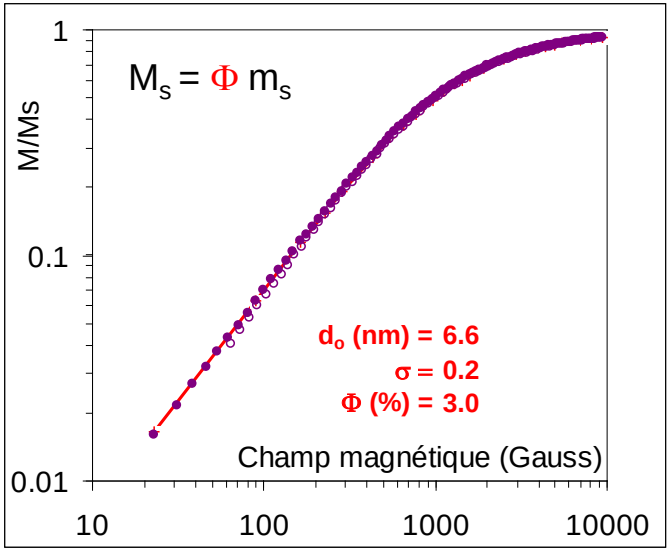

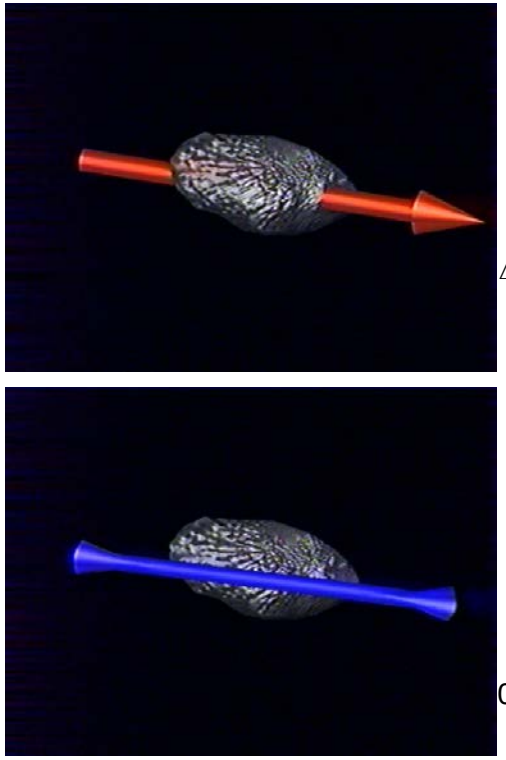

Birefringence

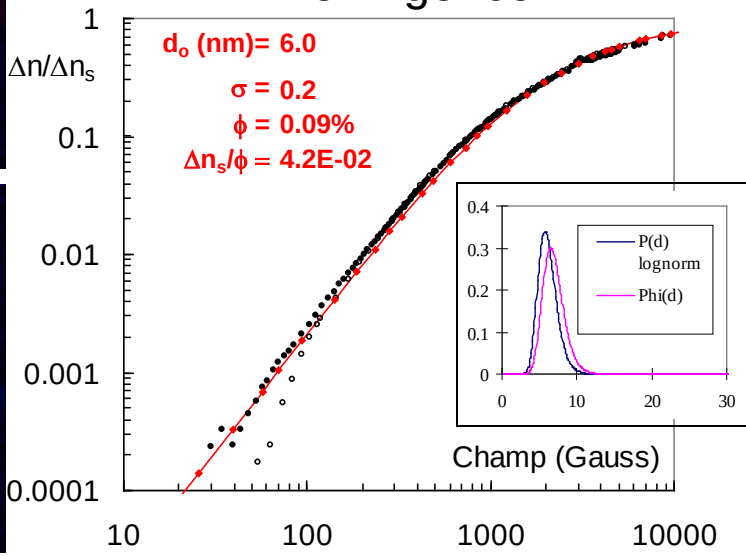

Improved properties of the larger magnetic NPs

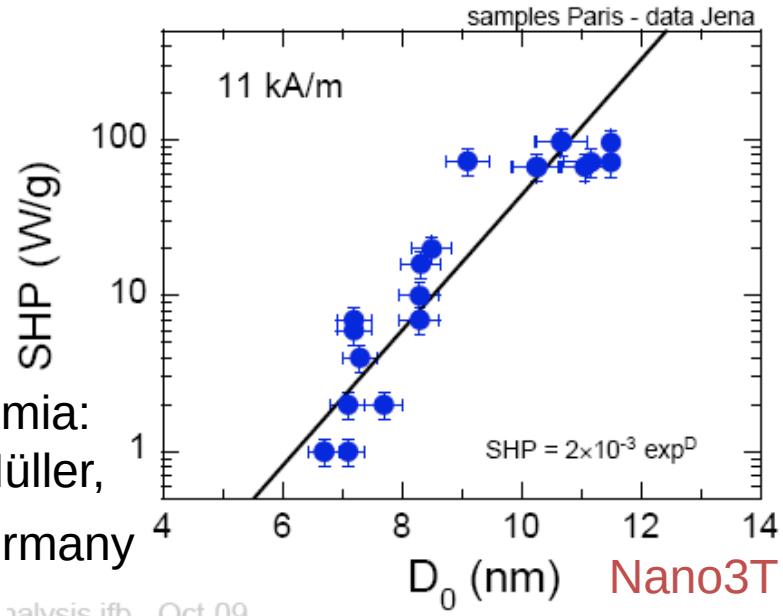

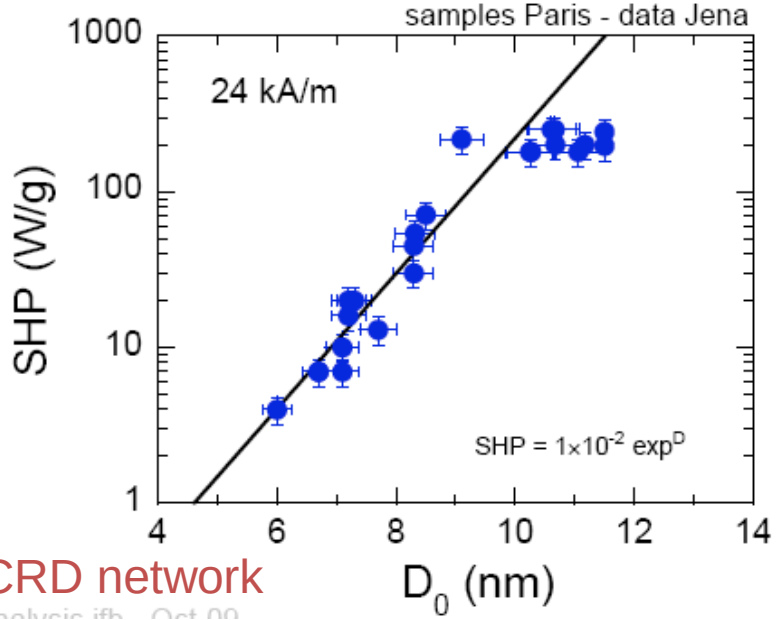

Hypethermia:
Robert Müller,
Jena, Germany

Nano3T 7th PCRD network

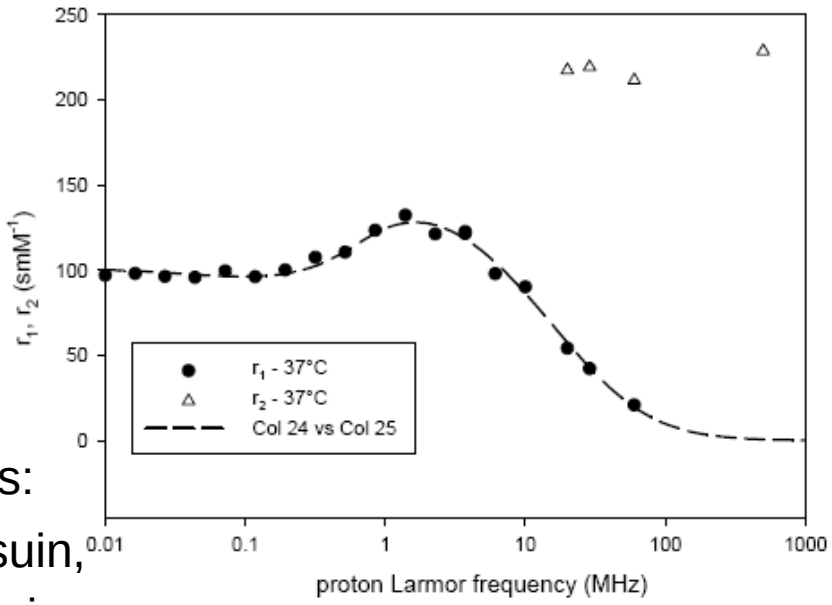

C1C2C3C4S5-PAA5K

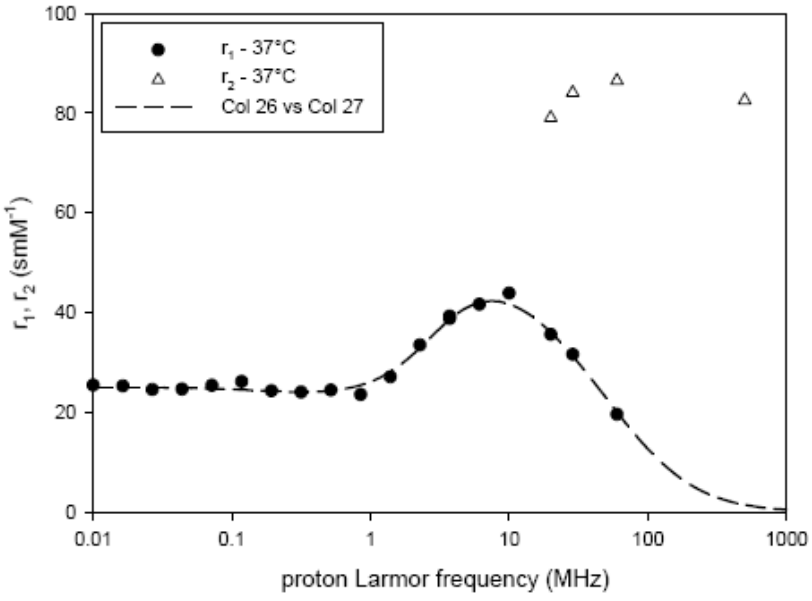

S2C14

Relaxivities:
Yves Gossuin,
Mons, Belgium

High Frequency Magnetic Susceptometry / Hyperthermia

Astalan, A.; Ahrentorp, F.; Jonasson, C.; Blomgren, J.; Yan, M.; Courtois, J.; Berret, J.-F.; Fresnais, J.; Sandre, O.; Müller, R.; Dutz, S.; Johansson, C., AIP Conf. Proc. Series 2010

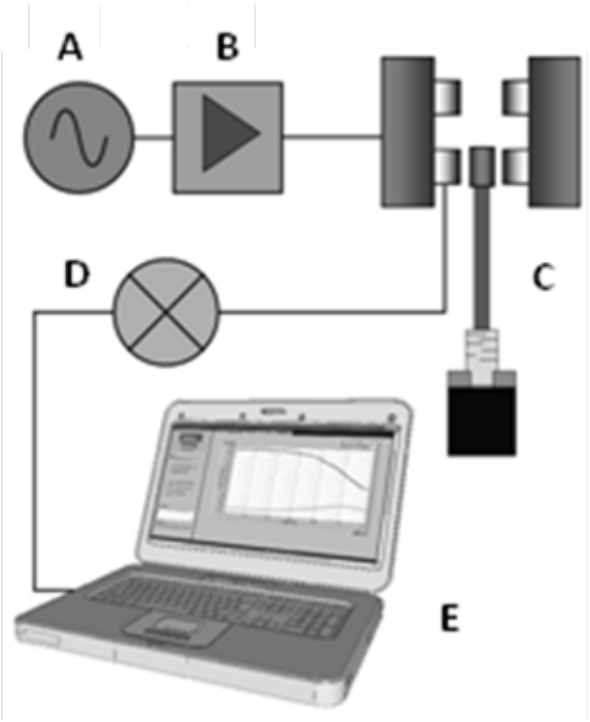

High frequency AC susceptometer built at the IMEGO company (Sweden)
AC signal source (A), current amplifier (B), coil system and mechanics (C), lock-in amplifier (D) and user interface software (E)

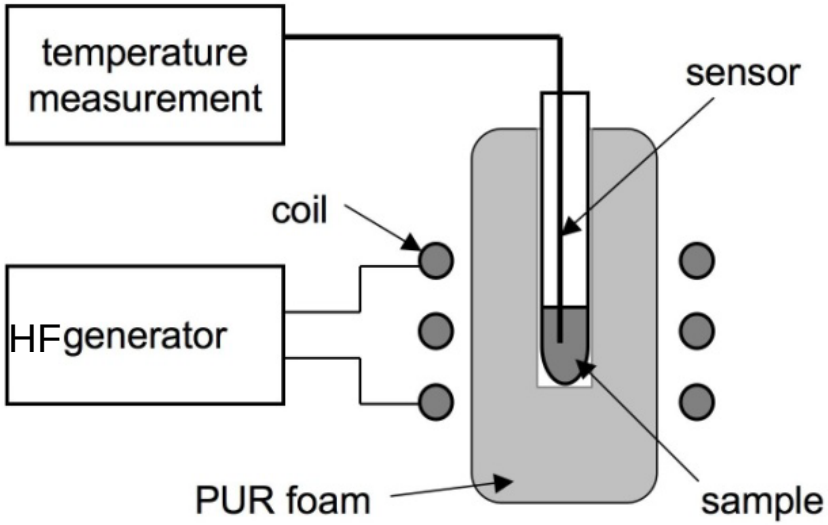

Hyperthermia set-up built by R. Müller, Jena (Germany)

$$SHP = \pi \mu_0 \chi'' f_{RF} H_0^2 V_S$$

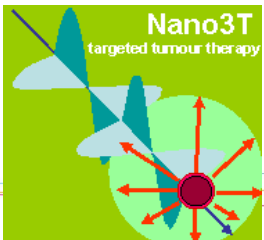

Role of the sizes' (mono)dispersity on the SHP effect

G. Glöckl, R. Hergt, J. Phys.: Condens. Matter 18 (2006) S2935–S2949: resonance effect

5,3nm / 0,19	6,8nm / 0,20	8,0nm / 0,21	10,2nm / 0,28	≈ 20nm / 0,3

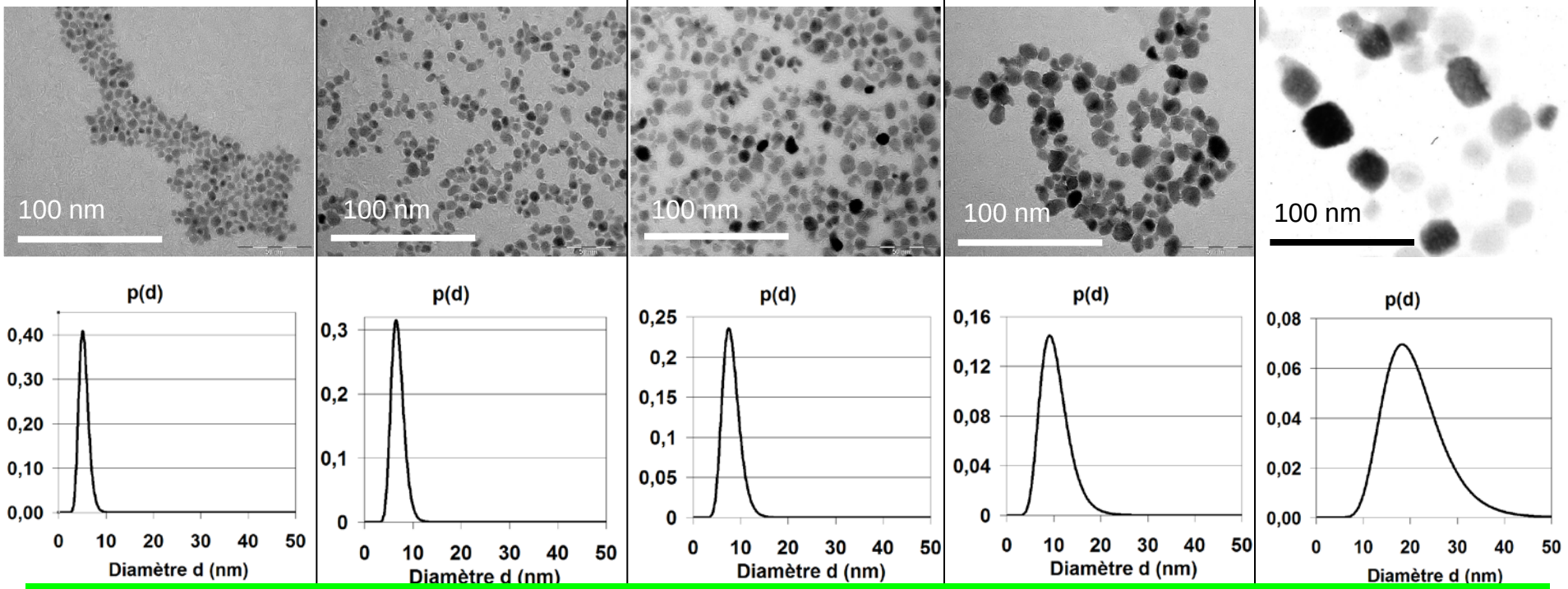

SHP (at f =700 kHz, H_0=24.8 kAm^{-1}) =

4 W/g 14 W/g 37 W/g 275 W/g 1650 W/g

J-P. Fortin, C. Wihelm, J. Servais, C. Ménager, J-C. Bacri, F. Gazeau, J. Am. Chem. Soc. 129 2628 (2007)

M. Lévy, C. Wilhelm, J-M. Siaugue, O. Horner, J-C. Bacri, F. Gazeau, J. Phys. Cond. Mat. 20 204133 (2008)

Calibration sample: monodisperse Fe_3O_4 nano-spheres

Astalan, A.; Ahrentorp, F.; Jonasson, C.; Blomgren, J.; Yan, M.; Courtois, J.; Berret, J.-F.; Fresnais, J.; Sandre, O.; Müller, R.; Dutz, S.; Johansson, C., AIP Conf. Proc. Series 2010

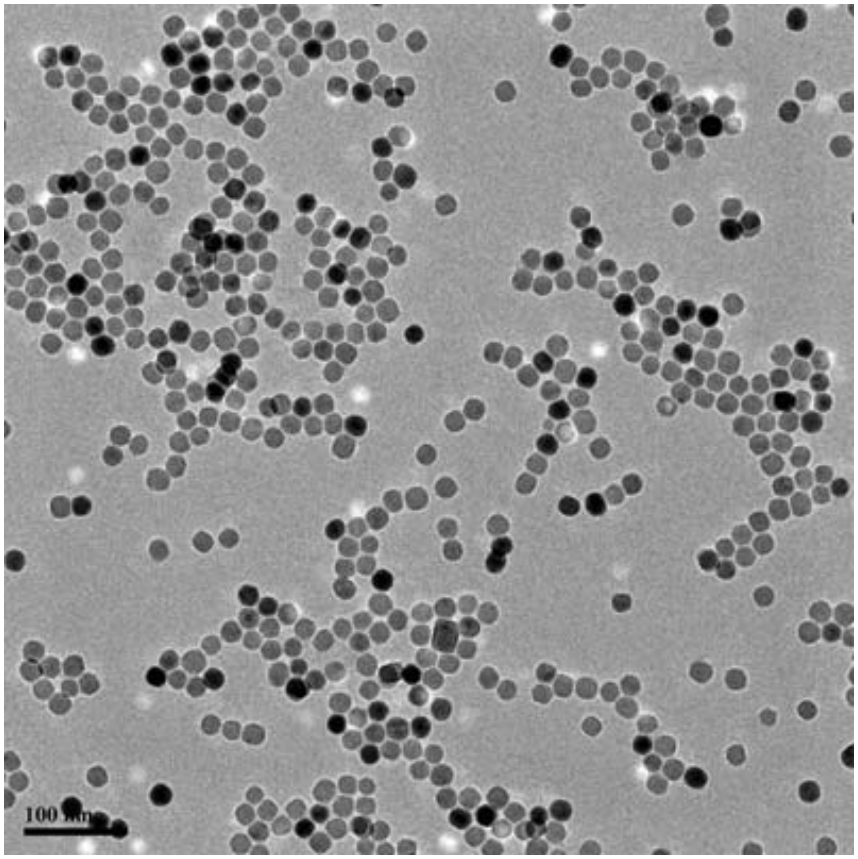

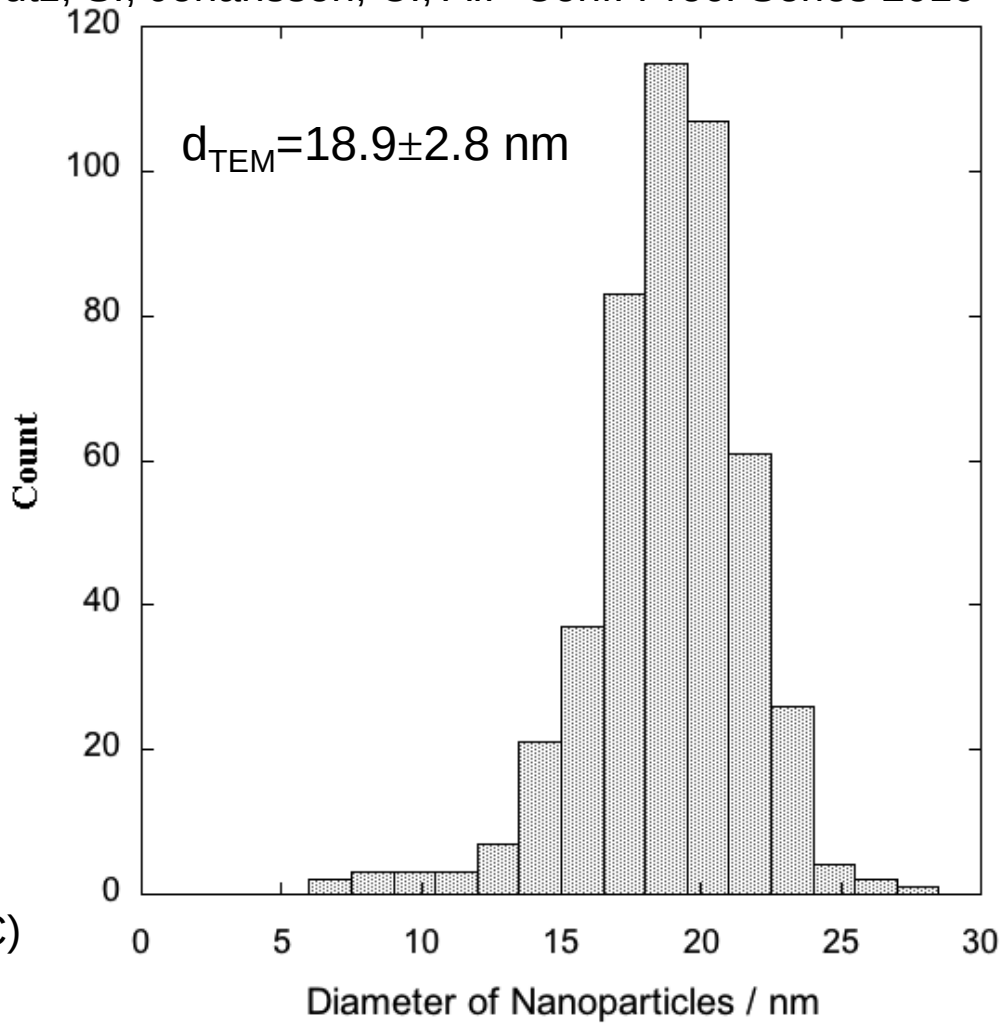

Fe-oleate decomposition in n-hexane (4h 70°C)
Q. Bin, O. T. Mefford (Clemson Univ, USA)
according to Park et al, Angew. Ch. 2005)

Role of MNP shape on the magnetic anisotropy K_a

Astalan, A.; Ahrentorp, F.; Jonasson, C.; Blomgren, J.; Yan, M.; Courtois, J.; Berret, J.-F.; Fresnais, J.; Sandre, O.; Müller, R.; Dutz, S.; Johansson, C., AIP Conf. Proc. Series 2010

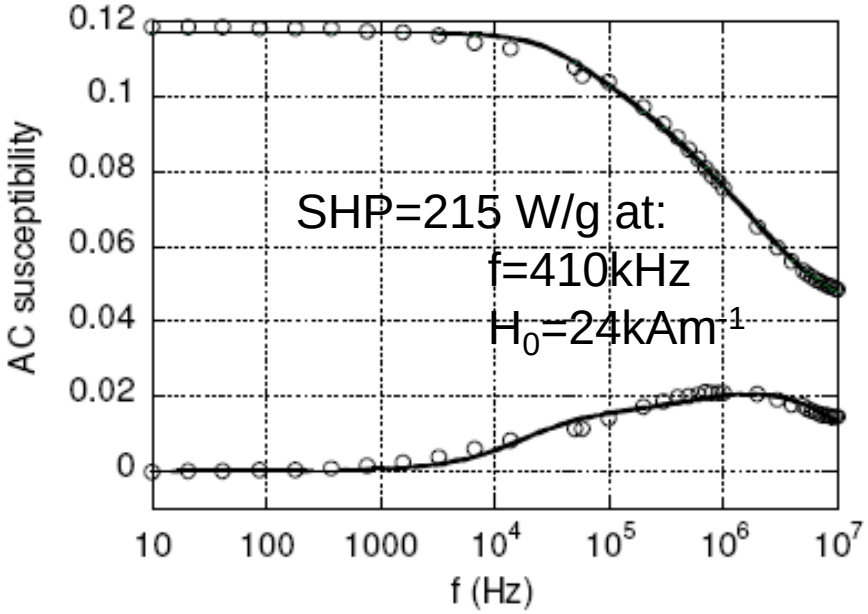

rock-like particles Ø16nm :
large χ'', Néel's band ~ 2MHz

$$\chi(\omega) = C \int \frac{r_C^6}{\left(1 + j\omega\tau_{eff}(r_H)\right)} f(r_H) dr_H + \chi_{high}$$

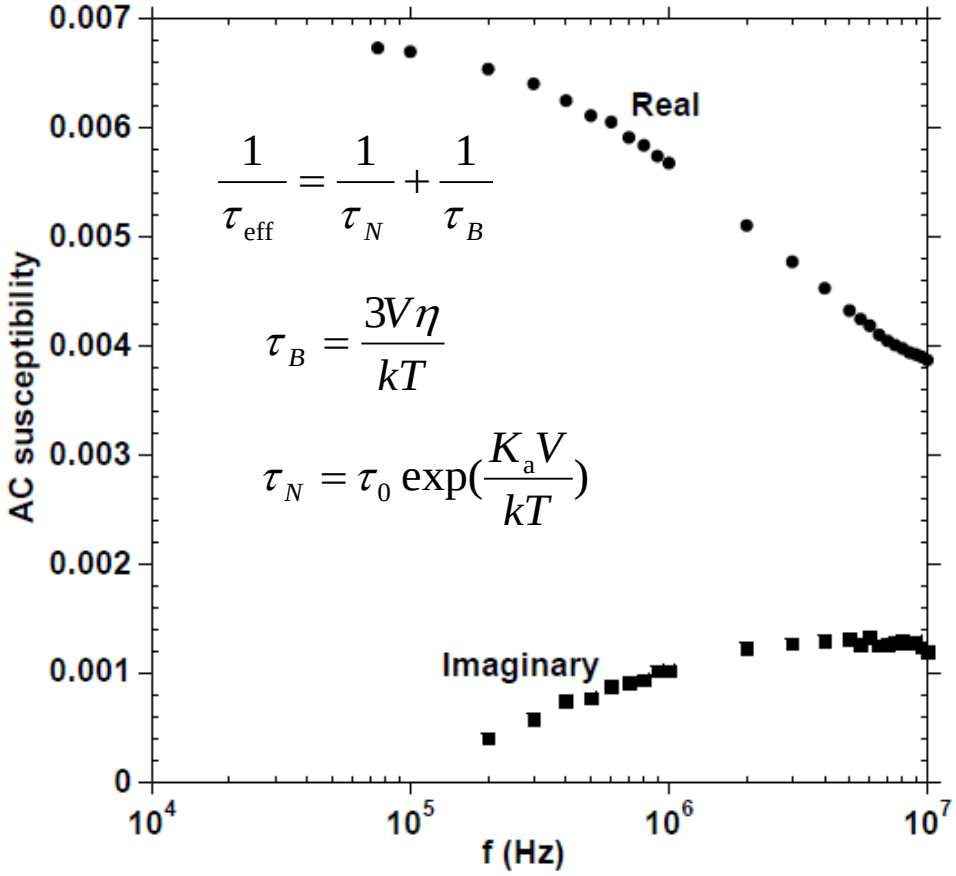

spheres Ø19nm: weak χ'', Néel's band ~ 5MHz

Improved properties of the larger magnetic NPs

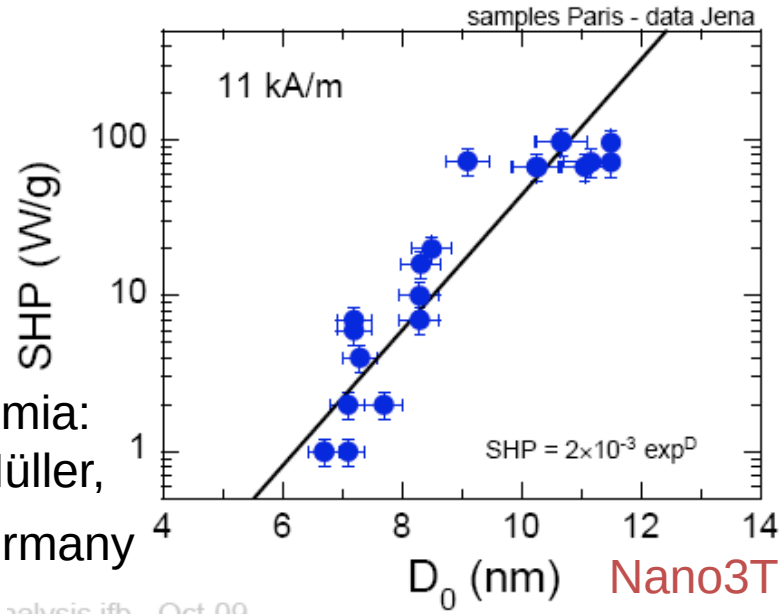

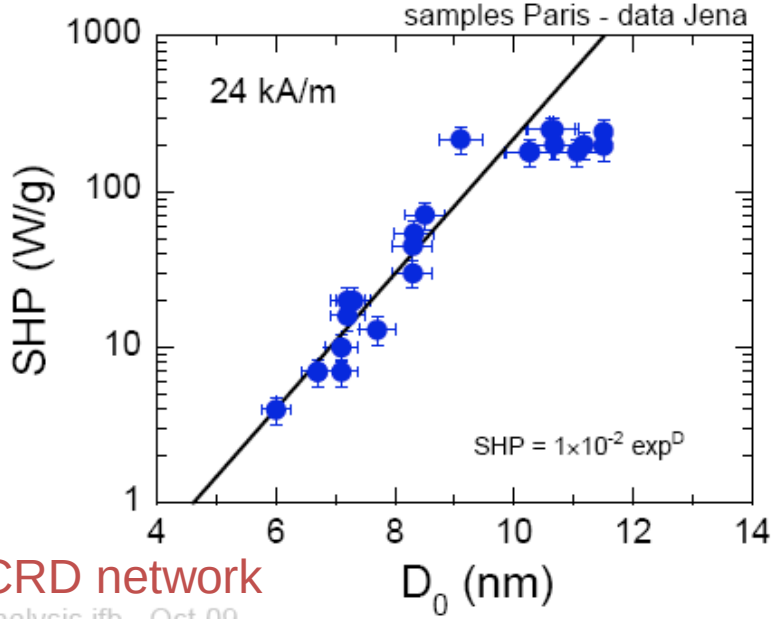

Hypethermia:
Robert Müller,
Jena, Germany

Nano3T 7th PCRD network

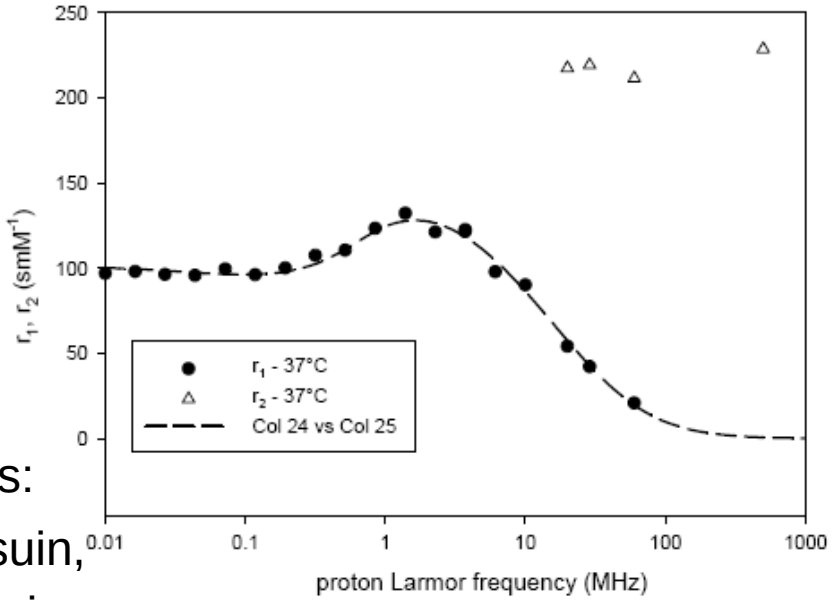

C1C2C3C4S5-PAA5K

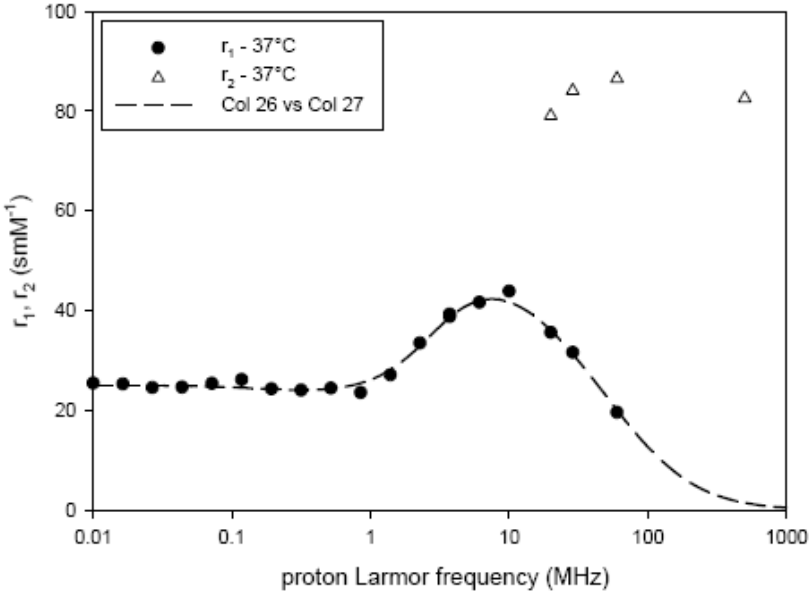

S2C14

Relaxivities:
Yves Gossuin,
Mons, Belgium

Ionic Ferrofluids: the coprecipitation synthesis

- Massart's process:

Alkaline coprecipitation of $FeCl_2$ & $FeCl_3$
→ magnetite Fe_3O_4 nanoparticles

$$Fe^{2+}_{(aq)} + 2Fe^{3+}_{(aq)} + 8OH^-_{(aq)} \rightarrow Fe_3O_{4(s)} + 4H_2O_{(l)}$$

R. Massart *IEEE Trans. Magn.* **17** 1247 (1981)

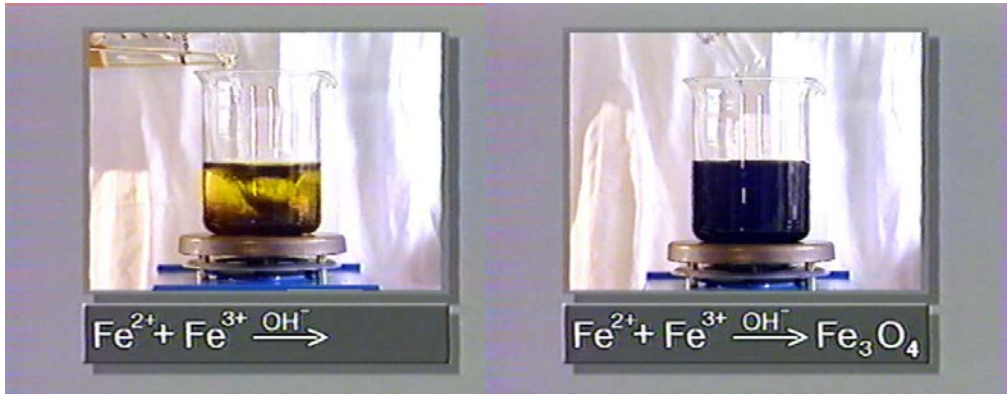

Oxidation by $Fe(NO_3)_3$
→ maghemite γ-Fe_2O_3 nanoparticles
in acidic medium (HNO3): stabilized by electrostatic surface charges (PZC≈7)

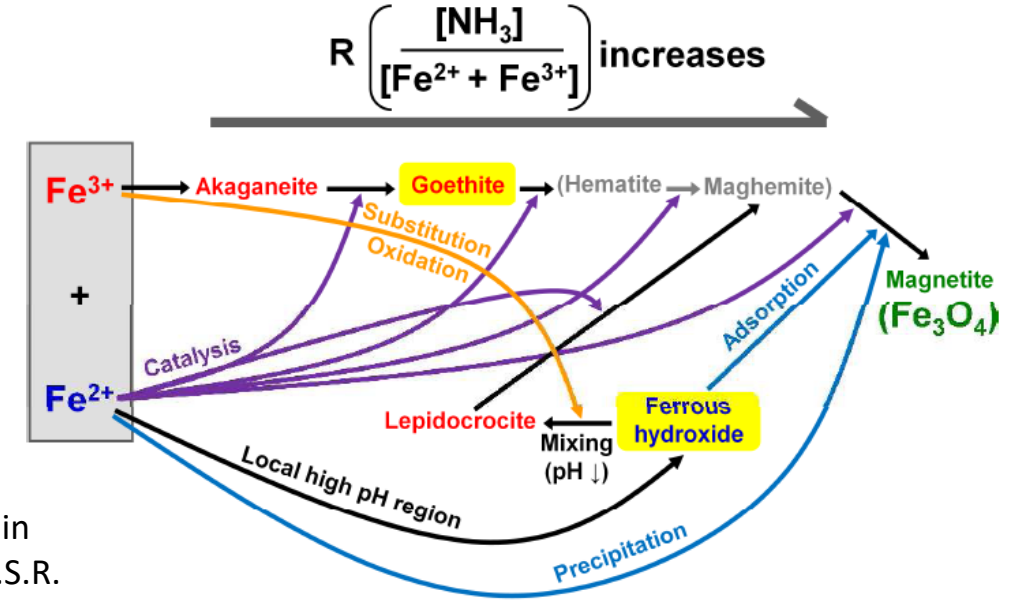

A. Abou-Hassan, O. Sandre, and V. Cabuil, *Chapter 9: Microfluidics for the synthesis of iron oxide nanoparticles*, in Microfluidic Devices in Nanotechnology: Applications, C.S.S.R. Kumar, Editor. **2010**, John Wiley & Sons, Inc: Hoboken, NJ, USA. p. 323-360

T. Ahm at al. *J. Phys. Chem.* (2012) pre-print

Microfluidics as a tool to get an insight of the kinetics of the coprecipitation reaction

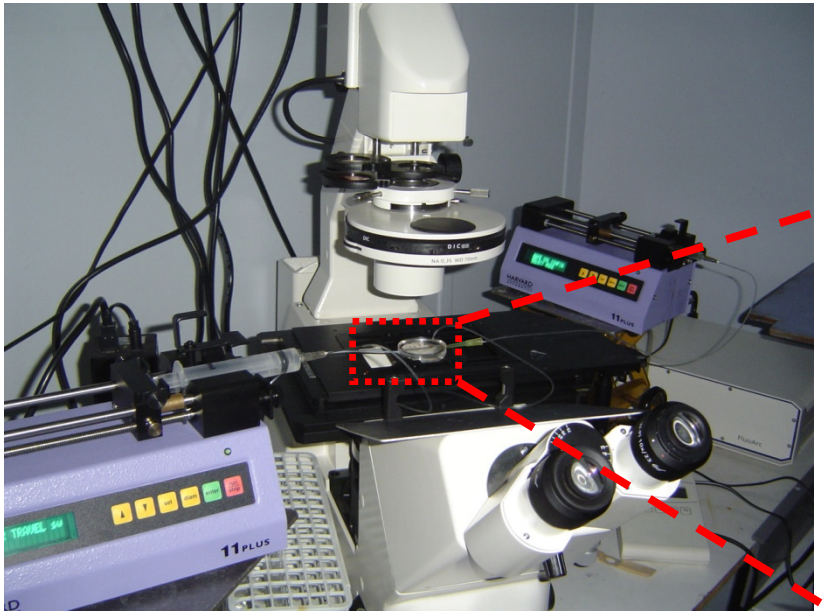

Answer to clogging issue: 3D geometry and non flocculating counterion of base TMA⁺

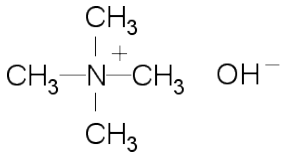

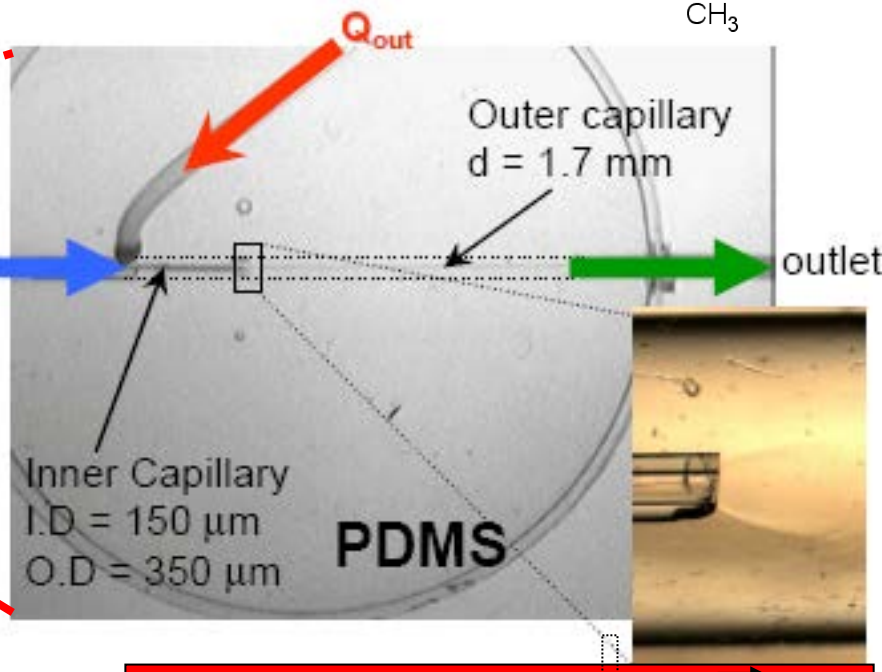

PhD thesis Ali Abou Hassan (2 oct 2009)

A. Abou Hassan, O. Sandre, V. Cabuil, P. Tabeling, *Chem. Commun.* 2008, 1783

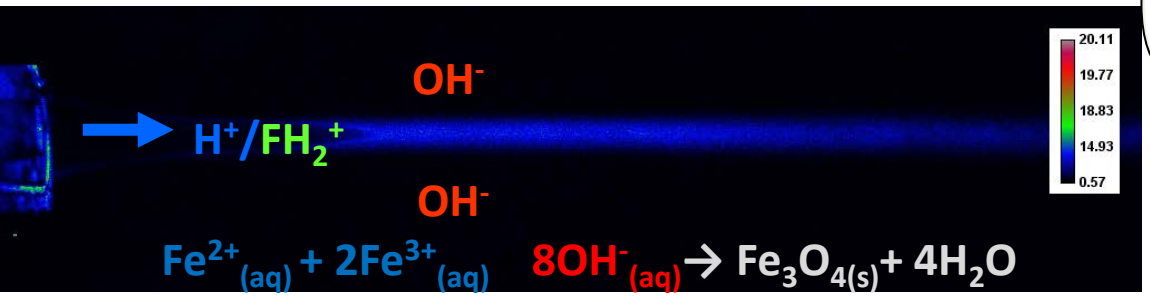

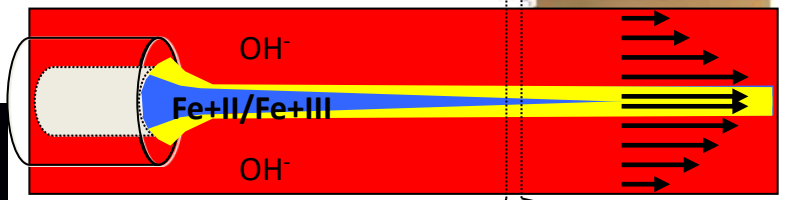

Nanoparticles at the interface

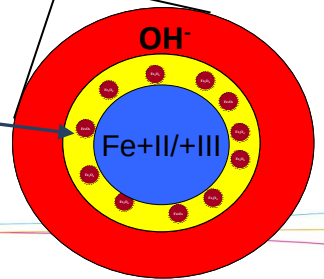

Microfluidics as a tool to get an insight of the mechanism of goethite formation

Two micro-reactors in-line

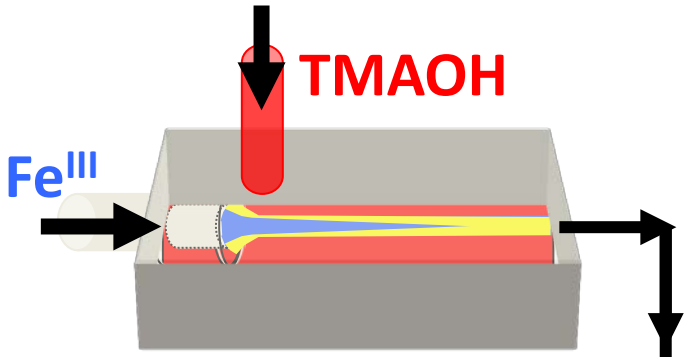

µR1: nucleation (seeds)

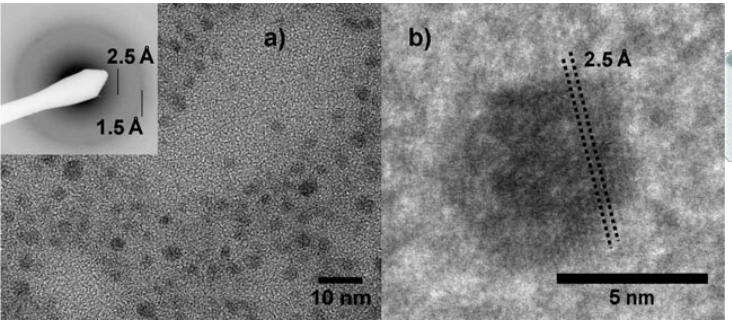

“2-lines ferrihydrite” nanodots ∅ = 4±1 nm

µR2: growth T=60°C

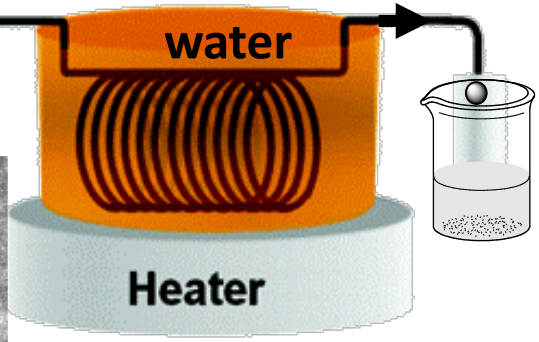

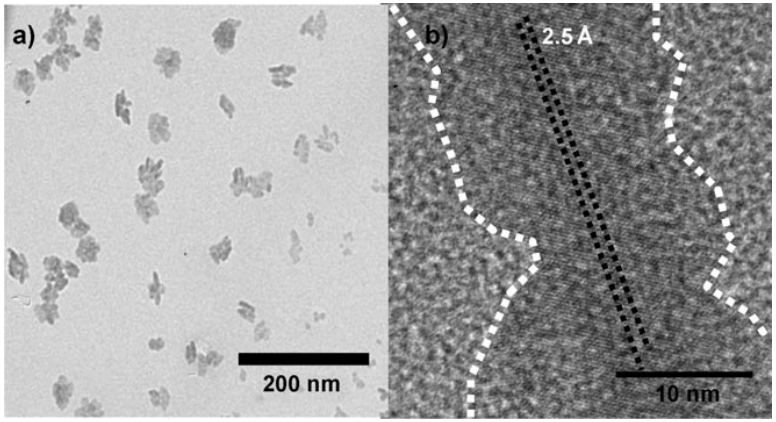

15 min / 60°C: Goethite nanorods

L=30±17 nm and w=7±4 nm

Final state as in macro synthesis

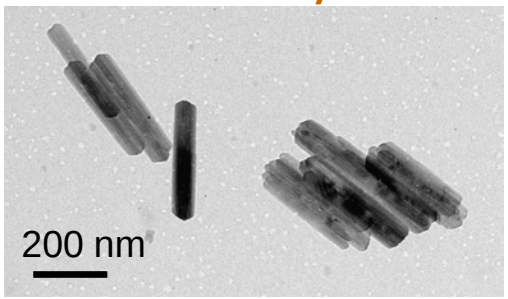

→ check “oriented aggregation” mechanism

J. F. Banfield et al. *Science* 2000, 289, 751

A. Abou-Hassan, O. Sandre, S. Neveu, V. Cabuil, *Angew. Ch.* **48** 1-5 (2009)

Microfluidics as a tool to get an insight of the mechanism of goethite formation

- **FEM lab simulations**

$$\frac{\partial C_i}{\partial t} + \mathrm{div}(C_i \mathbf{u} + \mathbf{j}_i) = \sigma_i$$

$$\mathbf{j}_i = -D_i \,\mathrm{grad} C_i + \frac{D_i}{k_B T} C_i Z_i e \mathbf{E}$$

(Nernst-Planck)

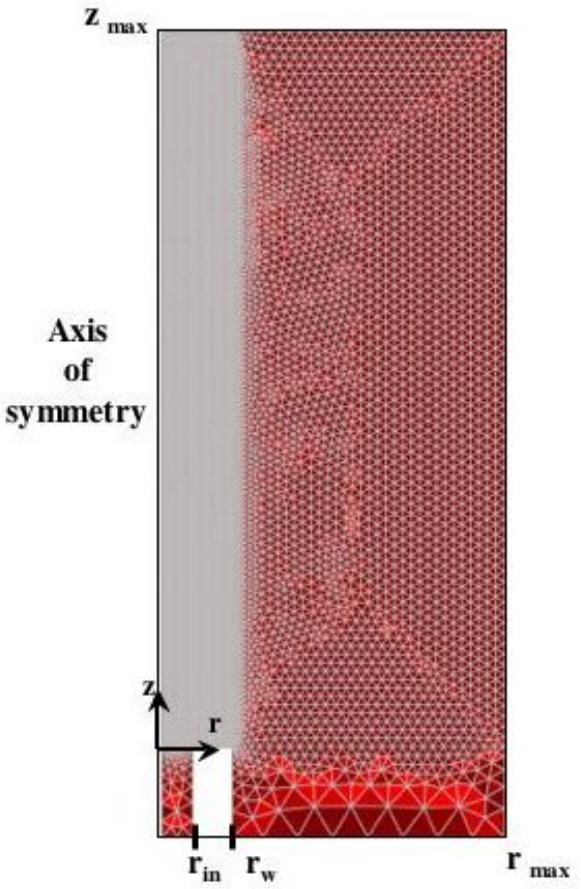

- **Confocal Laser Scanning Microscopy: Fluorescein as pH reporter dye**

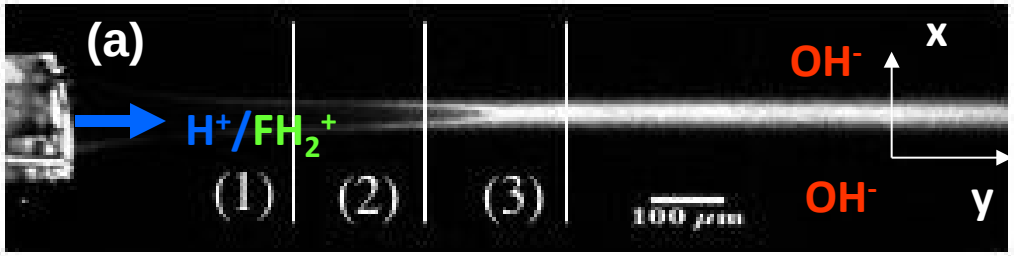

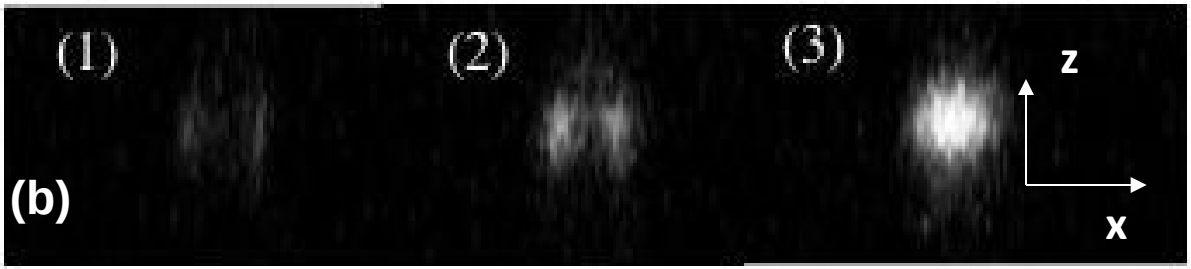

pH = f(α) with α = Q_{OH^-} / Q_{H^+}

A. Abou-Hassan, J-F. Dufrêche, O. Sandre, G. Mériguet, O. Bernard, V. Cabuil, *J. Chem. Phys.* C 2009

Microfluidics as a tool to get an insight of the mechanism of goethite formation

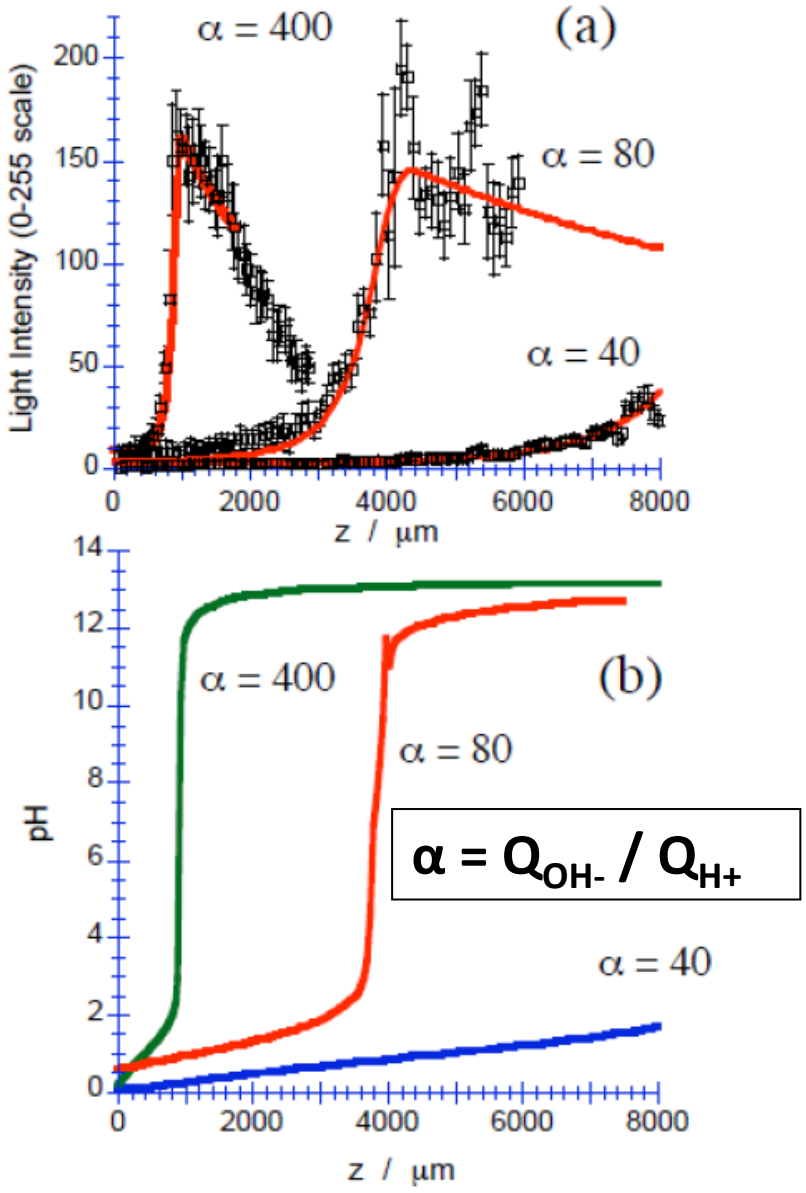

$\alpha = Q_{OH^-} / Q_{H^+}$

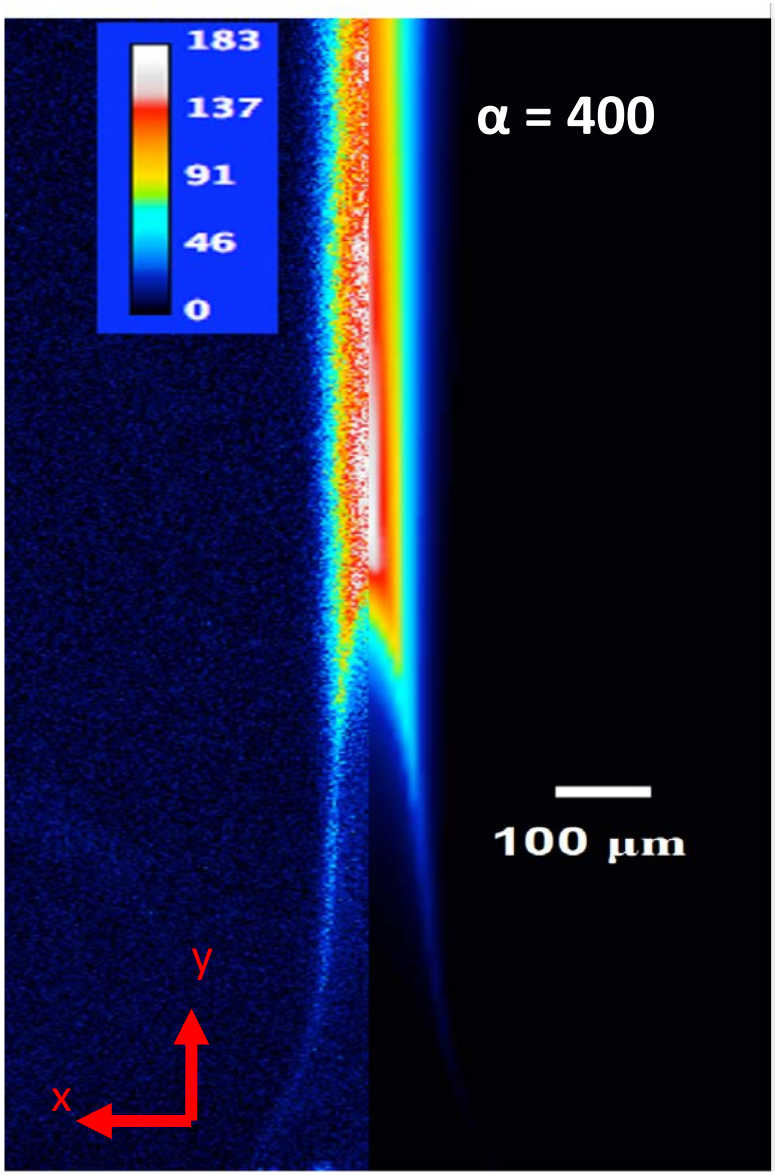

Detection of first seeds using SAXS in microfluidics

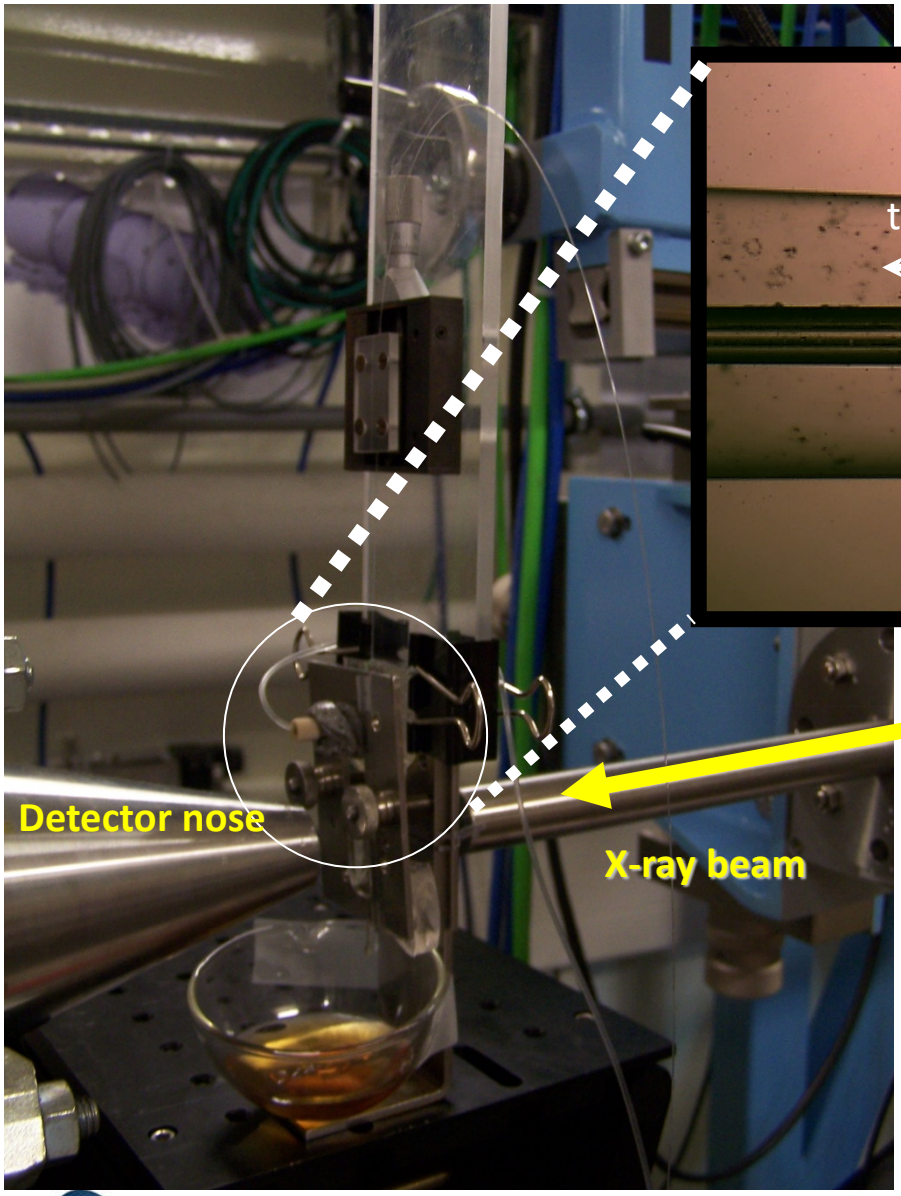

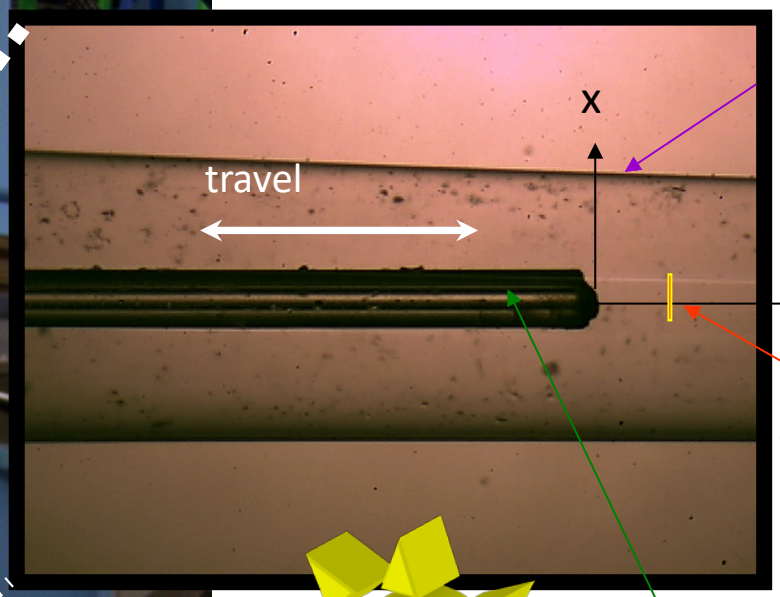

Lindemann glass capillary
∅ = 1,6 mm
(wall thickness = 10 µm)

beam 300 x 100 µm cross-section at fixed position

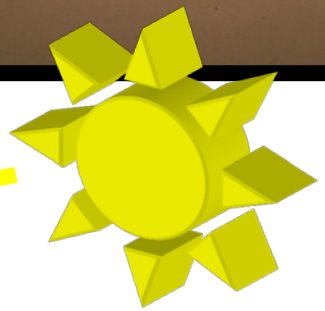

Internal capillary
$\varnothing_{int}$ = 100 µm
$\varnothing_{ext}$ = 350 µm

SAXS measurements on SWING line at SOLEIL synchrotron (July 2009)

Abou Hassan, O. Sandre,
V. Dupuis, Olivier Spalla

Detection of first seeds using SAXS in microfluidics

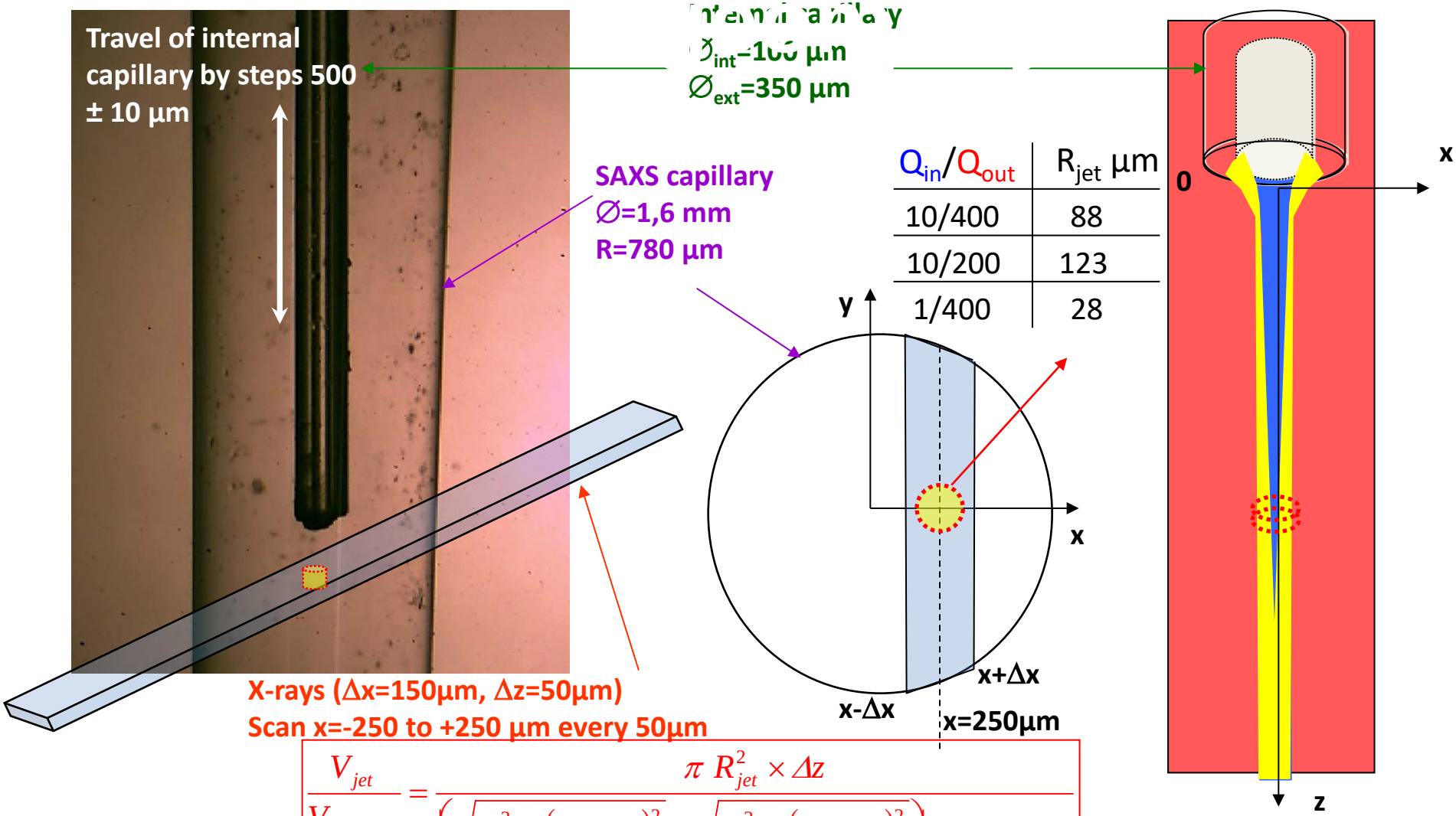

$$\frac{V_{jet}}{V_{diffusant}} = \frac{\pi R_{jet}^2 \times \Delta z}{\left(\sqrt{R^2-(x-\Delta x)^2}+\sqrt{R^2-(x+\Delta x)^2}\right)\times 2\Delta x \times \Delta z}$$

Preliminary SAXS results: intensity curves along z

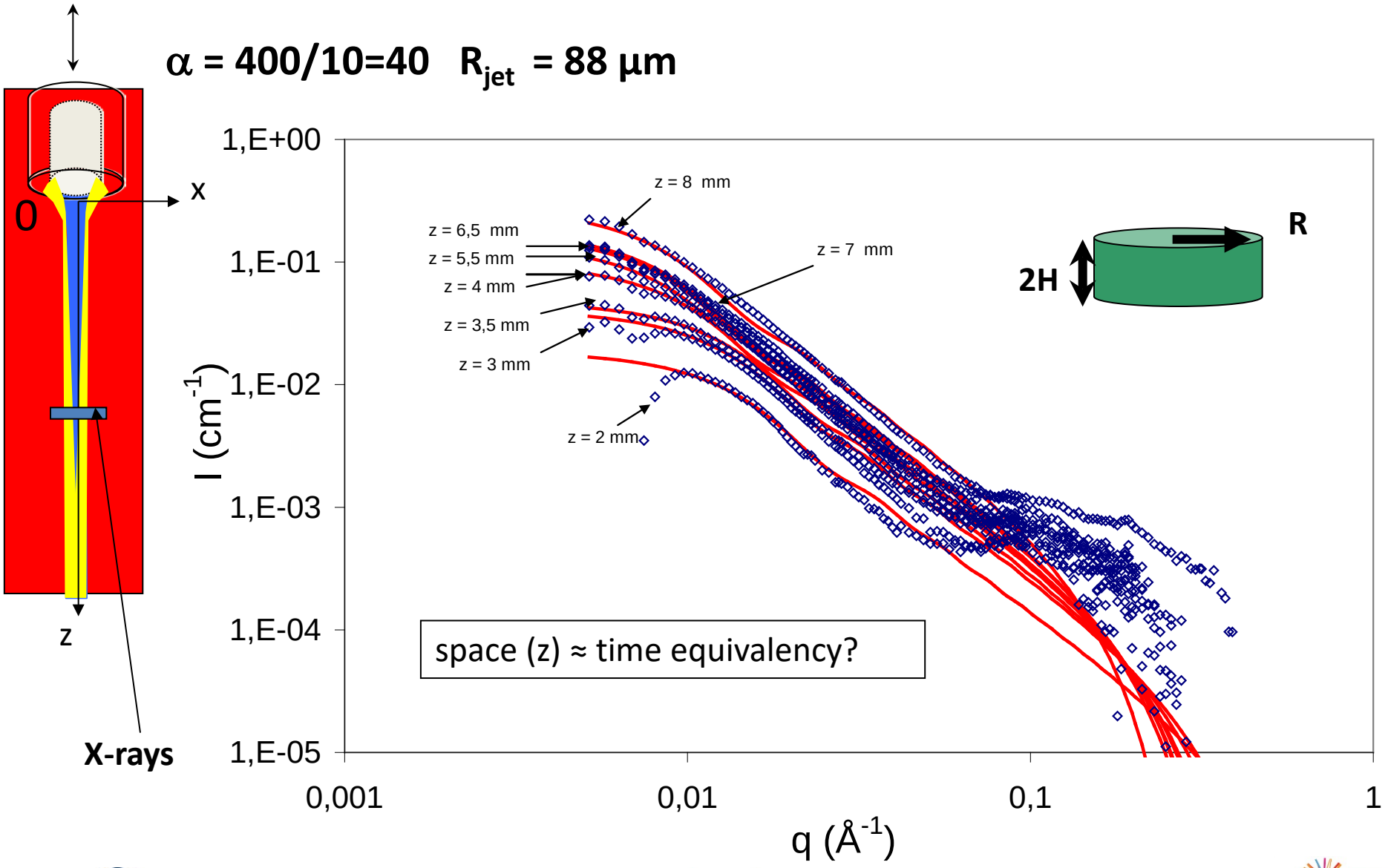

Preliminary SAXS results: fits as disk form factor

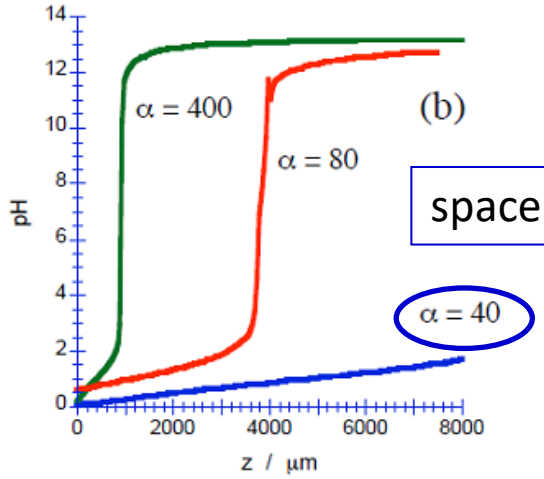

space (z) ≈ pH equivalency

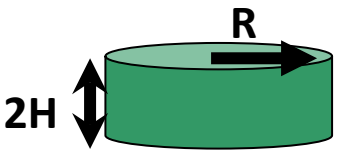

Anisotropy R/H ↘

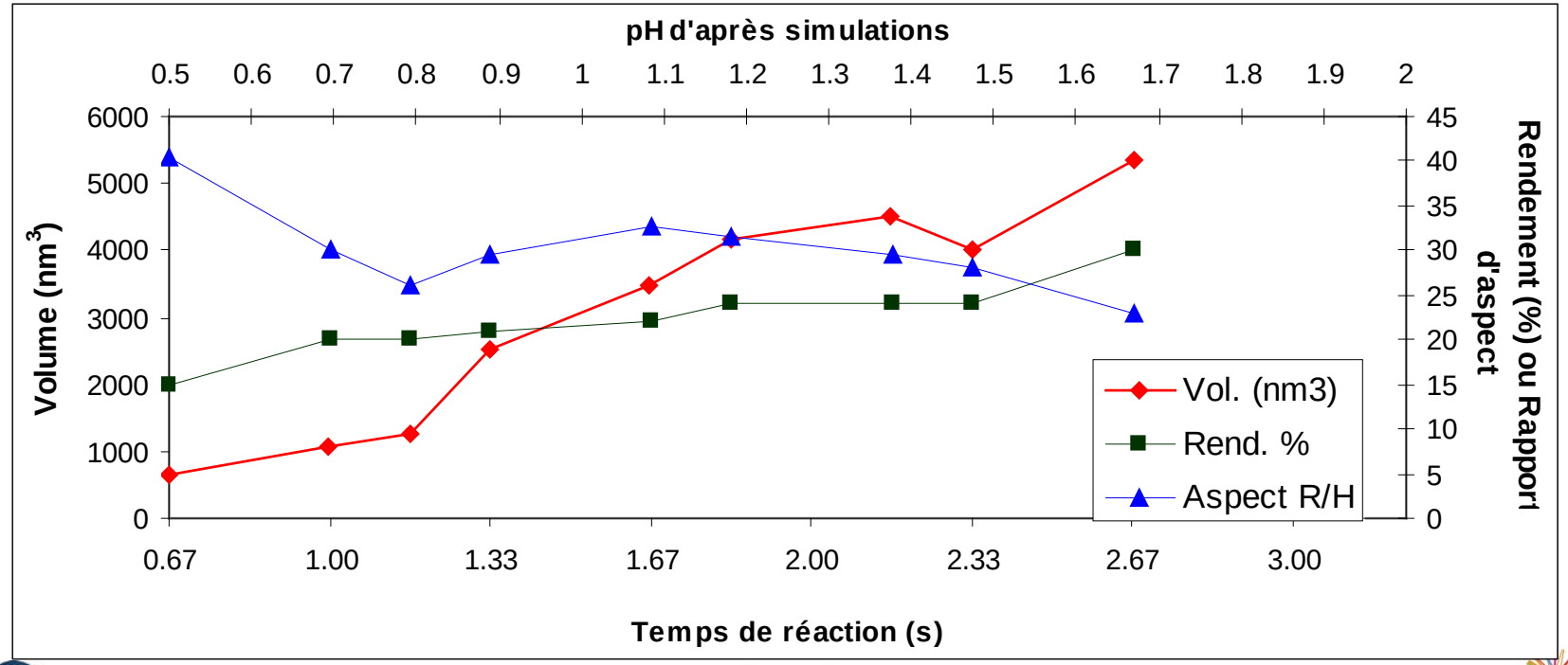

Preliminary SAXS results: fits as disk form factor

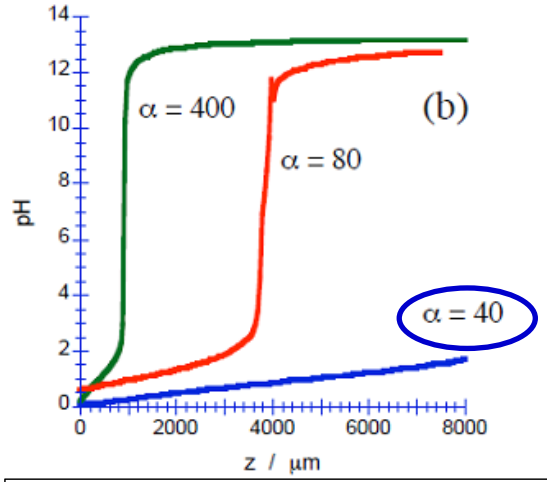

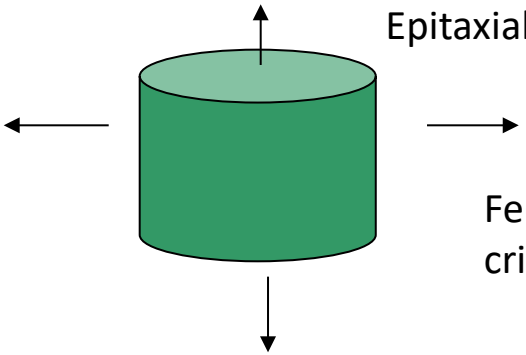

Epitaxial growth rate ≈ 9Å/s

$Fe(OH)_3$ as fractal gel or cristallyne structure Bernalite

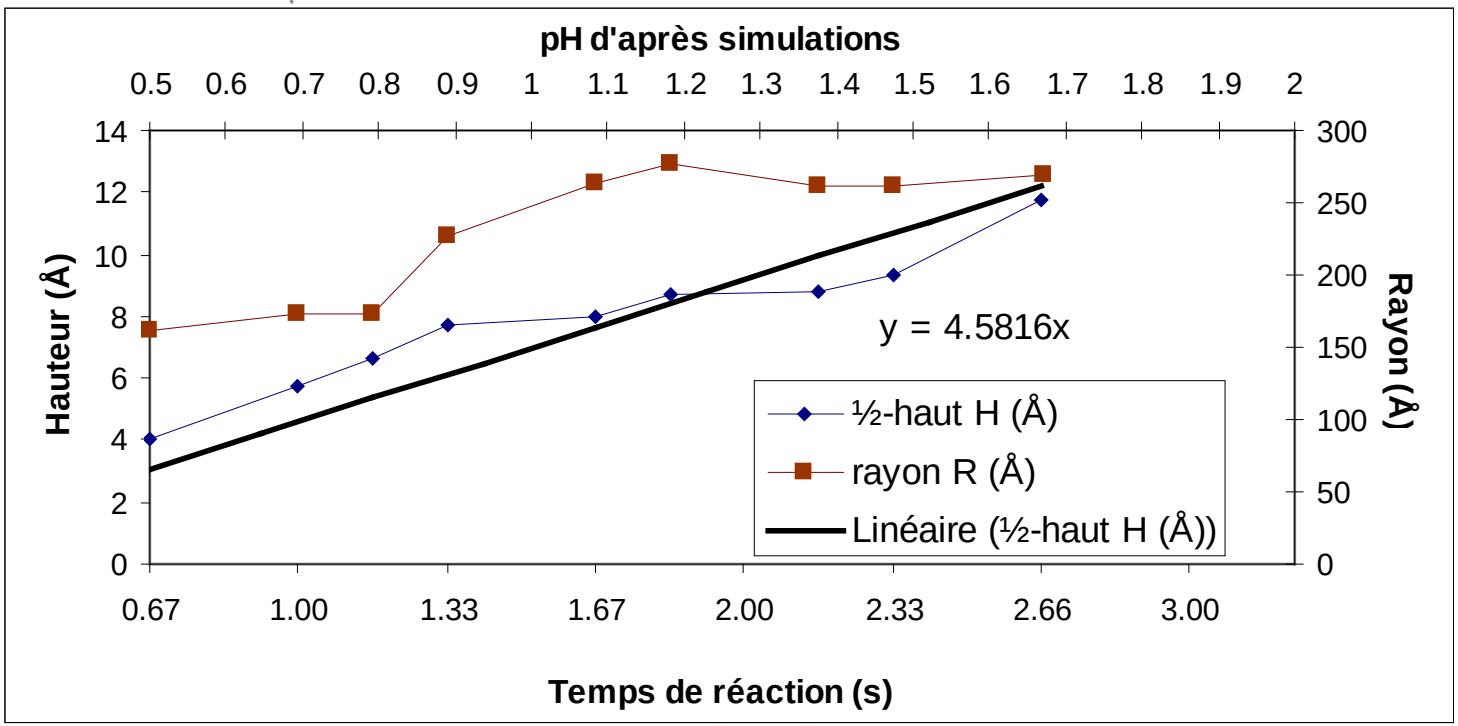

Coatings of iron oxide and oxo-hydroxide NPs for their dispersion in various media

Different coatings to insure colloidal stability :

- surfactants (oleic acid, phosporic di-ester ,…) for organic solvents (alkanes, chlorinated,…)

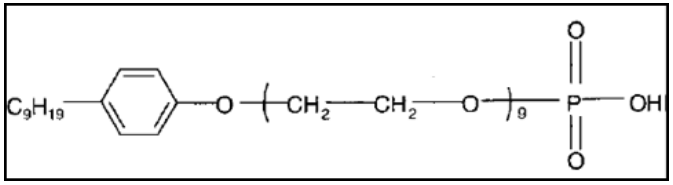

- sodium citrate in aqueous neutral medium (pH=7.2) or sodium polyacrylate (2000 or 5000 g/moL)

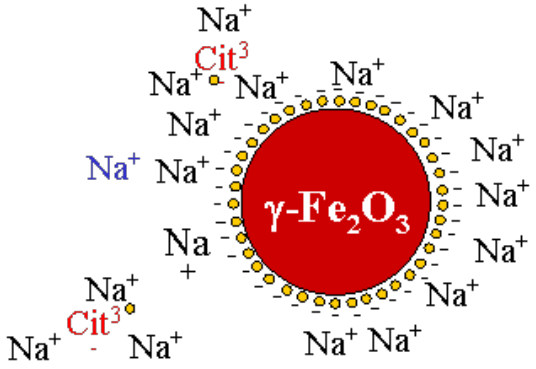

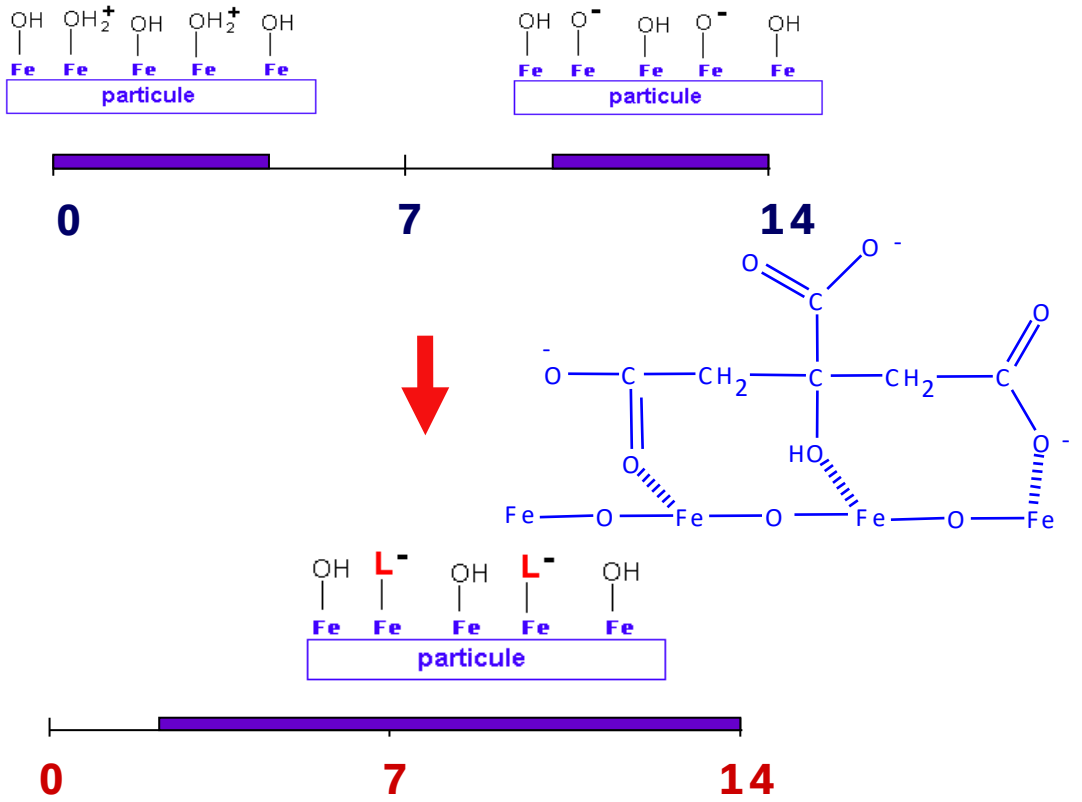

20 mol%/Fe addition precipitation-redispersion

J. A. Galicia, O. Sandre, F. Cousin, D. Guemghar, C. Ménager, V. Cabuil, *J. Phys.-Cond. Mat.* **2003**. 15 S1379.

Ionic Ferrofluids: demixtion & size sorting

- Size Polydispersity: P(d, nm)

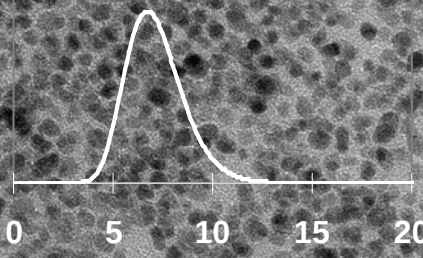

- Fractionated separations

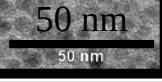

R. Massart, E. Dubois, V. Cabuil, E. Hasmonay, J. Magn. Magn. Mater. 149 1 (1995)

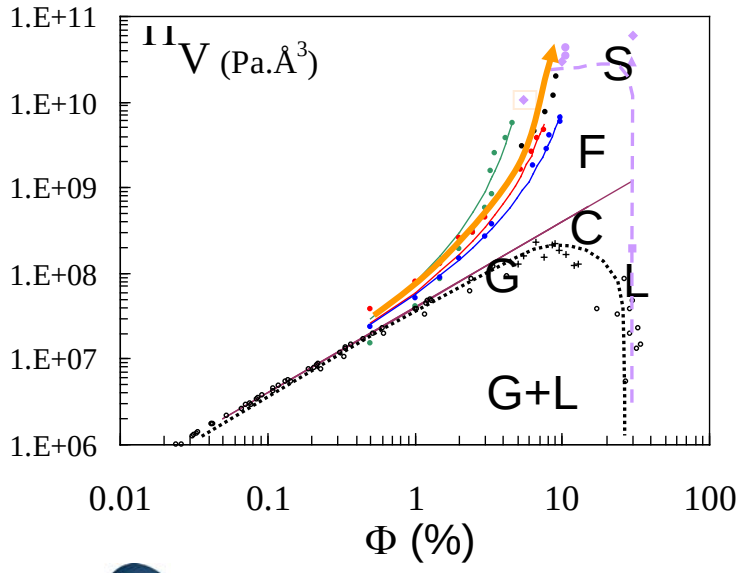

835mL ferrofluide acide DE1,
Φ=2.5% d_0=7nm σ=0.39

HNO3 en excès

C1
250mL Φ=6.4%
d_0=8.6nm σ=0.35

S1

HNO_3

HNO_3

C1C

C1S
200mL Φ=3.5%
d_0=7.6nm σ=0.30

S1C
65mL Φ=4.2%
d_0=7.4nm σ=0.25

S1S-HNO3
85mL Φ=1.8%
d_0=6.6nm σ=0.21

1) Na_3Cit 2) dialyse

S1S-Na3Cit
20mL Φ=3.2%
d_0=6.6nm σ=0.21
$[Na_3Cit]$ =1.4x10^{-2} M

HNO_3

C2
140mL Φ=2.8%
d_0=8.5nm σ=0.29

S2-HNO3
160mL Φ=1.2%
d_0=7.1nm σ=0.26

S2-CH_2Cl_2
25mL Φ=1.2%
d_0=6.8nm σ=0.24

Size-sorted "ionic ferrofluid" as elementary bricks

USPIO fraction	Given name in this work	D_H of bare MNPs in HNO_3 nm / PDI	Average diameters by TEM	Average diameters by VSM	Saturation magnetization emu/g A/m	r_2 (4.7T) $s^{-1}mM^{-1}_{Fe}$	SLP at f=800 kHz, H_0=11 kA/m W/g
S1S2S3	6-7 nm	11 / 0.12	d_n=4.9 nm, d_w=6.9 nm (N=600)	d_n=6.5 nm, d_w=7.5 nm	55±1 2.8×10^5	70	2±1

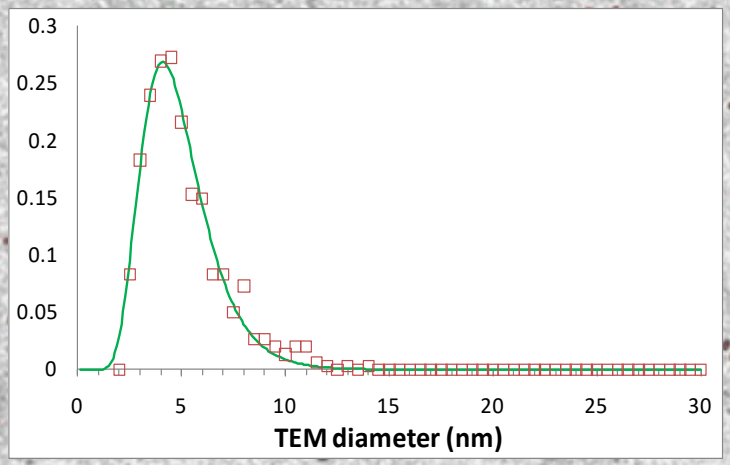

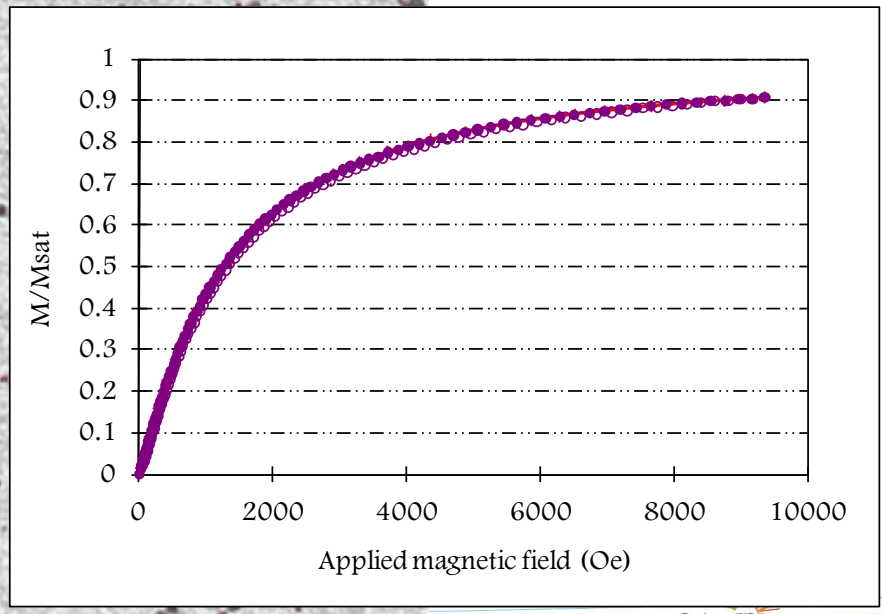

Size-sorted "ionic ferrofluid" as elementary bricks

USPIO fraction	Given name in this work	D_H of bare MNPs in HNO_3 nm / PDI	Average diameters by TEM	Average diameters by VSM	Saturation magnetization emu/g A/m	r_2 (4.7T) $s^{-1}mM^{-1}_{Fe}$	SLP at f=800 kHz, H_0=11 kA/m W/g
S1S2S3	6-7 nm	11 / 0.12	d_n=4.9 nm, d_w=6.9 nm (N=600)	d_n=6.5 nm, d_w=7.5 nm	55±1 2.8×10^5	70	2±1
S1C2	8-10 nm	23 / 0.16	d_n=8.5 nm, d_w=11.6 nm (N=3800)	d_n=8.2 nm, d_w=10.0 nm	60 3.0×10^5	104	9±1

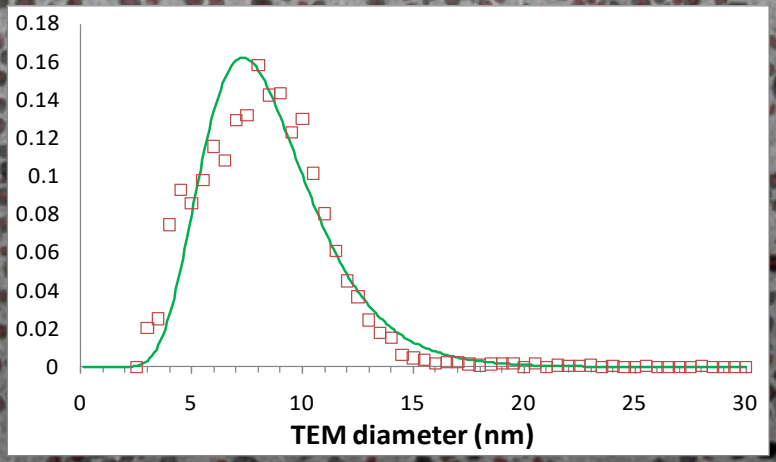

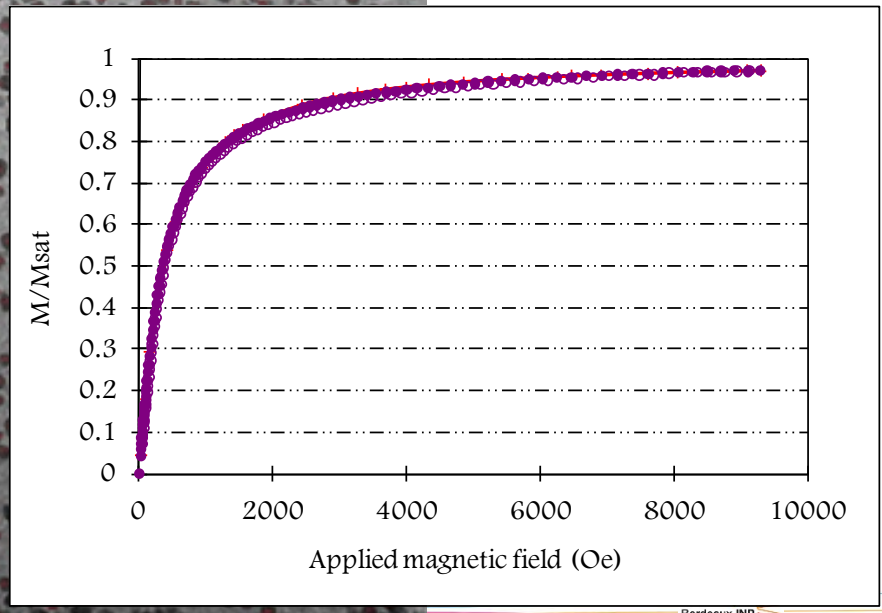

Size-sorted "ionic ferrofluid" as elementary bricks

USPIO fraction	Given name in this work	D_H of bare MNPs in HNO_3 nm / PDI	Average diameters by TEM	Average diameters by VSM	Saturation magnetization emu/g A/m	r_2 (4.7T) $s^{-1}mM^{-1}_{Fe}$	SLP at f=800 kHz, H_0=11 kA/m W/g
S1S2S3	6-7 nm	11 / 0.12	d_n=4.9 nm, d_w=6.9 nm (N=600)	d_n=6.5 nm, d_w=7.5 nm	55±1 2.8×10^5	70	2±1
S1C2	8-10 nm	23 / 0.16	d_n=8.5 nm, d_w=11.6 nm (N=3800)	d_n=8.2 nm, d_w=10.0 nm	60 3.0×10^5	104	9±1
C1C2S3S4	10-15 nm	38 / 0.26	d_n=13.8 nm, d_w=20 nm (N=1140)	d_n=10.4 nm, d_w=14.8 nm	70±1 3.5×10^5	293	80±5

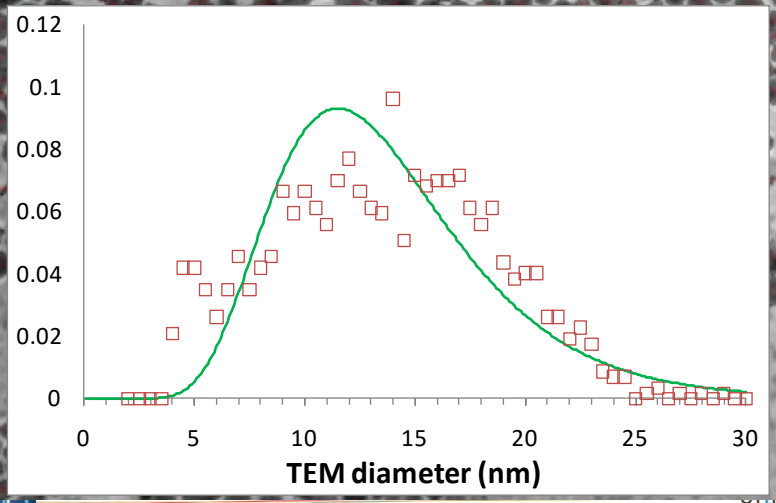

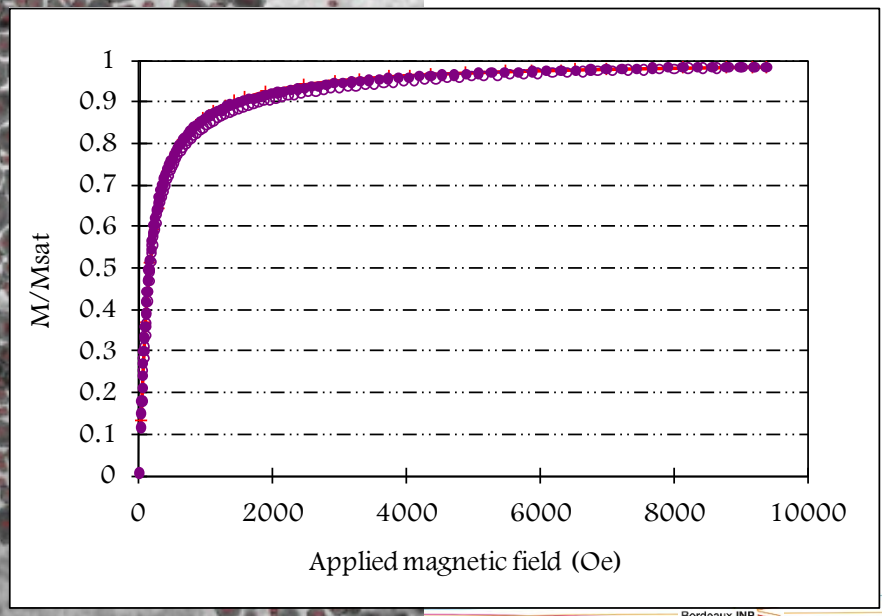

Magnetization curves along the size-grading process

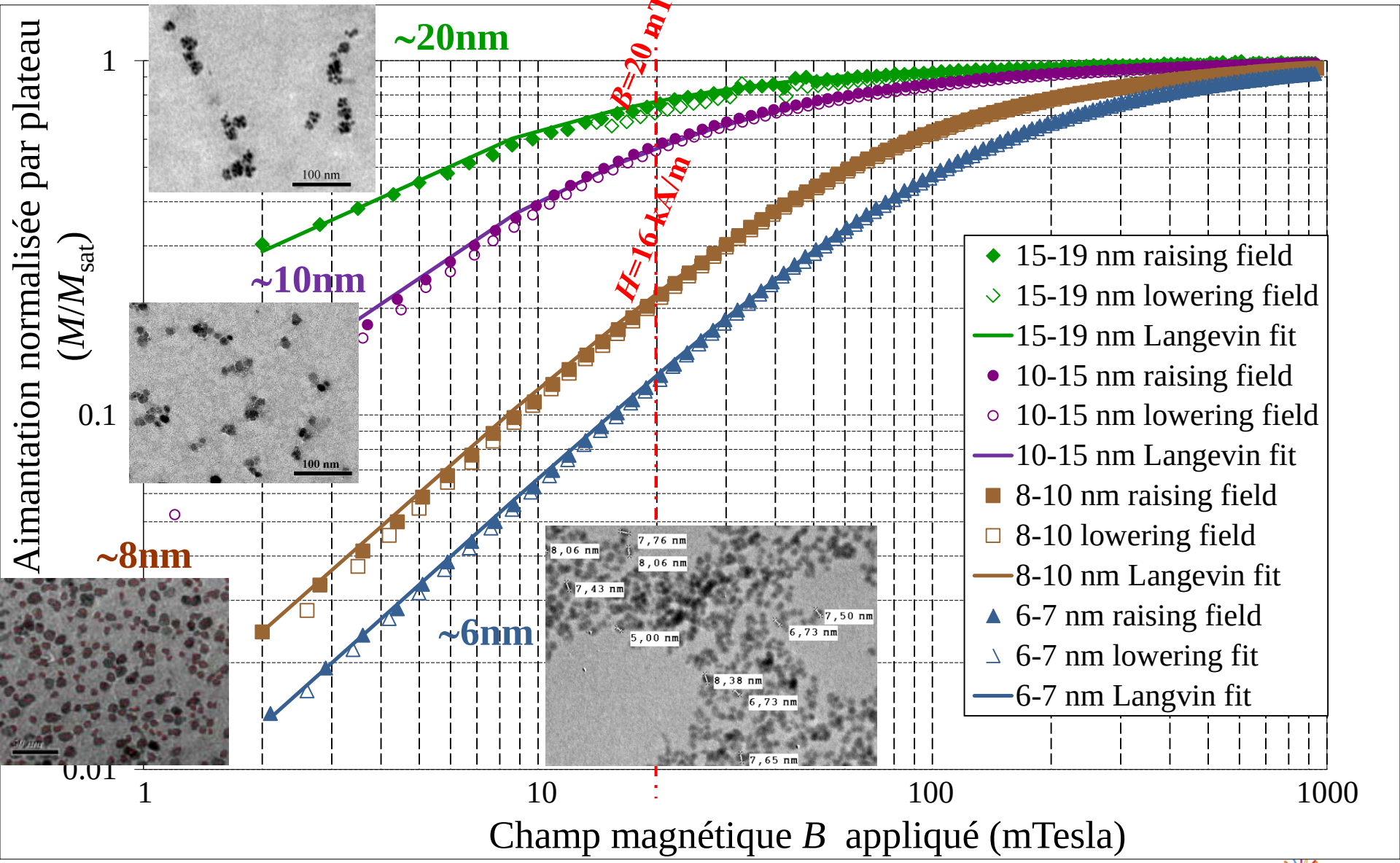

Larger nanoparticles for larger physical effects?

Obtained by multiple phase separation (C1C2C3C4)

$\langle d \rangle_{TEM}$ = 13.9 nm

$\langle d \rangle_{VSM}$ = 11.8 nm

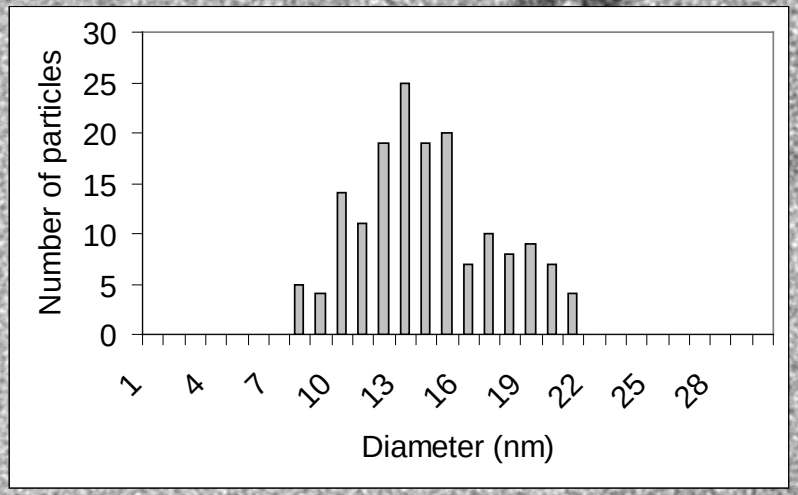

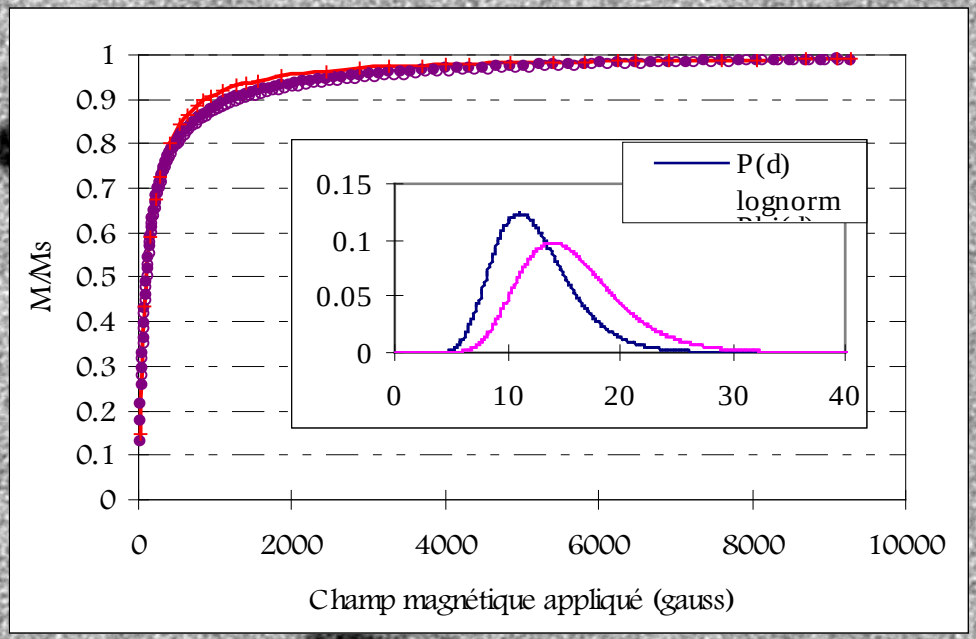

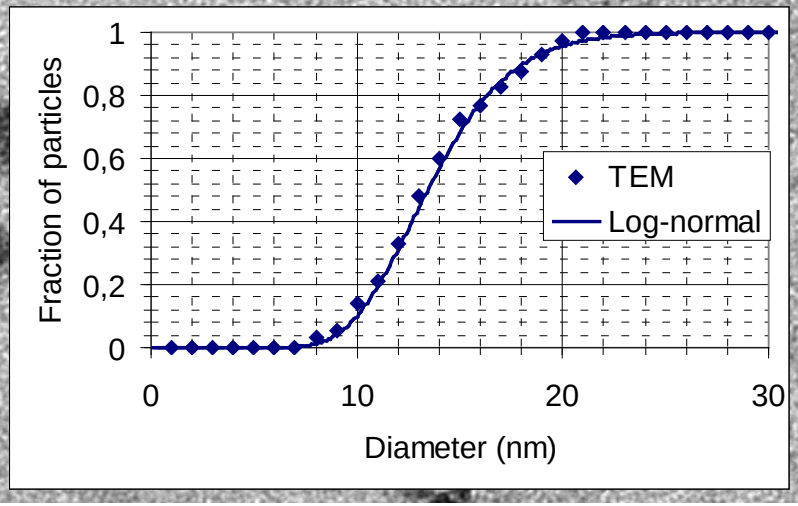

$d_w = \langle d^4 \rangle / \langle d^3 \rangle_{VSM \text{ or } TEM} \approx 16$ nm

100 nm

$\langle d^n \rangle = d_0^n \exp(n\sigma^2/2) \rightarrow d_w = \langle d^4 \rangle / \langle d^3 \rangle = d_0 \exp(3.5\sigma^2)$

Size-sorted fraction: C1C2S3S4

$\langle d \rangle_{TEM}$ = 13.3 nm

$d_w = \langle d^4 \rangle / \langle d^3 \rangle_{VSM}$ = 14.8 nm

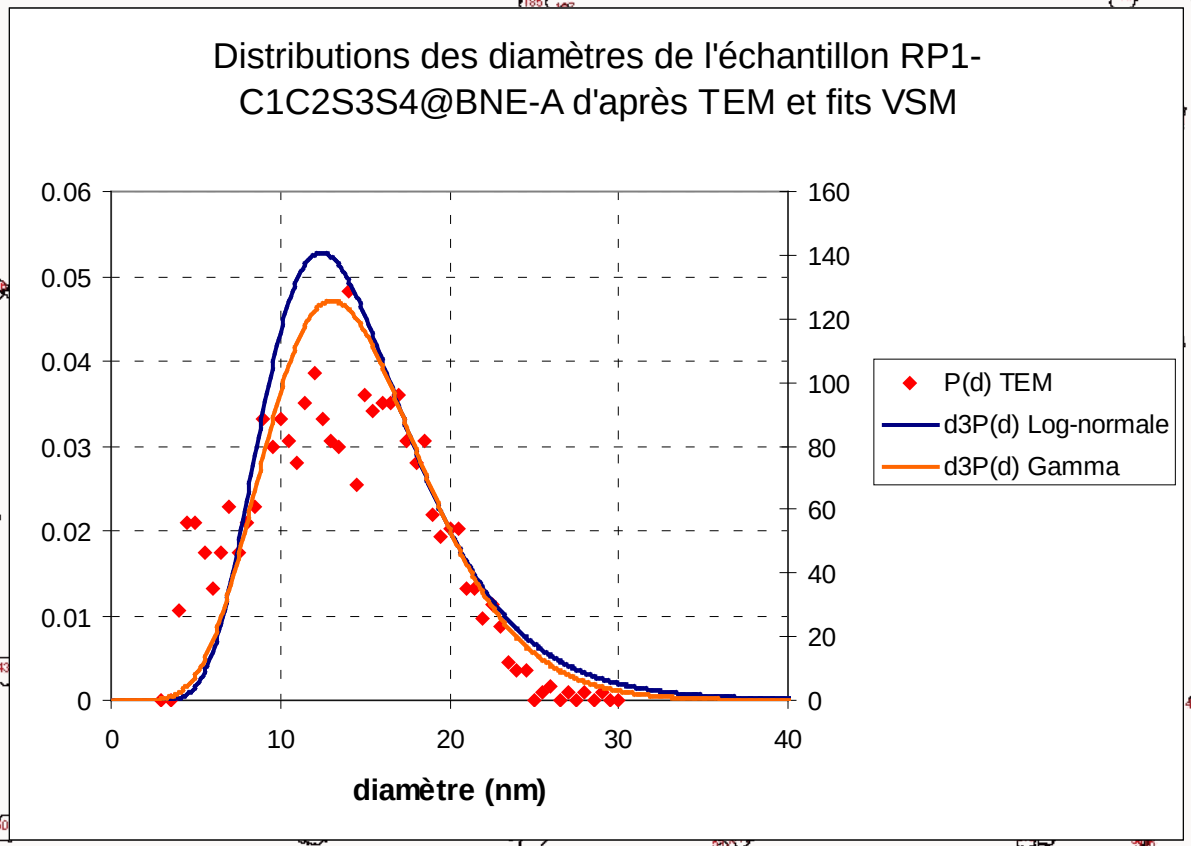

Magnetic/magneto-optical properties of size-sorted MNPs

Vibrating sample magnetometry

$$M = \frac{1}{V_S}\int M_S \frac{\pi}{6} D^3 L\left(\frac{\mu_0 M_S \pi D^3 H}{6kT}\right) f_{LN}(D)\,dD$$

Smaller NPs (S1S fraction d=6nm)

a.

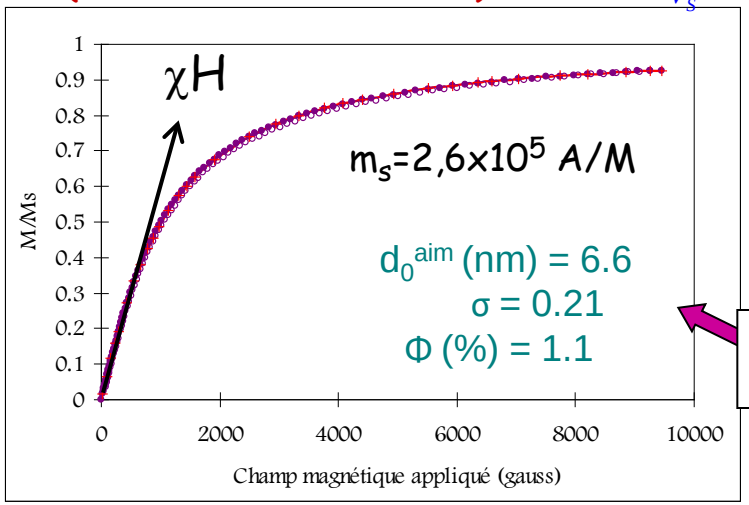

$M_{sat} = m_s \Phi$

1st order Langevin's curve

Larger NPs (C1C fraction d=9nm)

b.

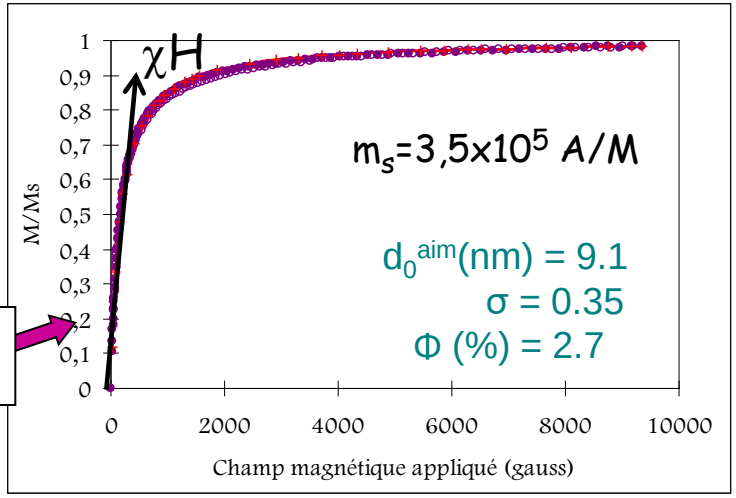

Static Magneto-birefringence

c.

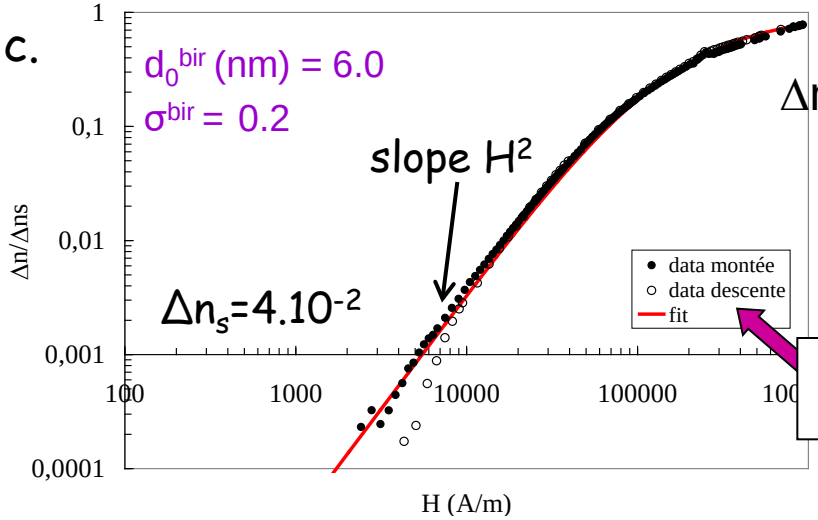

$\Delta n_{sat} = \Delta n_s \Phi$

2nd order Langevin's curve

d.

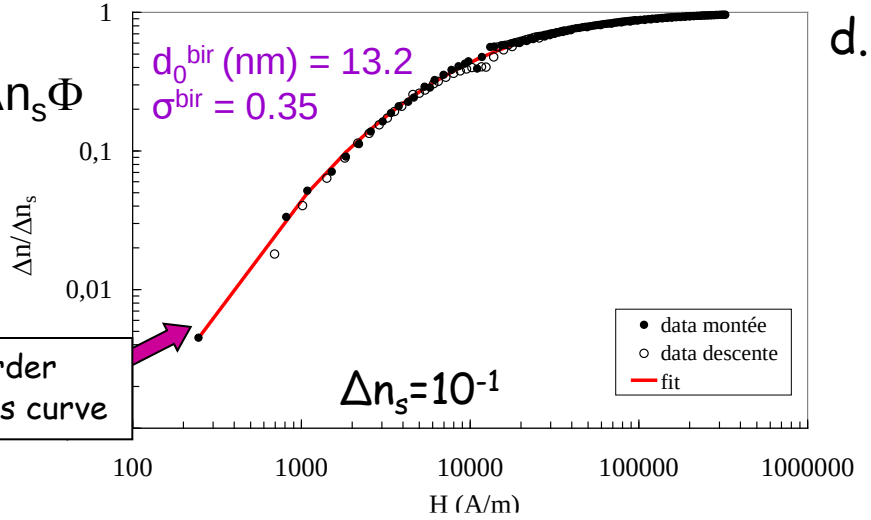

→ more monodisperse and superparamagnetic

→ larger, ferrimagnetic and more anisotropic

Particle form factors by small angle neutron scattering

SANS Intensity normalized by volume fraction Φ (cm^{-1})

PACE spectrometer with Annie Brûlet

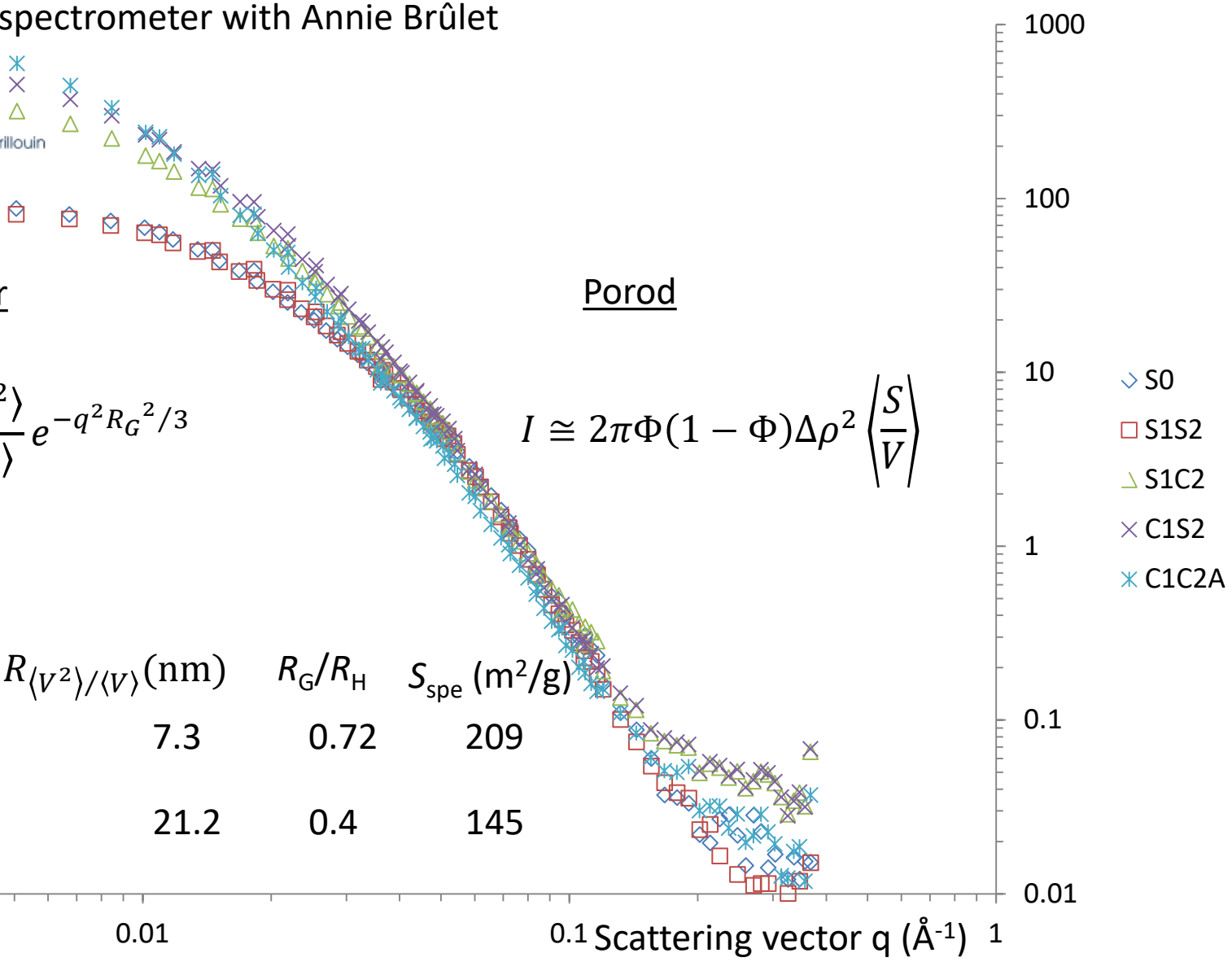

Guinier

$$I \cong \Phi \Delta\rho^2 \frac{\langle V^2 \rangle}{\langle V \rangle} e^{-q^2 {R_G}^2/3}$$

Porod

$$I \cong 2\pi\Phi(1-\Phi)\Delta\rho^2 \left\langle \frac{S}{V} \right\rangle$$

	R_G (nm)	$R_{\langle V^2 \rangle / \langle V \rangle}$ (nm)	R_G/R_H	S_{spe} (m^2/g)
S_0:	9.2	7.3	0.72	209
C_1C_2A:	16.7	21.2	0.4	145

Synthesis & properties of multi-core "nanoflowers"

L. Lartigue, P. Hugounenq, D. Alloyeau, S. P. Clarke, M. Lévy, J-C. Bacri, R. Bazzi, D. F. Brougham, C. Wilhelm, F. Gazeau, ACS Nano 6, 10935–10949 (2012)

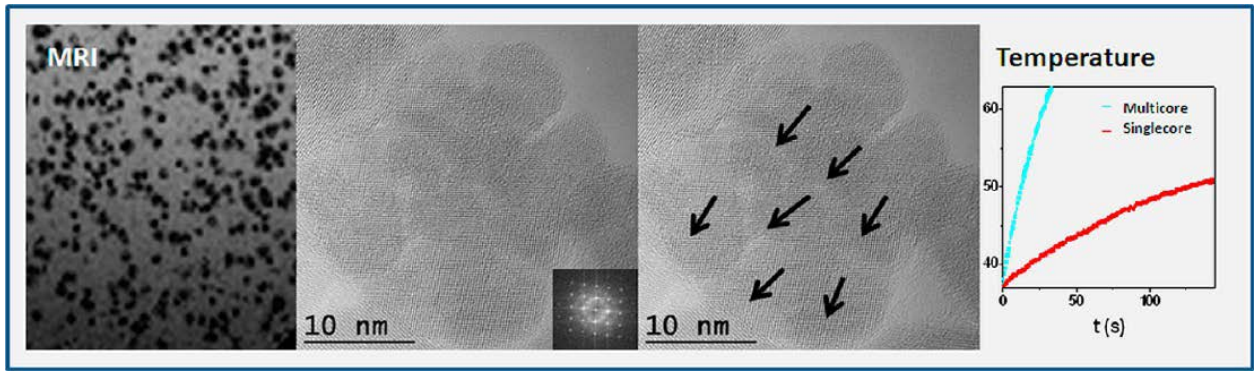

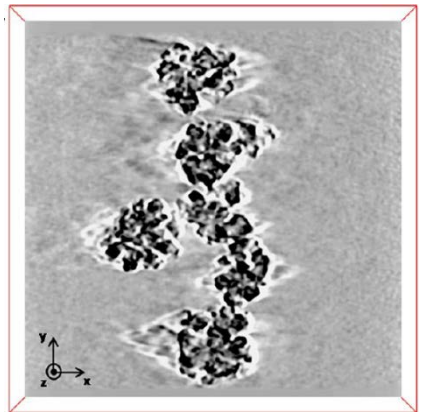

→ superior heating properties (here values at H_{max}=29 kA/m)

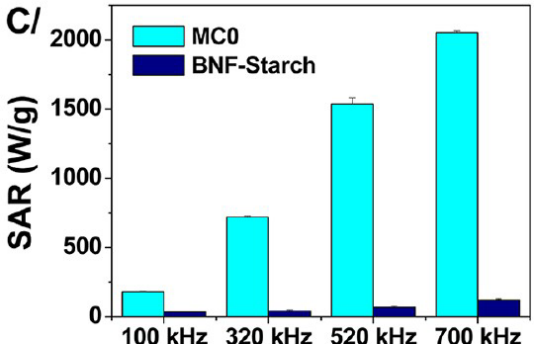

→ also high transverse relaxivity: r_2=365 $s^{-1}mM_{Fe}^{-1}$ at 9.25MHz (0.22T/37°C)

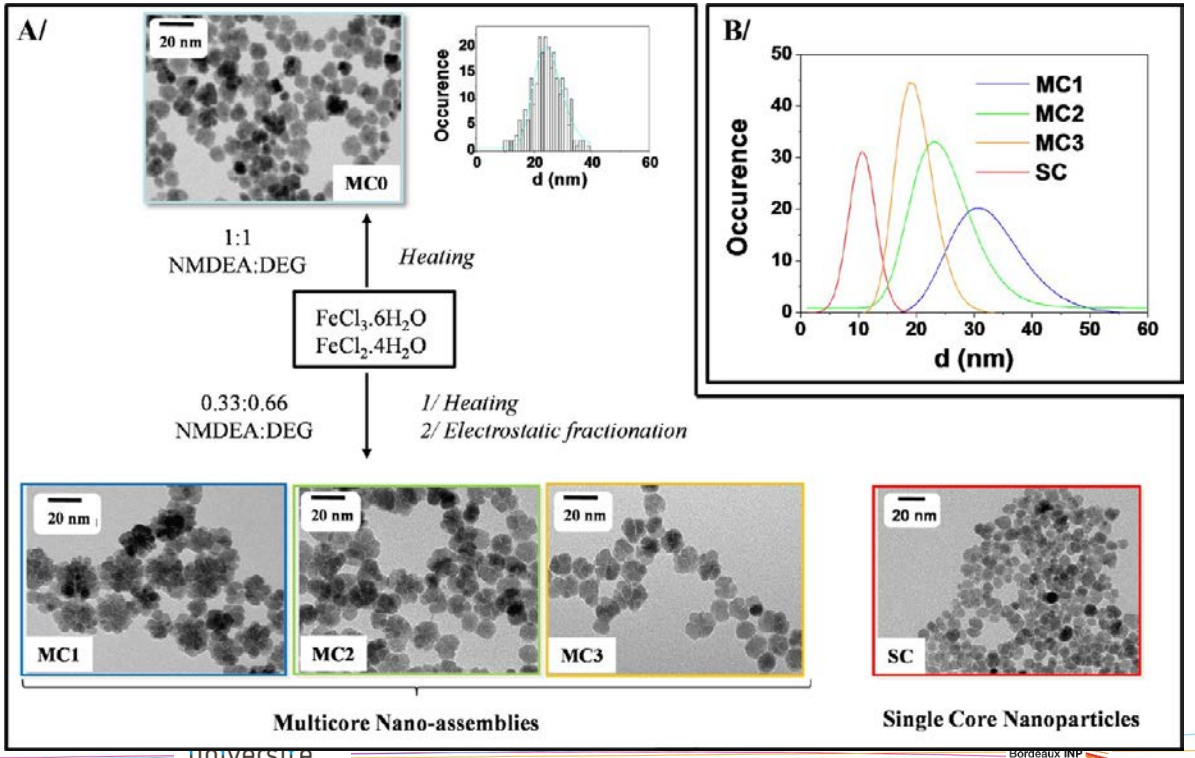

Nanoflower synthesis: the New Orleans method

D. Caruntu, G. Caruntu, Y. Chen, C. J. O'Connor, G. Goloverda, V. L. Kolesnichenko, *Chem. Mater.* **2004,** *16,* 5527-5534

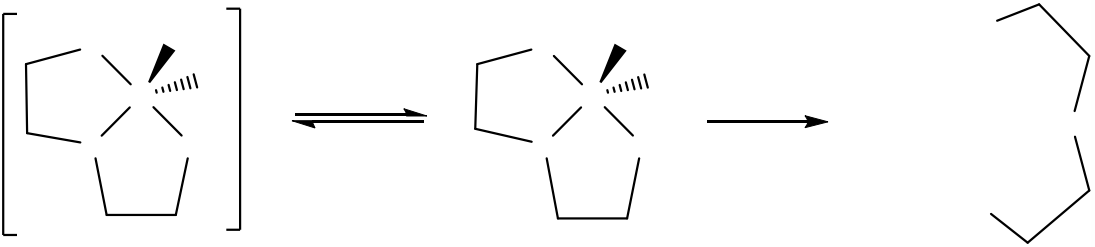

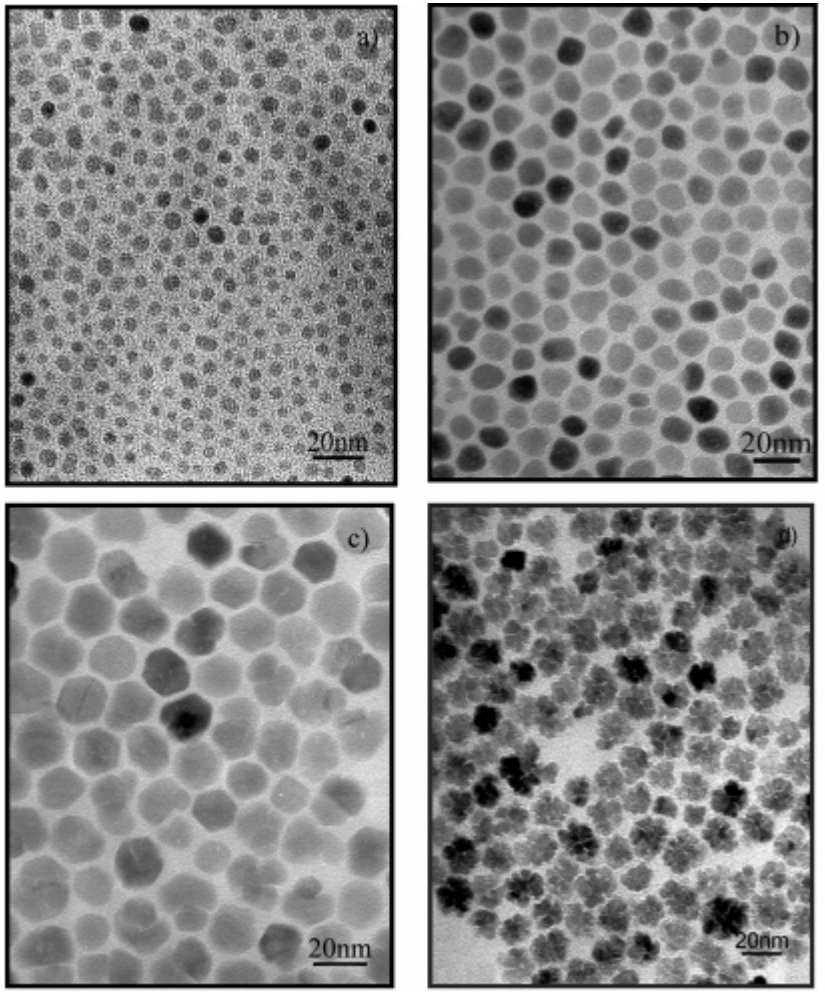

Polyol mixture: N-methyl diethanolamine / DEG (1:1)

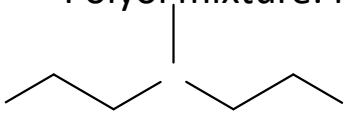

- 2 mmol $FeCl_2$
- 4 mmol $FeCl_3$
- 16 mmol NaOH
- 40 g DEG
- 40 g NMEDA
- 220°C 5h

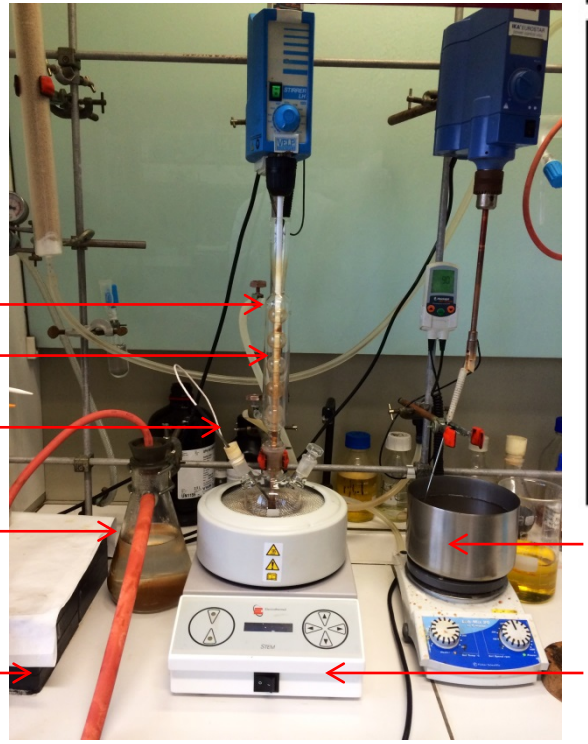

- Precursor
- Polyol composition
- Temp/Duration
- Water content

Forced hydrolysis mechanistic pathway (Caruntu)

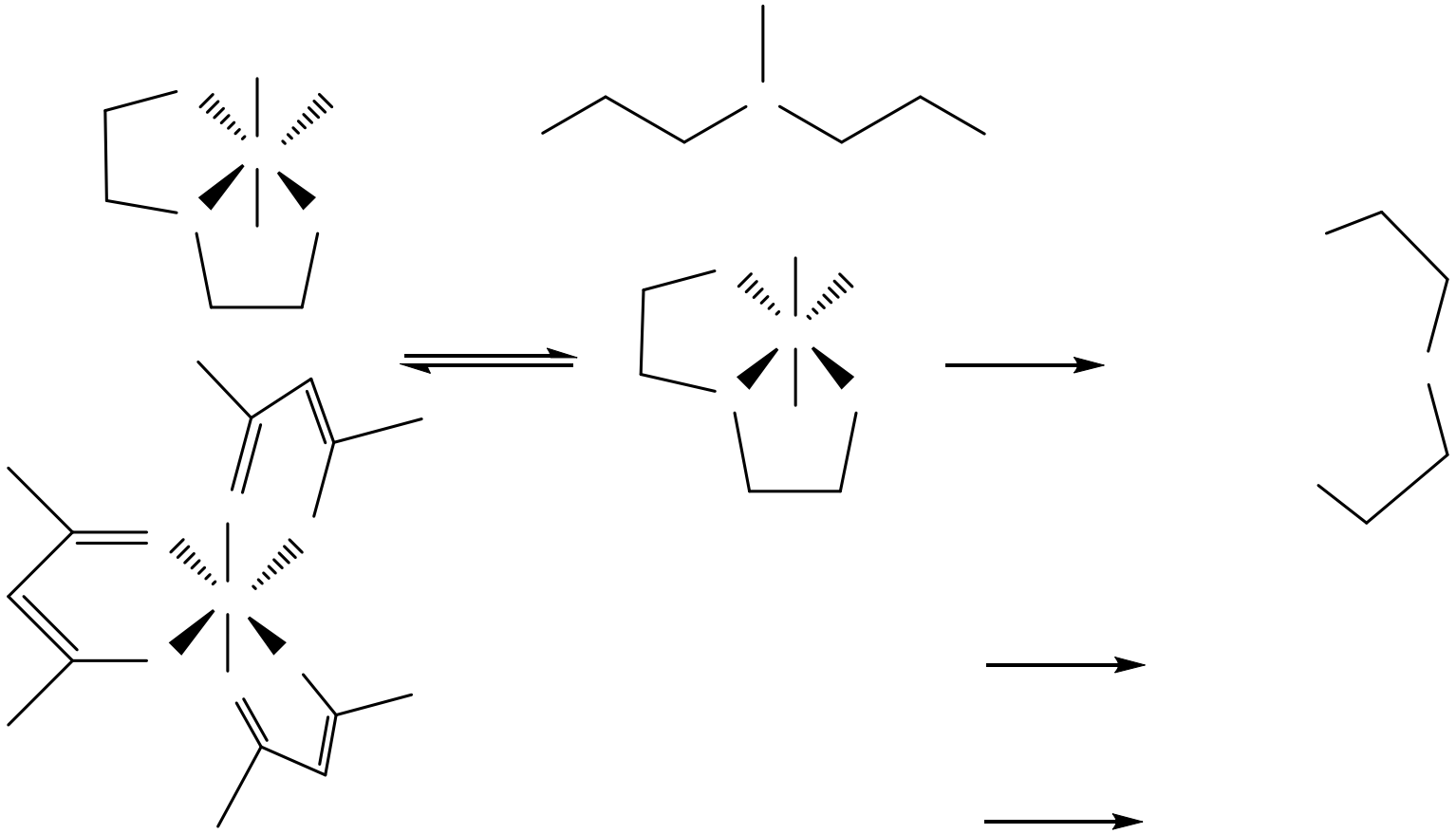

1) D. Caruntu, G. Caruntu, Y. Chen, C. J. O'Connor, G. Goloverda, V. L. Kolesnichenko, *Chem. Mater.* **2004,** *16,* 5527-5534;
2) S. Sun and H. Zeng et al, *J. A. C. S.*, **2002**, *124*, 8204-8205 and **2004**, *126*, 273-279
3) F.A. Tourinho, R. Franck, R. Massart, *J. Materials Science* **1990**, *25*, 3249-3254

Large library of sample batches

Batch name	Nomenclature
15ff	$DN1000_{HU}$-5h
17ff	$D5000_{HI}$-20m
25ff	$DN500_{HU}$-4h
30ff	$DN1000_{HU}$-5h
31ff	$DN500_{HU}$-1h
32ff	$DN500_{HU}$-5h
34ff	$DN100_{HU}$-5h*
35ff	$DN100_{HU}$-5h
36ff	$DN100_{HU}$-5h

Batch name	Nomenclature
28AA	$DN100_{HU}$-220-5h-Cl
29AA	$DN200_{HU}$-220-5h-Cl
02MA	$DN300_{HU}$-220-5h-Cl
09MA	$DN400_{HU}$-220-5h-Cl
10MA	$DN500_{HU}$-220-5h-Cl
11MA	$DN50_{HU}$-220-5h-Cl
27MA	DN0-220-5h-Acac
12MA	DN100-220-5h-Acac
17MA	DN200-220-5h-Acac
18MA	DN300-220-5h-Acac
19MA	DN400-220-5h-Acac
20MA	DN500-220-5h-Acac
15JA	DD100-250-5h-Cl
10JA	TD100-250-5h-Cl

Vary µL water in 120 g polyol mixture:

EG: Ethylene Glycol
DEG: Diethylene Glycol
TEG: Triethylene Glycol
DEA: Diethanolamine
NMDEA: N-methyldiethanolamine
TEA: Triethanolamine
DIA: N-ethyl Diisopropylamine

D=pure DEG
DN=DEG/NMDEA (1:1)
DD=DEG/DEA (1:1)
TD=TEG/DEA (1:1)

HU=heating up
HI=hot injection
* no stirring

Cl=2 mmol $FeCl_2$, 4 mmol$FeCl_3$,16 mmol NaOH
Acac=6 mmol $Fe(acac)_3$,16 mmol NaOH

Study of polyol route: fate of solvent molecules

a)

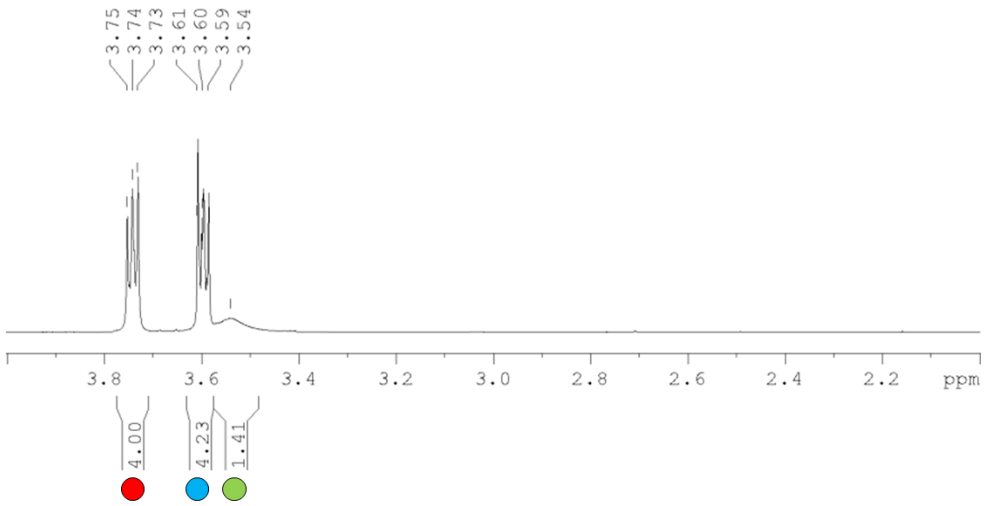

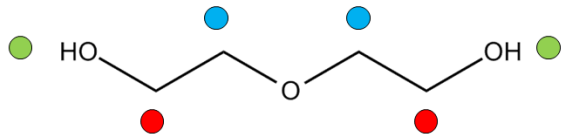

Diethylene glycol (DEG)

b)

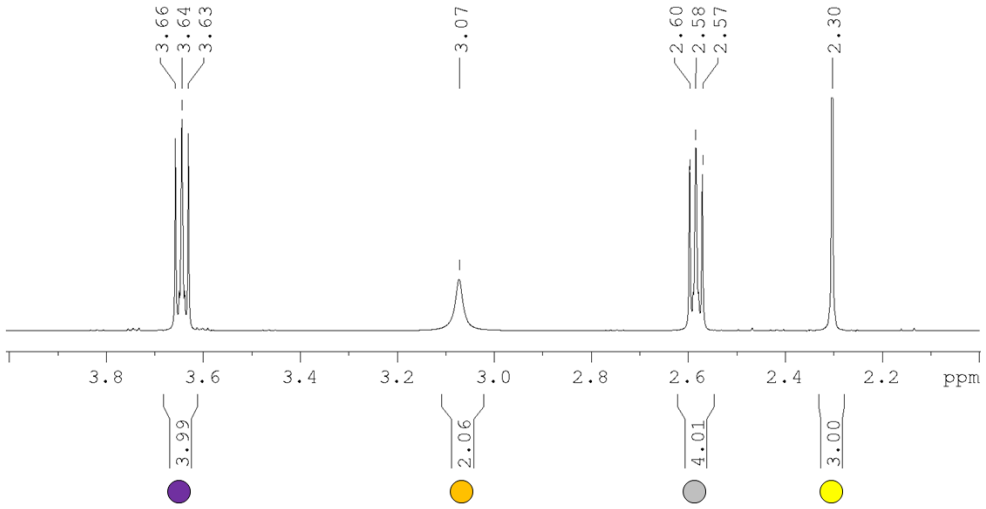

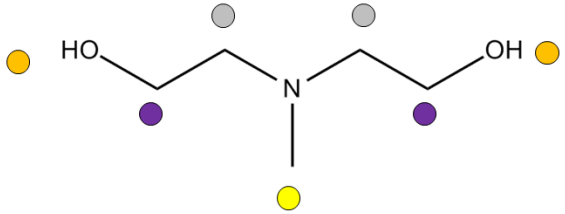

N-methyldiethanolamine (NMDEA)

Study of polyol route: fate of solvent molecules

c)

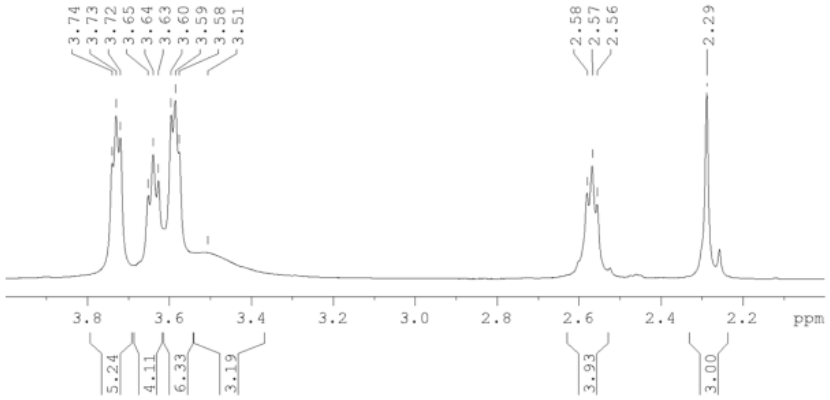

DEG, NMDEA, NaOH, $FeCl_2$, $FeCl_3$

d)

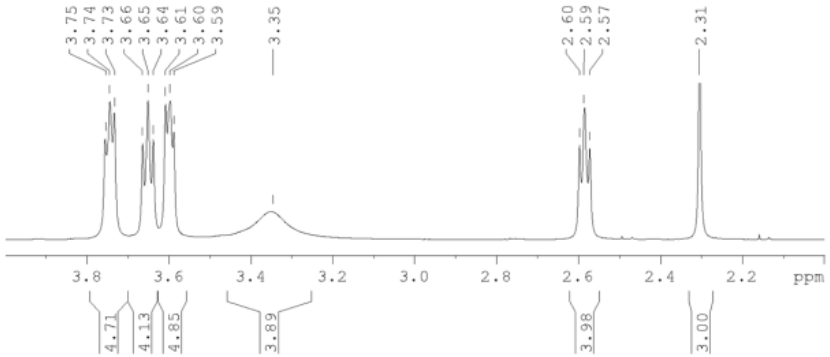

DEG, NMDEA, NaOH, $FeCl_2$, $FeCl_3$, H_2O
Before reaction

e)

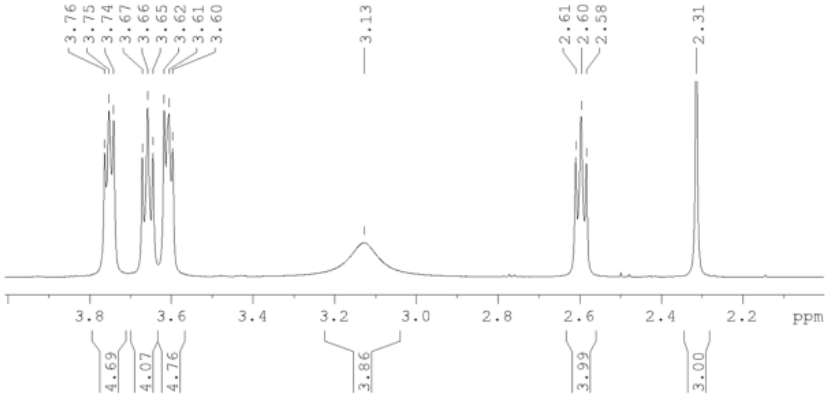

DEG, NMDEA, NaOH, $FeCl_2$, $FeCl_3$, H_2O
After reaction

Study of polyol route: fate of solvent molecules

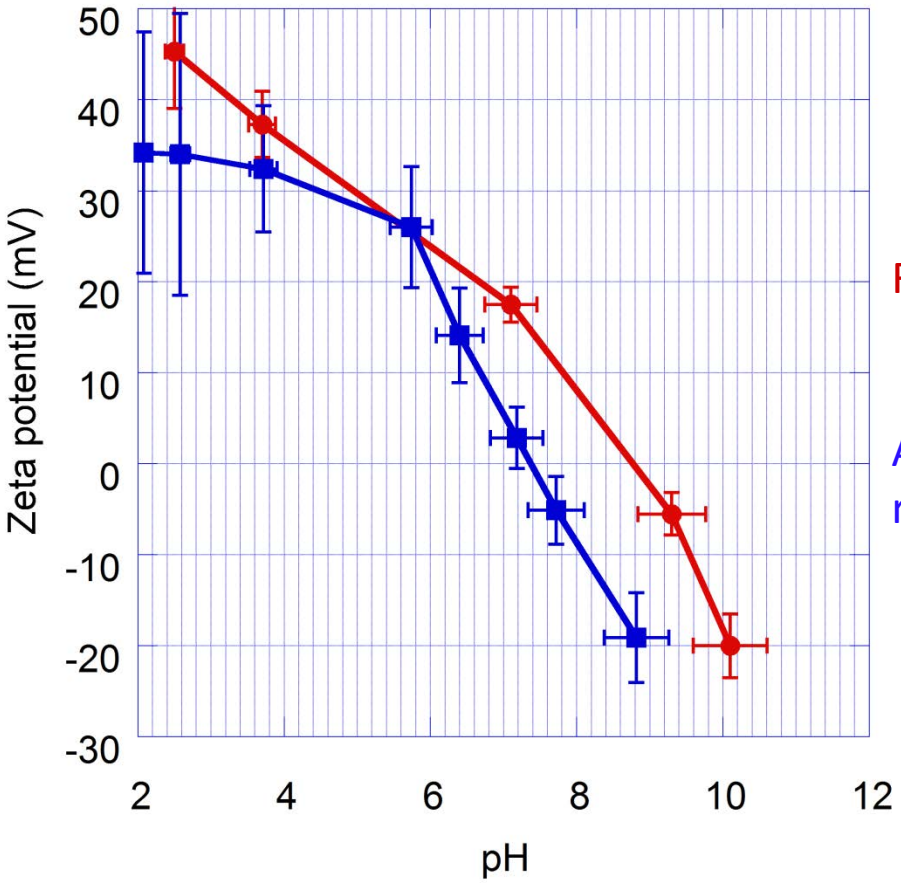

Right after synthesis

→ PZC = pKa of NMDEA

After washings (precipitation-redispersion cycles at alkaline pH)

- Can be oxidized in boiling $Fe(NO_3)_3$: $Fe_3O_4 \rightarrow \gamma\text{–}Fe_2O_3$
- Washed and stabilized in water at pH~7 with citrate ligand or PEG-phosphonate

Hydrodynamic size by DLS

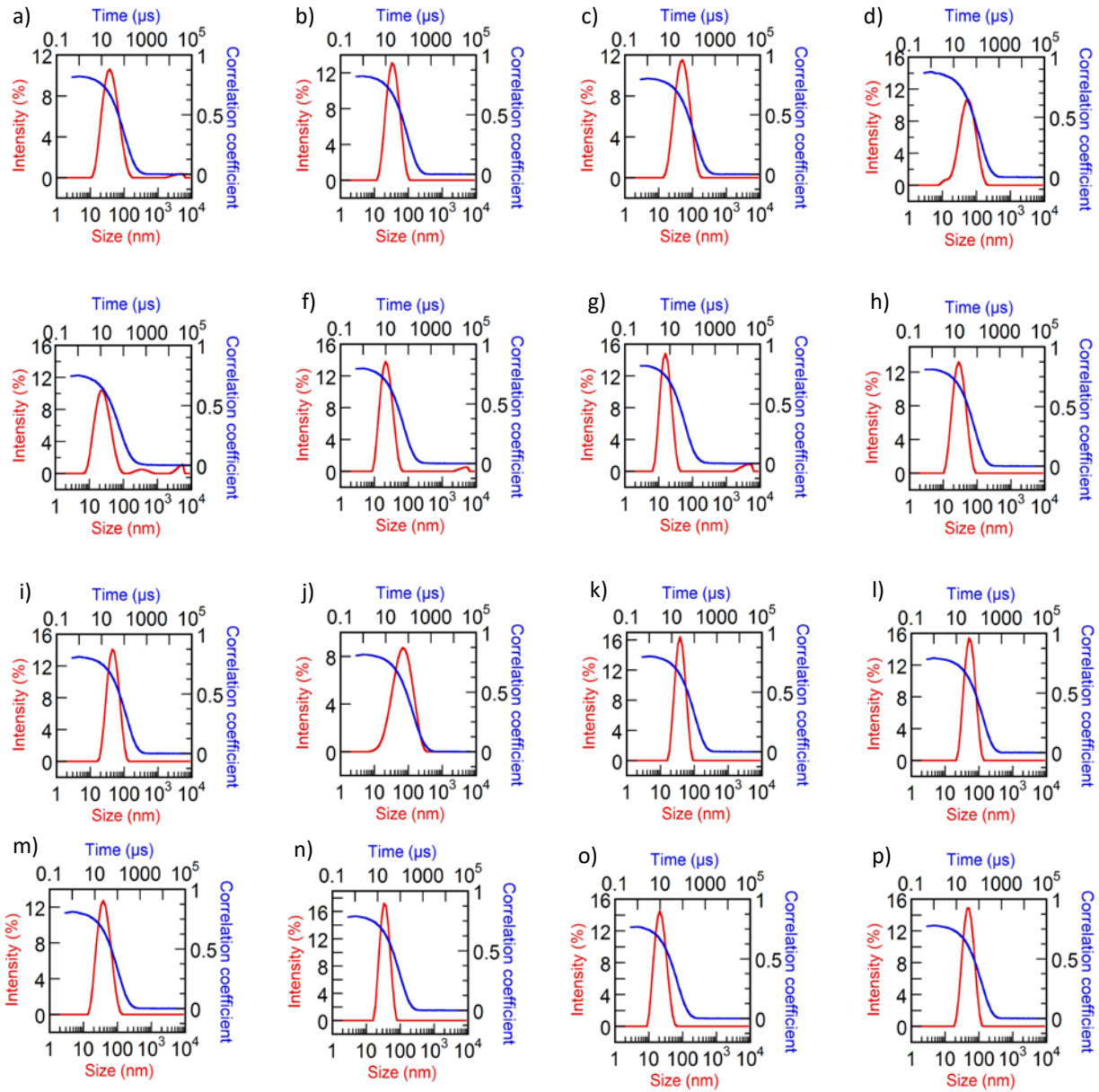

Figure	Batch	D_h (nm)	PDI
a	5ff	36	0.22
b	7ff	32	0.14
c	12ff	44	0.18
d	15ff	46	0.23
e	17ff	24	0.32
f	19ff	22	0.18
g	20ff	16	0.21
h	21ff	27	0.14
i	22ff	43	0.14
j	25ff	55	0.26
k	26ff	36	0.10
l	27ff	50	0.11
m	29ff	37	0.16
n	31ff	33	0.08
o	32ff	21	0.13
p	33ff	45	0.12
q	34ff	30	0.19
r	35ff	36	0.13

Variety of Fe_3O_4 NP batches synthesized in DEG:NMDEA

$$\langle d \rangle = d_0 e^{\sigma^2/2} \qquad var(d) = {d_0}^2 \left(e^{\sigma^2/2} - 1\right)$$

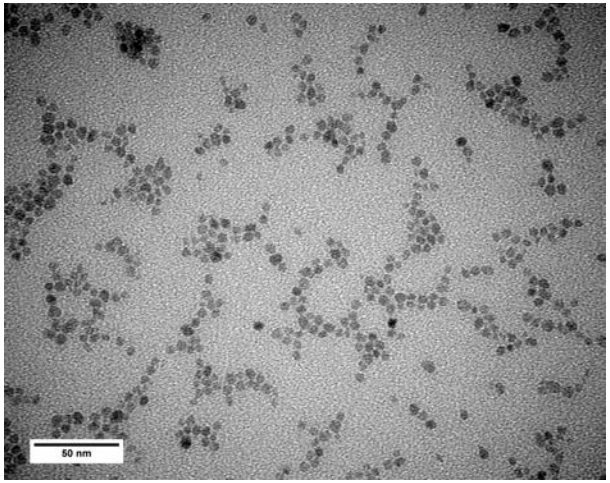

4FF: *d*=6.2±1.0 nm

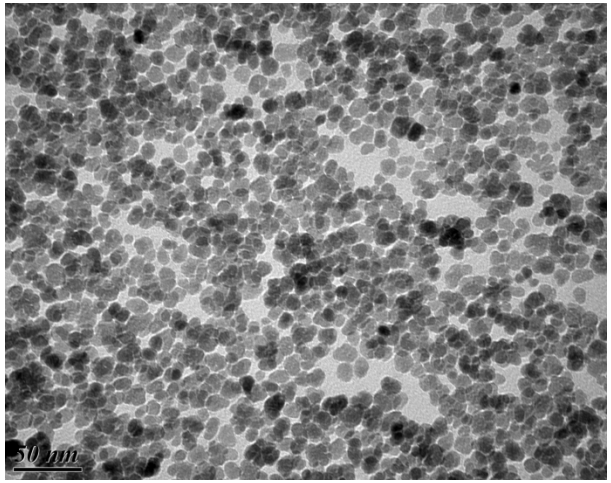

23FF: *d*=10.5±1.9 nm

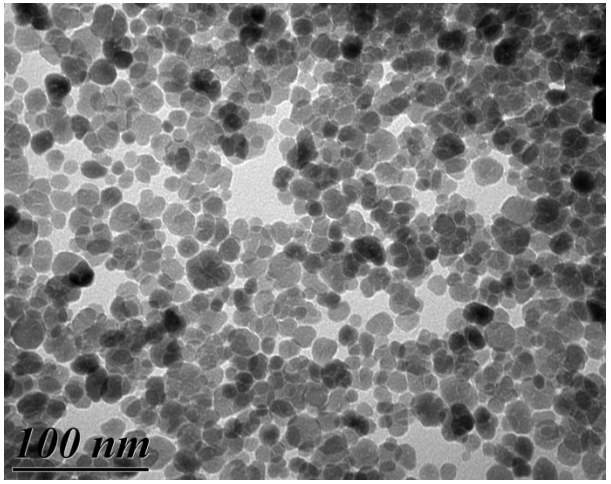

25FF: *d*=14.2±3.2 nm

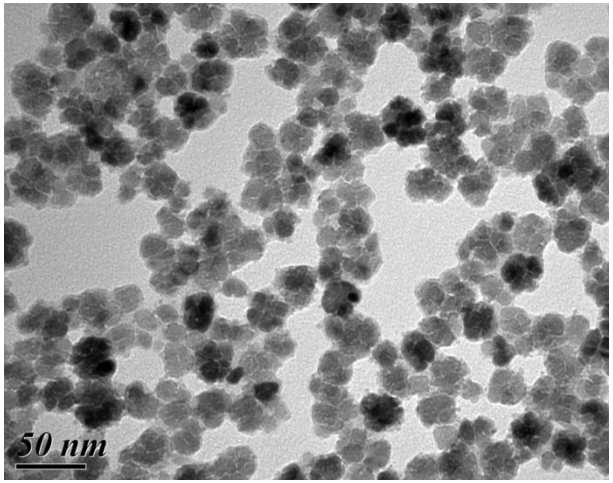

29FF: d_{out}=26.6±4.2 nm

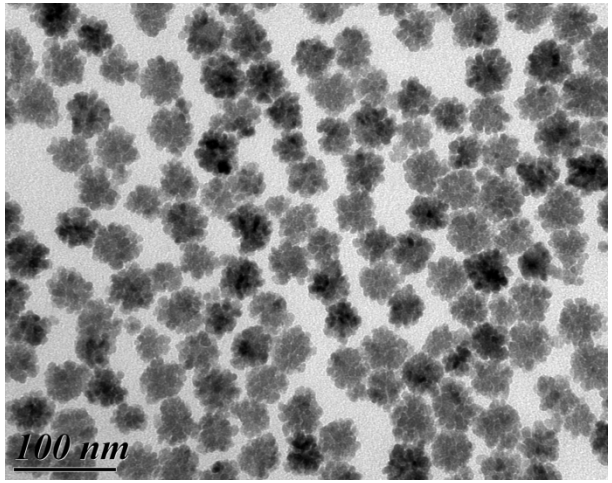

15FF: d_{out}=36.3±4.8 nm

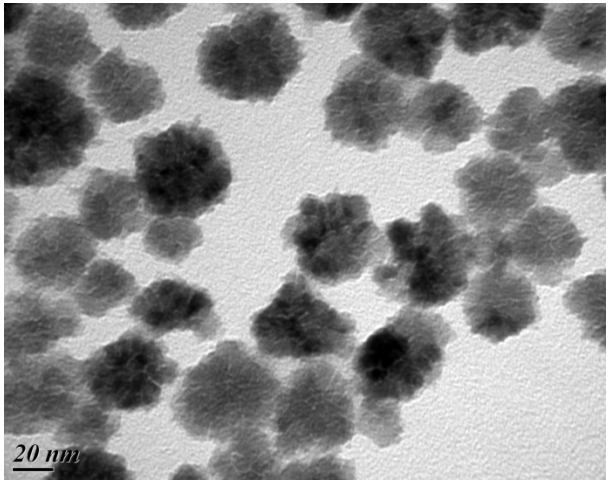

30FF: d_{out}=41.1±8.6 nm

G. Hemery, A. C. Keyes Jr., E. Garaio, I. Rodrigo, J. A. Garcia, F. Pazaola, E. Garanger, O. Sandre, arXiv preprint: 1701.05858

Example of ultra-small nanosphere sample: 17FF

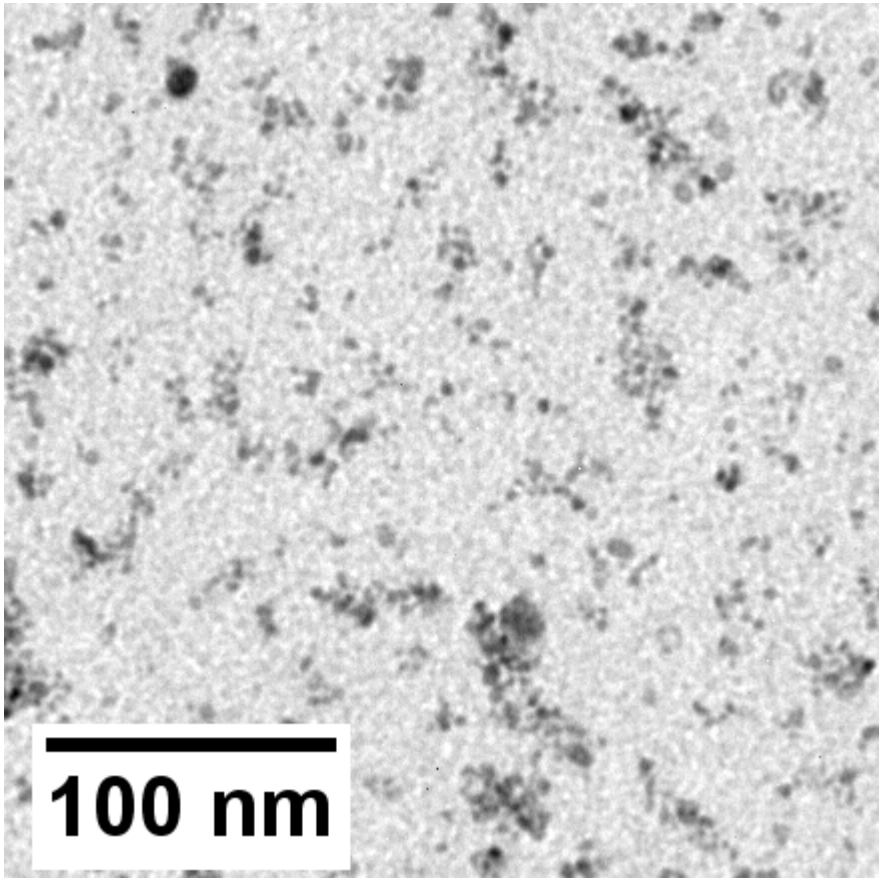

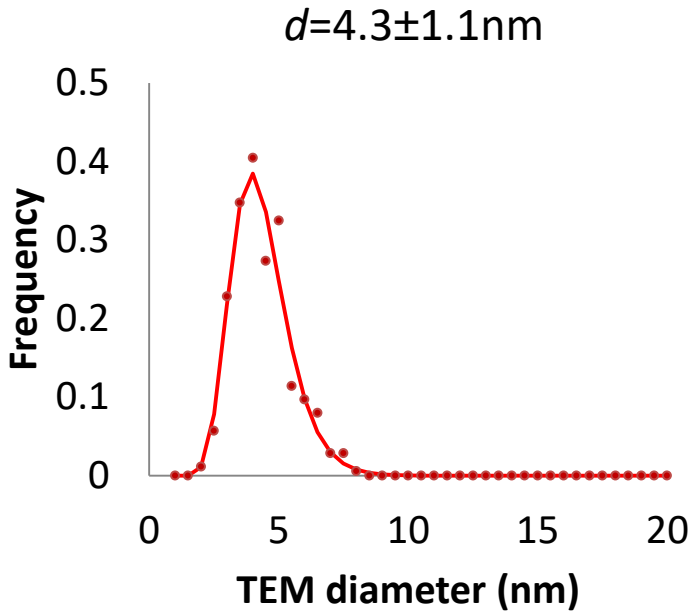

Example of medium size nanosphere sample: 25FF

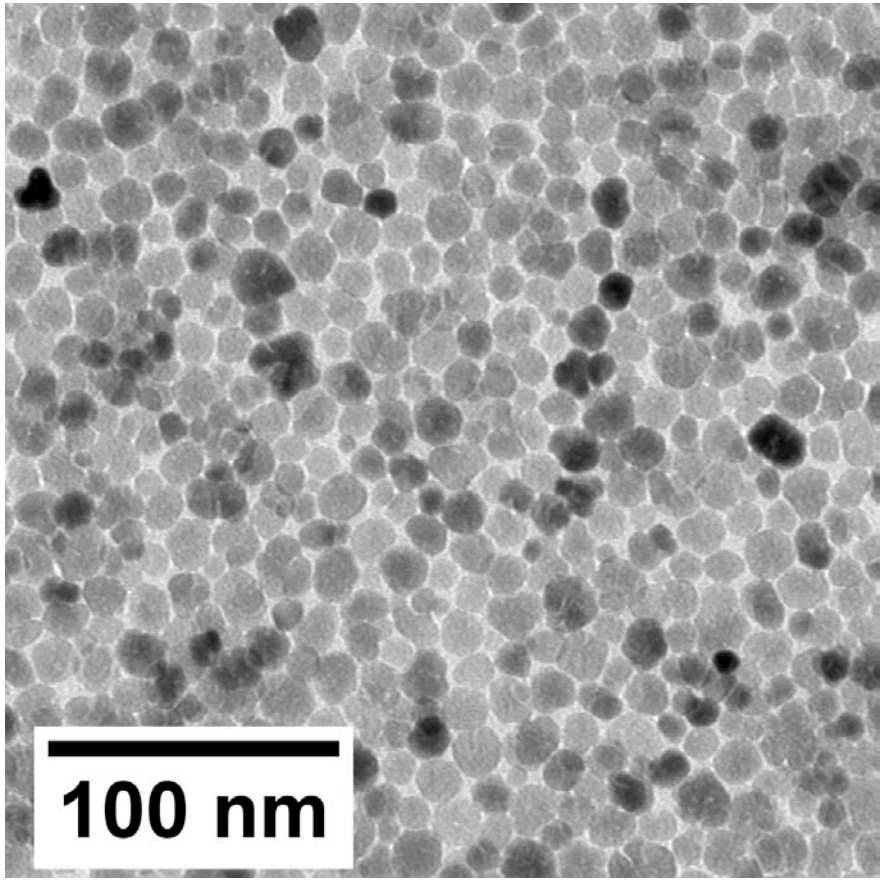

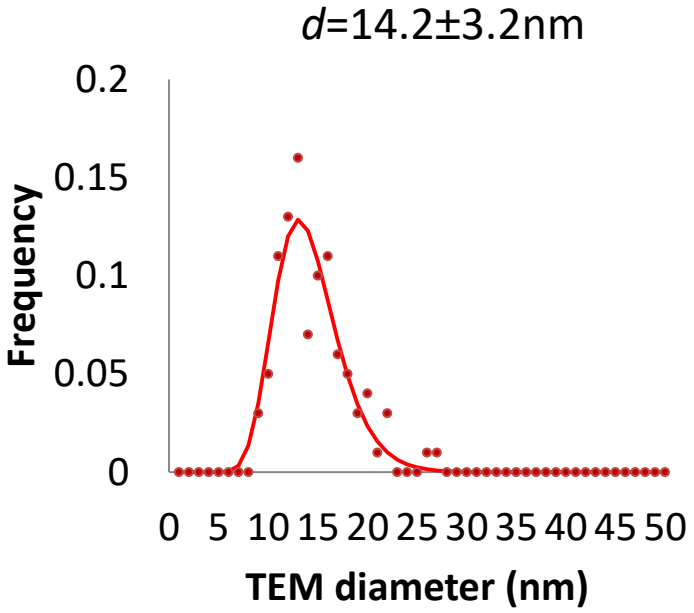

Example of very large size nanosphere sample: 34FF

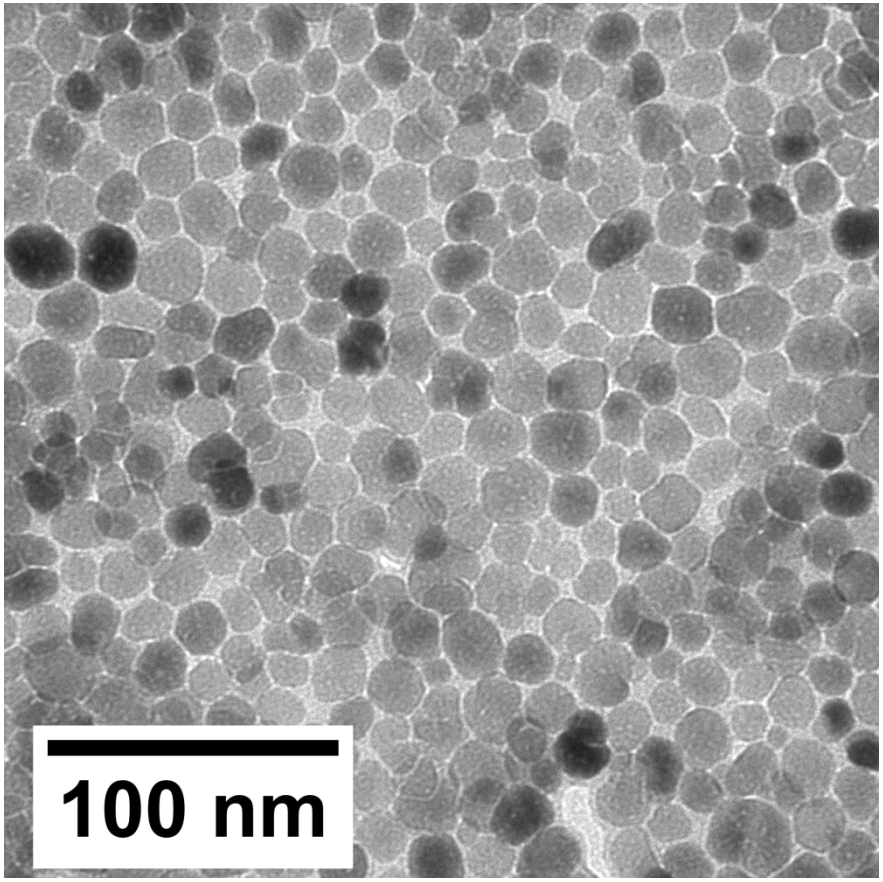

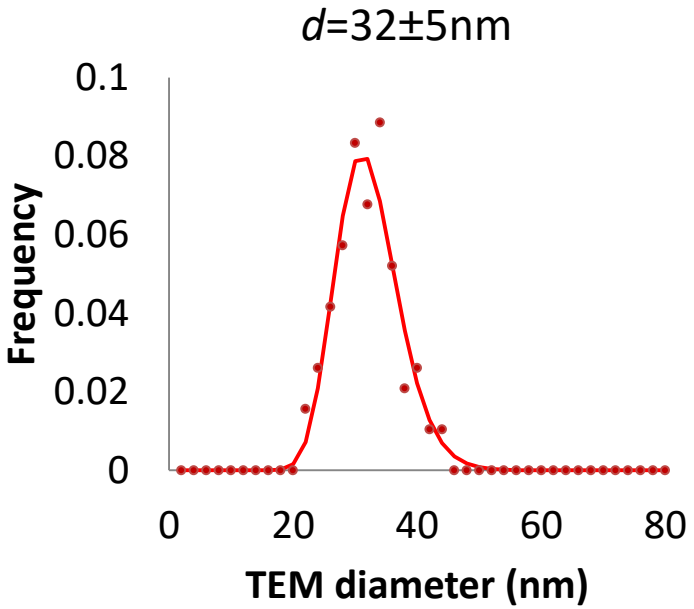

Example of nanoflower sample: 15FF

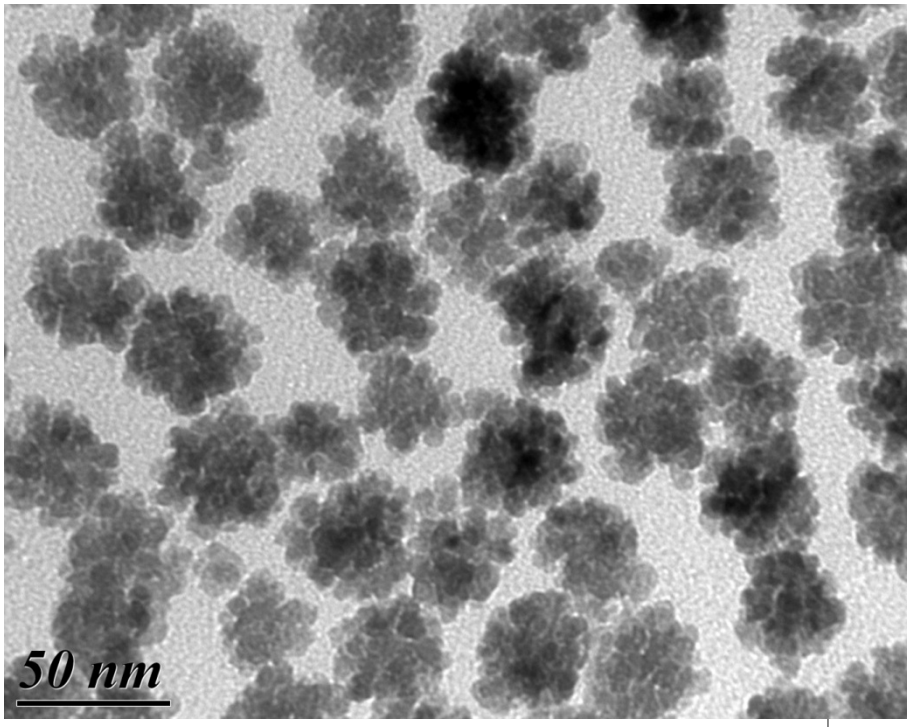

d_{out}=36.3±4.8 nm

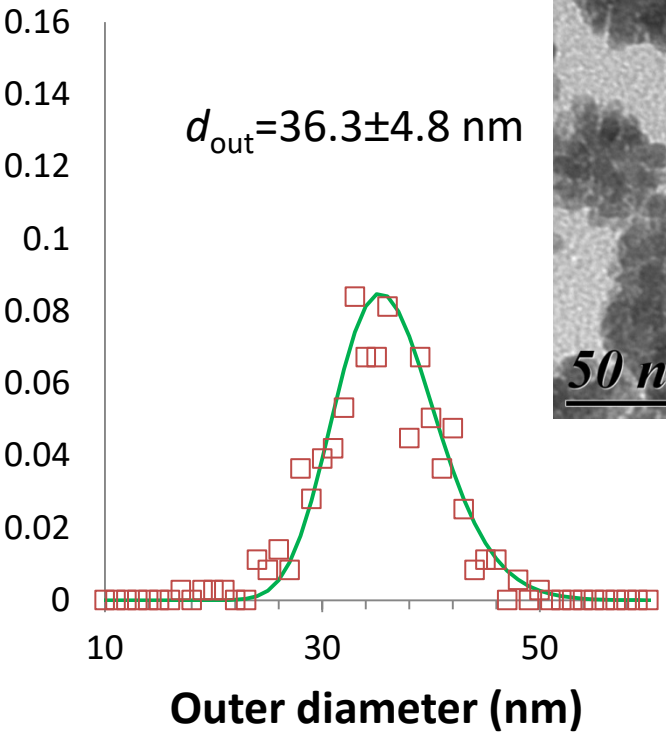

d_{core}=7.4±1.4 nm

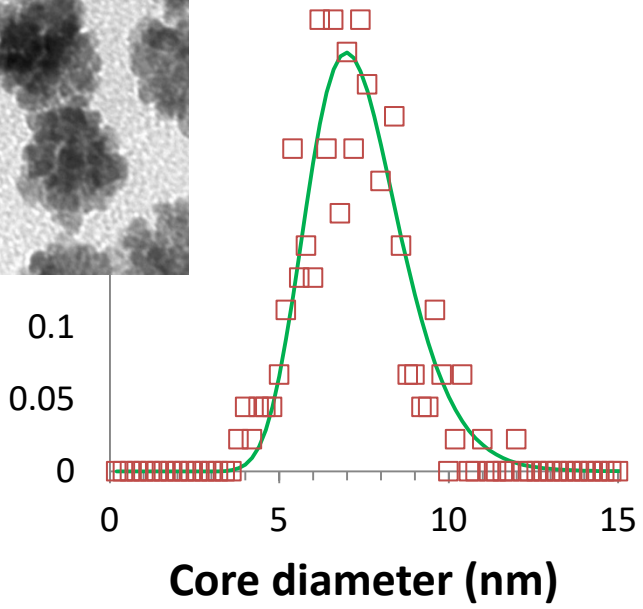

Particle form factors by small angle neutron scattering

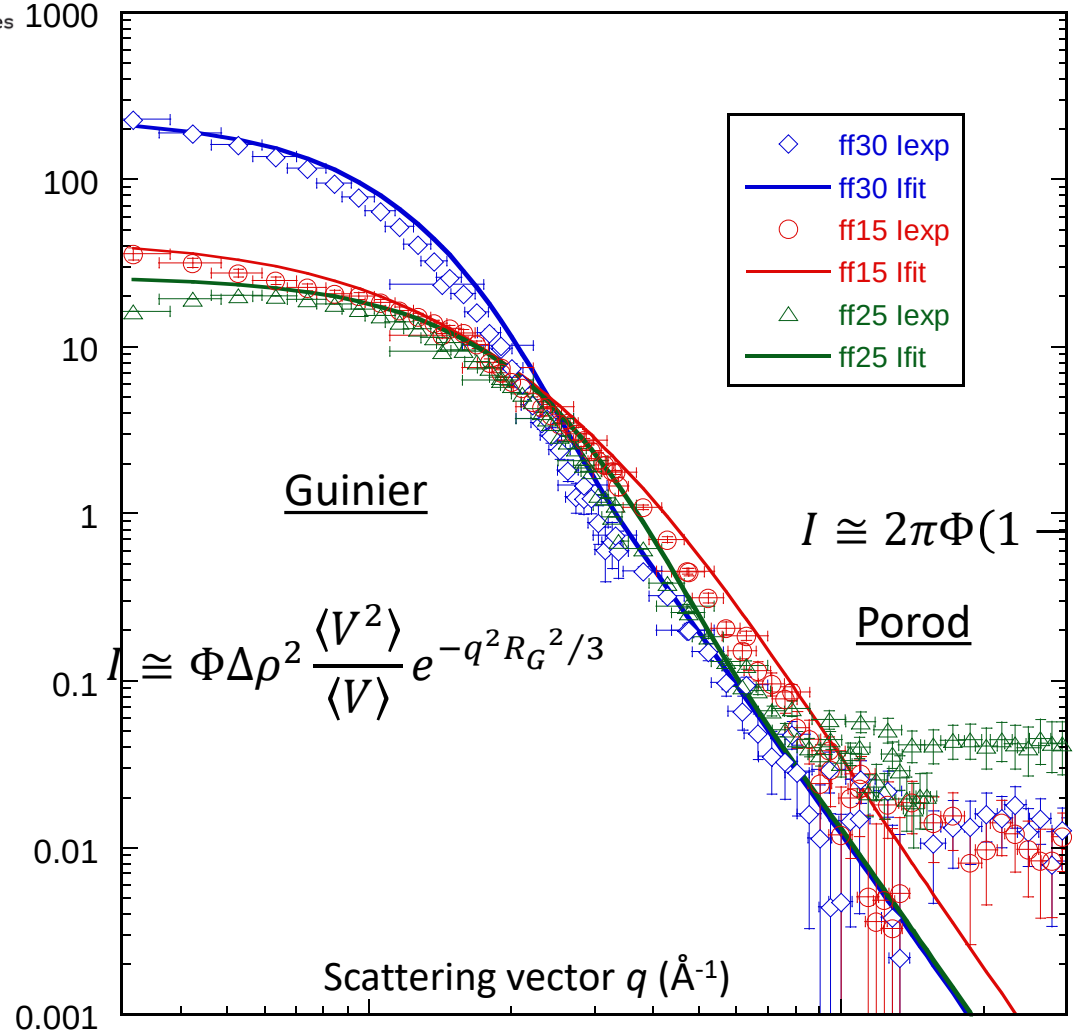

PACE spectrometer
with Annie Brûlet

Orphée
Laboratoire Léon Brillouin

Guinier

$$I \cong \Phi\Delta\rho^2 \frac{\langle V^2 \rangle}{\langle V \rangle} e^{-q^2 {R_G}^2/3}$$

Porod

$$I \cong 2\pi\Phi(1-\Phi)\Delta\rho^2 \left\langle \frac{S}{V} \right\rangle$$

$$\left\langle \frac{S}{V} \right\rangle^{\text{the}} = 3 \Big/ \left(R_{\langle V^2 \rangle / \langle V \rangle} \right)$$

	R_G (nm)	$R_{\langle V^2 \rangle / \langle V \rangle}$(nm)	R_{TEM}(nm)	S_{spe} (m²/g)	S_{spe}^{the}
30ff:	18.9	18.1±3.9	23.5 ± 4.2	31.7	33.1
25ff:	10.5	10.4±2.3	7.1 ± 1.6	52.6	57.7
15ff:	19	10.6±3.9	17.5 ± 2.4	89.9	56.6

Necessity to measure precisely iron oxide concentration

Experimental measurement of all properties (m_S, Δn_S, SHP, P(q), r_1, r_2…) require the total iron concentration.

Available methods are:

• Atomic Absorption Spectroscopy (or ICP): sensitive (10^{-5}M) but ±5%

• Redox titration (Charlot) by $K_2Cr_2O_7/SnCl_2$: precise (±1%) but not sensitive (10^{-1}M)

• Whole UV-Vis curve: precise (±1%) and sensitive (10^{-4}M)

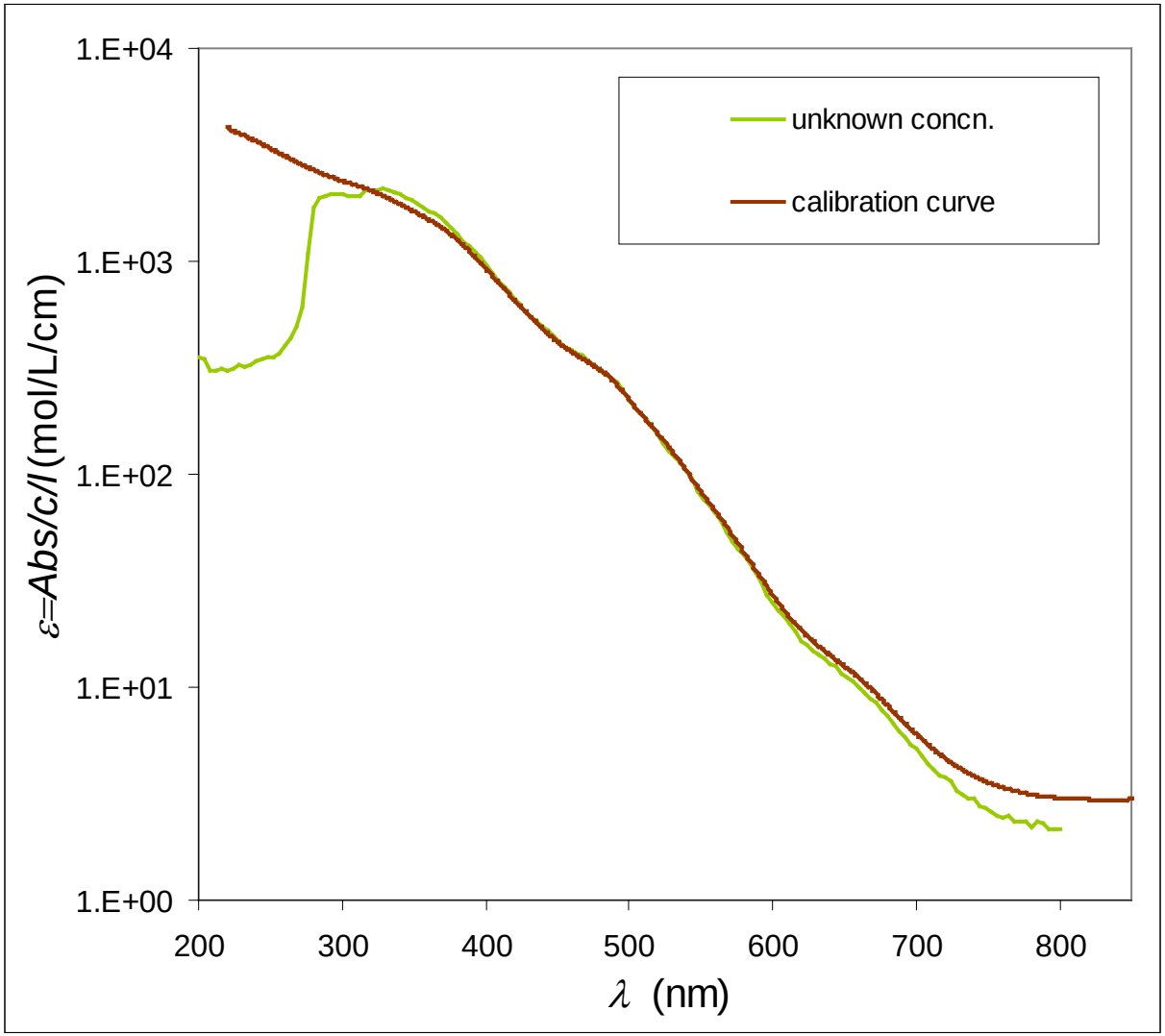

• "Ferrozine assay": highly sensitive (10^{-7}M) from OD_{562nm} according to *Small* 5 (2009) 256

UV-Vis extinction is independent on MNP size distribution

Constant → $c(h\nu - E_g^{bulk})^{1/2}$ ← 3,6 eV for Fe_2O_3 Shannon, *J. Phys. Chem. Ref. Data* 2002

UV-Vis molar extinction coefficient → $\varepsilon = \dfrac{c(h\nu - E_g^{bulk})^{1/2}}{h\nu}$

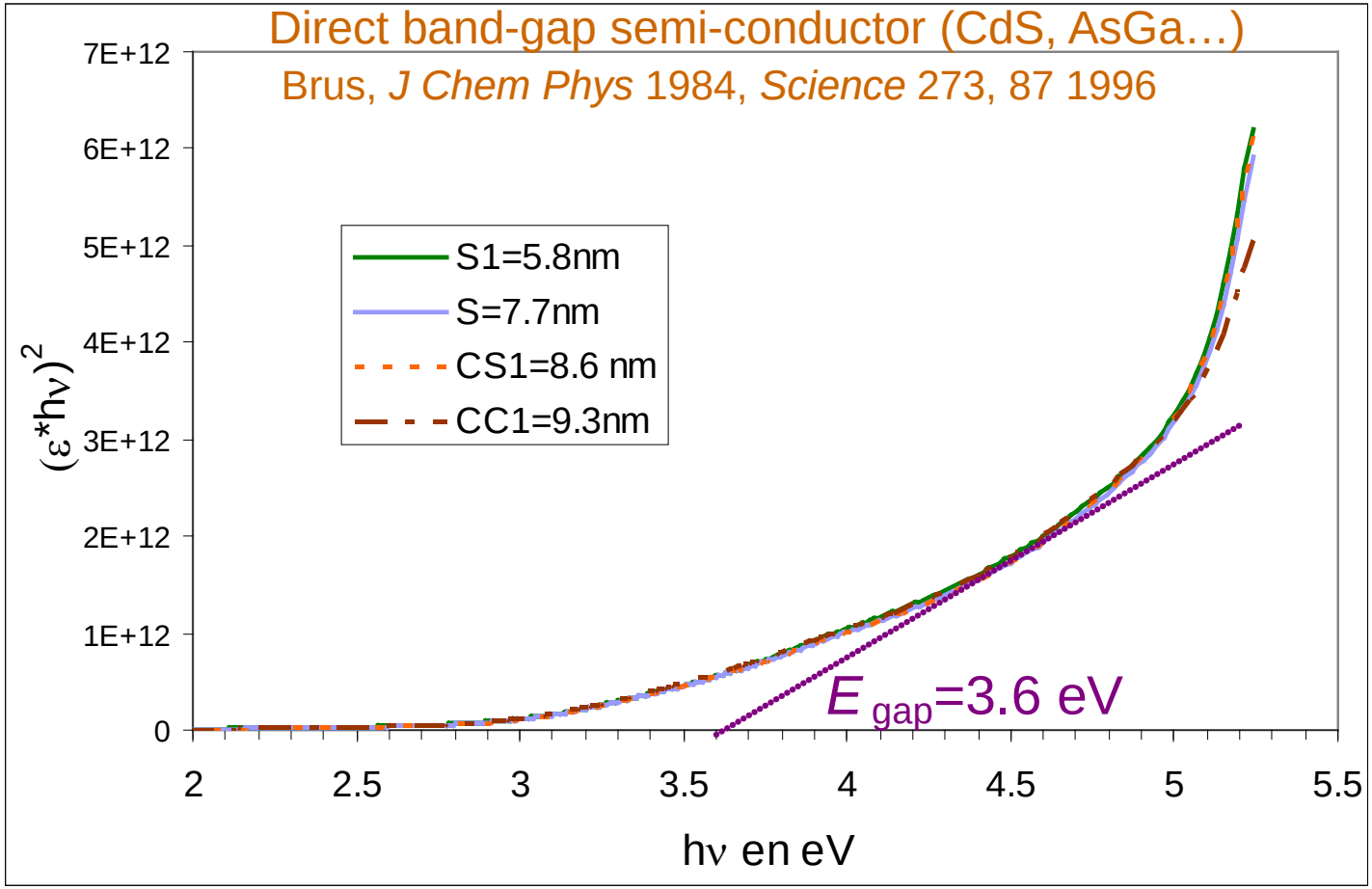

A. Abou-Hassan UPMC thesis 2009 2010 Best thesis prize in physical chemistry (SFP/SCF)
→ no size-dependent gap in the case of γ-Fe_2O_3
(the exciton diffusion length is presumably much smaller than the size of the USPIOs, thus no confinment)

Conclusion on Part 1 (Synthesis & Properties of MNPs)

- Since 30 years, the aqueous route (alkaline coprecipitation) leads to a quantitative production (~100g dry γ–Fe_2O_3) of magnetic nanoparticles that can be further functionalized (organic solvent, polymer matrix, biological coatings...). Today the up-scalable method is polyol route.

- Samples have inherent size / shape polydispersity, which can be a drawback for long-range ordering (*e.g.* colloidal or liquid crystals) but, according to Curie's principle, this is a great advantage to get large physical properties!

- The outlooks for biological applications (MRI contrast agents and magnetic hyperthermia) might be to play on the anisotropy constant K_a (shape anisotropy or other "irregularity") rather than on the size only, because of the difficulty to stabilize large MNPs (*e.g.* Ø>20nm) in biological media (ionic strength and flocculent proteins).